

ตัวเร่งปฏิกิริยาชนิดสารประกอบเหล็กบนตัวรองรับเคลย์สำหรับออกซิเดชันของไซโคลออกเทน



นางสาวปาริชาติ ดำรงพงษ์

สถาบันวิทยบริการ
จุฬาลงกรณ์มหาวิทยาลัย

วิทยานิพนธ์นี้เป็นส่วนหนึ่งของการศึกษาตามหลักสูตรปริญญาวิทยาศาสตรมหาบัณฑิต

สาขาวิชาเคมี ภาควิชาเคมี

คณะวิทยาศาสตร์ จุฬาลงกรณ์มหาวิทยาลัย

ปีการศึกษา 2547

ISBN 974-17-6411-1

ลิขสิทธิ์ของจุฬาลงกรณ์มหาวิทยาลัย

CLAY SUPPORTED IRON COMPOUND CATALYSTS FOR OXIDATION OF
CYCLOOCTANE



Miss Parichat Damrongpong

สถาบันวิทยบริการ

A Thesis Submitted in Partial Fulfillment of the Requirements
for the Degree of Master of Science in Chemistry

Department of Chemistry

Faculty of Science

Chulalongkorn University

Academic Year 2004

ISBN 974-17-6411-1

Thesis Title CLAY SUPPORTED IRON COMPOUND CATALYSTS
FOR OXIDATION OF CYCLOOCTANE
By Miss Parichat Damrongpong
Field of Study Chemistry
Thesis Advisor Associate Professor Wimonrat Trakarnpruk, Ph.D.

Accepted by the Faculty of Science, Chulalongkorn University in Partial
Fulfillment of the Requirement for the Master's Degree

.....Dean of the Faculty of Science
(Professor Piamsak Menasveta, Ph.D.)

Thesis Committee

.....Chairman
(Associate Professor Sirirat Kokpol, Ph.D.)

.....Thesis Advisor
(Associate Professor Wimonrat Trakarnpruk, Ph.D.)

.....Member
(Assistant Professor Korbratna Kriausakul, Ph.D.)

.....Member
(Soamwadee Chaianansutcharit, Ph.D.)

ปาริชาต คำรงพงษ์ : ตัวเร่งปฏิกิริยาชนิดสารประกอบเหล็กบนตัวรองรับเคลย์สำหรับ
ออกซิเดชันของไซโคลออกเทน (CLAY SUPPORTED IRON COMPOUND
CATALYSTS FOR OXIDATION OF CYCLOOCTANE)

อ. ที่ปรึกษา : รศ. ดร. วิมลรัตน์ ตระการพุกภัย, 100 หน้า. ISBN 974-17-6411-1.

ตัวเร่งปฏิกิริยาสารประกอบเหล็กบนตัวรองรับเบนโทไนท์ คาโอลิน และ ทาลคัม ซึ่งได้ทำ
การสังเคราะห์ขึ้นสำหรับออกซิเดชันของไซโคลออกเทนด้วยวิธีแลกเปลี่ยนไอออนนั้น สารประกอบ
เหล็กที่ใช้ศึกษาคือ เหล็ก(II) ซัลเฟต เหล็ก(II) คลอไรด์ เหล็ก(II) ไนเตรท เหล็ก(II) อะซิทิลอะซิโท
เนท เหล็ก(II) ไพราซิเนท เหล็ก(II) พิโคลิเนท และเหล็ก(II) โบไฟริดิน ในงานนี้ได้ทำการวิเคราะห์
ตัวเร่งปฏิกิริยาโดยใช้เทคนิคหลายอย่าง ได้แก่ XRD XRF หรือ AAS FT-IR และ SEM สเปคโตรส
โกปี ตัวเร่งปฏิกิริยาเหล็กนำมารองรับบนเคลย์เพื่อใช้ศึกษาหาความสามารถในการเร่งปฏิกิริยา
ออกซิเดชันของไซโคลออกเทน ได้วิเคราะห์ไซโคลออกทานอนและไซโคลออกทานอลซึ่งเป็นผลิต
ภัณฑ์ของปฏิกิริยาด้วยเทคนิค GC พบว่า ปฏิกิริยามีความเลือกจำเพาะต่อการเกิดไซโคลออกทานอน
ศึกษาปัจจัยที่มีผลต่อการออกซิเดชันพบว่าภาวะที่เหมาะสมคือ ทำปฏิกิริยาที่อุณหภูมิ 70 องศา
เซลเซียส เป็นเวลา 24 ชั่วโมง โดยใช้เทอร์เชียรีไฮโดรเปอร์ออกไซด์ 70% ในน้ำเป็นสารออกซิไดซ์
จากการทดลองพบว่าเคลย์ ลิแกนด์ และ สารออกซิไดซ์มีผลต่อความสามารถในการเร่งปฏิกิริยา ผล
การทดลองแสดงว่าเหล็ก(III) อะซิทิลอะซิโทเนทบนตัวรองรับเบนโทไนท์ที่มีปริมาณเหล็ก 4.4%
ให้เปอร์เซ็นต์การเปลี่ยนรูปสูงที่สุดเท่ากับ 17% และเหล็กบนตัวรองรับเบนโทไนท์ให้เปอร์เซ็นต์
การเปลี่ยนรูปมากกว่าคาโอลินหรือทาลคัม ได้เสนอกลไกปฏิกิริยาออกซิเดชันของไซโคลออก
เทนด้วยเทอร์เชียรีไฮโดรเปอร์ออกไซด์เป็นแบบเรดิคัล เกิดผ่านตัวกลางอัลคิลไฮโดรเปอร์ออกไซด์
นอกจากนี้ยังพบว่าตัวเร่งปฏิกิริยาสามารถนำมาใช้ใหม่ได้

ภาควิชา.....เคมี.....ลายมือชื่อนิสิต.....
สาขาวิชา.....เคมี.....ลายมือชื่ออาจารย์ที่ปรึกษา.....
ปีการศึกษา.....2547.....

4572381523 : MAJOR CHEMISTRY

KEY WORD: OXIDATION / CYCLOOCTANE / IRON / CLAY / SUPPORT

PARICHAT DAMRONGPONG : CLAY SUPPORTED IRON COMPOUND
CATALYSTS FOR OXIDATION OF CYCLOOCTANE

THESIS ADVISOR : ASSOC. PROF. WIMONRAT TRAKARNPRUK, Ph.D.

100 pp., ISBN 974-17-6411-1.

Bentonite, kaolinite and talcum-supported iron compound catalysts were synthesized for cyclooctane oxidation by ion exchange method. Iron compounds studied were: iron (II) sulfate, iron (III) chloride, iron (III) nitrate, iron (III) acetylacetonate, iron (III) pyrazinate iron (III) picolinate and iron (III) bipyridine. The catalysts were characterized by several techniques: XRD, XRF or AAS, FT-IR and SEM. The catalytic performance of clay supported iron catalysts was studied using oxidation of cyclooctane. The products of reaction, cyclooctanol and cyclooctanone were analyzed by GC and the selectivity to cyclooctanone was observed. Parameters affecting the oxidation were studied. The optimum condition was 70°C for 24 hours with 70% TBHP in water as an oxidant. It was found that clay, the ligand and oxidant affected the catalyst activity. The results showed that bentonite supported iron (III) acetylacetonate catalyst with iron content of 4.4% gave the highest %conversion (17%). Bentonite supported iron provided higher %conversion than that on kaolinite or talcum. The mechanism of the cyclooctane oxidation with *tert*-butyl hydroperoxide was proposed to occur *via* alkyl hydroperoxide intermediate in radical pathway. In addition, the catalysts can be reused.

Department.....Chemistry.....Student's signature.....

Field of study.....Chemistry.....Advisor's signature.....

Academic year.....2004.....

ACKNOWLEDGEMENTS

The author wishes to express her deep gratitude and appreciation to Associate Professor Dr. Wimonrat Trakarnpruk, her thesis adviser for her kind assistance, generous guidance and encouragement throughout the course of this research. She would like to express the deepest gratitude to Associate Professor Dr. Sirirat Kokpol, Assistant Professor Dr. Korbratna Kriausakul and Dr. Soamwadee Chaianansutcharit who serve as committees for their valuable suggestions.

Appreciation is also expressed to Cernic International Company Limited for providing clay supports. The author would like to gratefully thank Chulalongkorn University for the invaluable knowledge, experience and support throughout her entire education. Moreover, the author also gratefully thanks the Department of Chemistry, Faculty of Science, Chulalongkorn University for granting a teaching assistant fellowship during 2003 and to the Graduate School for financial support of part of this research work.

This thesis could not have been completed without generous help of the staff members of the Organometallics Group, the Material Chemistry and Catalysis Research Unit and the Supramolecular Research Unit for their kind assistance and generosity. Special thank is forwarded to her family and her best friends for their love, understanding, encouragement, and assistance. Without them, the author would have never been able to achieve this goal.

สถาบันวิทยบริการ
จุฬาลงกรณ์มหาวิทยาลัย

CONTENTS

	Page
ABSTRACT IN THAI.....	iv
ABSTRACT IN ENGLISH.....	v
ACKNOWLEDGEMENTS.....	vi
CONTENTS.....	vii
LIST OF FIGURES.....	xii
LIST OF SCHEMES.....	xiv
LIST OF TABLES.....	xv
LIST OF ABBREVIATIONS.....	xvii
CHAPTER I INTRODUCTION.....	
1.1 Homogeneous catalysts.....	1
1.2 Heterogeneous catalysts.....	1
1.3 Oxidation of cycloalkane.....	4
1.4 Objectives of thesis.....	5
CHAPTER II THEORY.....	6
2.1 Clay.....	6
2.1.1 Tetrahedral sheets.....	6
2.1.2 Octahedral sheets.....	7
2.2 Clays structure and chemical composition.....	7
2.2.1 The 1:1 layer type.....	7
2.2.1.1 Kaolin.....	8
2.2.2 The 2:1 layer type.....	9
2.2.2.1 Talc-pyrophyllite, $x = 0$	9
2.2.2.2 Smectite $x \sim 0.2-0.6$	9
2.3 Properties of clays.....	10
2.3.1 Ion exchange.....	10
2.3.2 Swelling.....	10
2.3.3 Intercalation and cation-exchange.....	11
2.3.4 Acidity.....	11

CONTENTS (CONT.)

	Page
2.4 Oxidants.....	12
2.4.1 Air.....	12
2.4.2 Oxygen.....	12
2.4.3 Ozone.....	12
2.4.4 Hydrogen peroxide.....	13
2.4.5 <i>Tert</i> -butyl hydroperoxide.....	13
2.4.6 Peroxyacetic acid.....	14
2.4.7 Iodosobenzene.....	14
2.4.8 Potassium permanganate.....	14
 CHAPTER III LITERATURE REVIEWS.....	 16
3.1 Homogeneous iron catalyzed oxidation.....	16
3.2 Heterogeneous iron catalyzed oxidation.....	23
 CHAPTER IV EXPERIMENTAL.....	 30
4.1 Equipment.....	30
4.1.1 Schlenk line.....	30
4.1.2 Schlenk flask.....	31
4.1.3 Vacuum pump.....	31
4.1.4 Inert gas supply.....	32
4.1.5 Heating bath.....	32
4.2 Chemicals.....	32
4.3 Analytical measurements.....	34
4.3.1 Fourier transform infrared spectrometer (FT-IR).....	34
4.3.2 UV-Visible spectrophotometry (UV-vis).....	34
4.3.3 Gas chromatography (GC).....	34
4.3.4 X-ray diffractometer (XRD).....	35
4.3.5 X-ray fluorescence spectrometer (XRF).....	35
4.3.6 Atomic absorption spectrometer (AAS).....	35

CONTENTS (CONT.)

	Page
4.3.7 Scanning electron microscope (SEM).....	36
4.3.8 Nitrogen adsorption/desorption (Brunauer - Emmett-Teller method, BET).....	36
4.3.9 Furnace.....	36
4.4 Determination of cation exchange capacity.....	36
4.5 Preparation of bentonite supported iron catalysts.....	37
4.5.1 Bentonite supported iron catalysts.....	37
A. Bentonite supported iron (II) sulfate catalysts.....	37
B. Bentonite supported iron (III) chloride catalysts.....	37
C. Bentonite supported iron (III) nitrate catalysts.....	38
D. Bentonite supported iron (III) acetylacetonate catalysts.....	38
E. Bentonite supported iron (III) bipyridine catalyst.....	38
F. Bentonite supported iron (III) picolinate catalyst.....	38
G. Bentonite supported iron (III) pyrazinate catalyst.....	39
4.5.2 Kaolinite and talcum supported iron catalyst.....	39
4.5.3 Silica-supported iron catalysts.....	39
4.6 Synthesis of goethite.....	40
4.7 Preparation of iodosobenzene oxidant.....	40
4.8 Oxidation procedure for cyclooctane.....	40
A. Effect of catalyst types.....	41
B. Effect of oxidant types.....	41
C. Effect of oxidant amounts.....	41
D. Effect of solvent types.....	41
E. Effect of reaction time.....	42
4.9 Homogeneous iron complex catalysts.....	42
4.10 Test of iron leaching.....	42
4.11 Reusability of clay supported iron catalysts.....	43

CONTENTS (CONT.)

	Page
CHAPTER V RESULTS AND DISCUSSION	
5.1 Characterization of clays.....	44
5.1.1 X-ray diffraction (XRD).....	43
5.1.2 X-ray fluorescence (XRF) and atomic absorption spectrometer (AAS).....	46
5.1.3 Fourier transform infra-red spectrometer (FT-IR).....	46
5.1.4 Cation exchange capacity (CEC).....	47
5.2 Preparation and characterization of clay-supported iron catalysts	49
5.2.1 X-ray diffraction (XRD).....	49
5.2.2 X-ray fluorescence (XRF) and atomic absorption spectrometer (AAS).....	52
5.2.3 Fourier transform infra-red spectrometer (FT-IR).....	54
5.2.4 Cation exchange capacity (CEC).....	60
5.2.5 Scanning electron microscope (SEM).....	61
5.2.6 Nitrogen adsorption/desorption (Brunauer - Emmett- Teller method, BET).....	63
5.3 Preparation and characterization of goethite	64
5.4 Oxidation of cyclooctane.....	65
5.4.1 Optimization of reaction condition.....	66
A. Effect of iron amount.....	66
B. Effect of oxidant types.....	68
C. Effect of oxidant amounts.....	69
D. Effect of solvent types	70
E. Effect of reaction time.....	71
5.4.2 Bentonite supported iron compound catalysts.....	71
5.4.3 Bentonite supported iron(III) complex catalysts.....	73
5.4.4 Kaolinite and talcum supported iron catalysts.....	76
5.4.5 Silica supported iron(II) sulfate catalysts.....	76
5.4.6 Iron oxide catalysts.....	77
5.4.7 Homogeneous iron compound catalysts.....	78

CONTENTS (CONT.)

	Page
5.5 Test of leaching.....	80
5.6 Recycling of clay supported iron catalyst.....	81
5.7 Proposed mechanism.....	82
CHAPTER V CONCLUSION AND SUGGESTION.....	84
REFERENCES.....	87
APPENDIX.....	94
VITAE.....	100



สถาบันวิทยบริการ
จุฬาลงกรณ์มหาวิทยาลัย

LIST OF FIGURES

		Page
Figure 2.1	(a) A single silica tetrahedral unit (b) sheet structure of silica tetrahedra arranged in a hexagonal network.....	7
Figure 2.2	(a) A single octahedral unit (b) sheet structure of octahedral unit arranged in a hexagonal network.....	7
Figure 2.3	Structure of kaolinite.....	8
Figure 2.4	Structure of talc-pyrophyllite.....	9
Figure 3.1	Structure of [Fe(pic) ₂ py ₂] and [Fe(<i>o</i> -phenCO ₂)]......	16
Figure 3.2	Structure of [Fe ₂ (HPTB)(μ-OH)(NO ₃) ₂] ²⁻ cation.....	21
Figure 3.3	Structure of Fe(II) tetrasulfophthalocyanine (Na ₄ [FeTSPc]), Fe(II) perchlorinated phthalocyanine (FePc(Cl) ₁₆) and <i>m</i> -CPBA.....	21
Figure 3.4	Structure of the metal porphyrin.....	22
Figure 3.5	Proposed structure of the active site of Fe(NC ₃)Si-MCM-41.....	24
Figure 3.6	Geometry of (A) zeolite Y and (B) mordenite.....	25
Figure 3.7	Structures of iron porphyrins.....	25
Figure 3.8	Structures of TPP and TMPyP porphyrins.....	27
Figure 3.9	The heteropolynuclear hydrolysis of binary mixture.....	27
Figure 3.10	Gallery space and surface of the phyllosilicate (A) Sil _x and (B) Tal _x , where R is the attached organic group bound to the inorganic backbone.....	28
Figure 3.11	Structure of the iron porphyrin Na ₄ [Fe(TDFSPP)Cl].....	29
Figure 3.12	Synthesis of 3-aminopropyltriethoxysilanized kaolinite (4) and 5,10, 15,20 -tetrakis(2,6-difluoro-3-sulfonatophenyl) porphyrinato iron(III) silanized kaolinite (5).....	29
Figure 4.1	Schlenk line.....	31
Figure 4.2	Round-bottomed Schlenk flask.....	31
Figure 5.1	XRD patterns of clays (a) bentonite, (b) kaolinite and (c) talcum.....	44
Figure 5.2	FT-IR spectra of bentonite, kaolinite and talcum clay.....	47

LIST OF FIGURES (CONT.)

		Page
Figure 5.3	Calibration curve of $\text{Cu}(\text{EDA})_2^{2+}$ complex at $\lambda_{\text{max}} = 548 \text{ nm}$	48
Figure 5.4	XRD patterns of bentonite-supported iron(II) sulfate catalysts...	49
Figure 5.5	XRD patterns of bentonite-supported iron(III) compound catalysts.....	50
Figure 5.6	XRD patterns of kaolinite-supported iron(II) sulfate catalysts....	51
Figure 5.7	XRD patterns of talcum-supported iron(II) sulfate catalysts.....	52
Figure 5.8	FT-IR spectra of bentonite-supported FeSO_4 , FeCl_3 and $\text{Fe}(\text{NO}_3)_3$ catalysts.....	55
Figure 5.9	FT-IR spectra of uncalcined and calcined Ben/ $\text{Fe}(\text{acac})_3$ catalysts.....	56
Figure 5.10	FT-IR spectra of bentonite-supported $\text{Fe}(\text{bpy})_2\text{Cl}_3$, $\text{Fe}(\text{pyrazinate})_2\text{Cl}_3$ and $\text{Fe}(\text{picolinate})_2\text{Cl}_3$ catalysts.....	57
Figure 5.11	FT-IR spectra of kaolinite and Kao/ FeSO_4 catalysts	58
Figure 5.12	FT-IR spectra of talcum, mTal and Talc/ FeSO_4 catalysts.....	59
Figure 5.13	SEM photographs of the bentonite supported iron catalysts.....	62
Figure 5.14	Iron distributions on surface of the bentonite supported iron catalysts.....	63
Figure 5.15	XRD pattern of goethite.....	64
Figure 5.16	FT-IR spectrum of goethite.....	65
Figure 5.17	Structures of (a) $\text{Fe}(\text{picolinate})_2^{3+}$ and (b) $\text{Fe}(\text{pyrazinate})_2^{3+}$	80
Figure 5.18	XRD pattern of calcined Ben/ FeSO_4 catalyst after reusing.....	82

LIST OF SCHEMES

	Page
Scheme 3.1 Mechanism of two-substrate competitive reaction.....	20
Scheme 3.2 Proposed mechanism in oxidation of hydrocarbons with metalloporphyrins.....	22



สถาบันวิทยบริการ
จุฬาลงกรณ์มหาวิทยาลัย

LIST OF TABLES

		Page
Table 1.1	Comparison of homogeneous and heterogeneous catalysts.....	2
Table 4.1	Chemicals and suppliers.....	32
Table 5.1	The iron content in the raw clay using XRF and AAS techniques.....	46
Table 5.2	The assignment for the FT-IR spectra of clays.....	47
Table 5.3	UV-Vis data of $\text{Cu}(\text{EDA})_2^{2+}$ complex at $\lambda_{\text{max}} = 548 \text{ nm}$	48
Table 5.4	Cation exchange capacity of clays.....	48
Table 5.5	The iron content in the clay-supported iron catalysts using XRF and AAS.....	53
Table 5.6	The assignment for the FT-IR spectra of bentonite-supported iron(II) sulfate catalysts	54
Table 5.7	The assignment for the FT-IR spectra of bentonite-supported iron compound catalysts	55
Table 5.8	The assignment for the FT-IR spectra of bentonite-supported iron(III) acetylacetonate catalysts	56
Table 5.9	The assignment for the FT-IR spectra of bentonite-supported iron(III) complex catalysts	57
Table 5.10	The assignment for the FT-IR spectra of kaolinite and Kao/ FeSO_4	58
Table 5.11	The assignment for the FT-IR spectra of talcum, mTalc and Talc/ FeSO_4	59
Table 5.12	Cation exchange capacity of catalysts.....	60
Table 5.13	BET specific surface area of Ben/ $\text{Fe}(\text{acac})_3$ catalysts.....	64
Table 5.14	XRD data of goethite.....	65
Table 5.15	Oxidation of cyclooctane using iron(II)sulfate supported on bentonite catalysts.....	66
Table 5.16	Effect of oxidants for cyclooctane oxidation using calcined Ben/ FeSO_4 catalyst.....	68
Table 5.17	Oxidation of cyclooctane using calcined Ben/ FeSO_4 catalyst.....	69

LIST OF TABLES (CONT.)

		Page
Table 5.18	Effect of type of solvents for cyclooctane oxidation using calcined Ben/FeSO ₄ catalyst.....	70
Table 5.19	Effect of time for cyclooctane oxidation using calcined Ben/FeSO ₄ catalyst.....	71
Table 5.20	Oxidation of cyclooctane using iron(III)chloride supported on bentonite catalysts.....	72
Table 5.21	Results from different types of iron catalysts.....	72
Table 5.22	Oxidation of cyclooctane using bentonite-supported iron(III) acetylacetonate catalyst.....	73
Table 5.23	Oxidation of cyclooctane using Ben/Fe(acac) ₃ catalyst.....	74
Table 5.24	Oxidation of cyclooctane using bentonite-supported iron(III) complexes catalyst.....	75
Table 5.25	Oxidation of cyclooctane using kaolinite- and talc-supported iron catalyst.....	76
Table 5.26	Oxidation of cyclooctane using silica-supported iron(II) catalysts.....	77
Table 5.27	Oxidation of cyclooctane using iron oxides catalyst.....	77
Table 5.28	Cyclooctane oxidation using homogeneous iron catalysts.....	78
Table 5.29	Effect of oxidants for cyclooctane oxidation using iron(III) complex catalysts.....	79
Table 5.30	Amount of iron leached from calcined Ben/FeSO ₄ catalyst.....	81
Table 5.31	Oxidation of cyclooctane using recycled calcined Ben/FeSO ₄ catalyst.....	81
Table 5.32	Cyclooctane oxidation using Ben/FeSO ₄ catalysts.....	82

LIST OF ABBREVIATIONS

AAS	=	Atomic absorption spectroscopy
acac	=	Acetylacetonate
Ben	=	Bentonite
BET	=	Brunauer-Emmett-Teller method
bpy	=	Bipyridine
°C	=	Degree Celsius
CEC	=	Cation exchange capacity
cm ⁻¹	=	Unit of wave number
EDX	=	Energy dispersive x-ray
FT-IR	=	Fourier transform infra-red
GC	=	Gas chromatography
Kao	=	Kaolinite
m.p.	=	Melting point
Nd	=	Not determined
PhIO	=	Iodosobenzene
SEM	=	Scanning Electron Microscope
Talc	=	Talcum
TBHP	=	<i>Tert</i> -butyl hydroperoxide
UV-Vis	=	UV-visible spectrometer
XRD	=	X-ray diffraction
XRF	=	X-ray fluorescence

CHAPTER I

INTRODUCTION

Catalysts are used in 80% of all current industrial chemical processes. A catalytic process provides reduced capital costs, improved chemical and energy efficiency, reduces the environmental impact and allows more rapid product development.

1.1 Homogeneous catalysts

The catalyst is in the same phase as the reactants, which provides a good contact with reactants so a more effective concentration can be achieved. The disadvantage of this type of catalyst is separation which usually involves distillation. In some cases this makes catalyst recovery difficult because the high temperature can destroy the catalyst, and aggregation of catalyst to form dimer or multi-nuclear cluster, leading to the loss of catalytic activity.¹

1.2 Heterogeneous catalysts

The catalyst is in a different phase from the reactants. Reactants might be gas or liquid and the catalyst is a solid. Separating and recycling of the catalyst are facile. The solid catalysts are generally easier and safer to handle than liquid or gaseous ones. Good dispersion of active sites can lead to significant improvements in reactivity. However, the reaction rate is generally slow because reaction occurs only on the exposed active surface and often requires vigorous condition.

Table 1.1 Comparison of homogeneous and heterogeneous catalysts ²

	Homogeneous	Heterogeneous
Active centers	all metal atoms	only surface atoms
Concentration	low	high
Selectivity	high	lower
Diffusion problems	practically absent	present
Reaction condition	mild (50-200°C)	severe (often > 250°C)
Application	limited	wide
Activity loss	irreversible reaction with products (cluster formation); poisoning	sintering of the metal crystallites; poisoning
Catalyst properties		
Structure/stoichiometry	defined	undefined
Modification possibilities	high	low
Thermal stability	low	high
Catalyst separation	sometimes laborious (chemical decomposition, distillation, extraction)	fixed-bed: unnecessary suspension: filtration
Catalyst recycling	possible	unnecessary
Cost of catalyst losses	high	low

Immobilized metal catalysts in solid supports are desirable for stabilizing the compounds against deactivating dimerization and other destructive processes under oxidizing condition. The activity of these systems is mainly based on the correct choice of the solvent, which determines the polarity of the medium and the size of the substrate that needs to be adsorbed at the catalytic surface.³

The solid support usually contains a pore network with pores ranging from micro (< 20 Å) to macro pores, approaching micron dimensions. The location of the catalytically active component within the porous structure is difficult to ascertain. The manner in which pores interconnect may in turn have an effect on the accessibility of reactants to the catalytically active site, and to the removal of products.

As much research work and care is involved in developing appropriate supports as in developing the catalyst itself, a catalyst support should allow the catalyst to be highly dispersed on the surface of the support. The support needs to be stable under reaction conditions, and under the conditions needed for regeneration. It must not be affected by any solvents used or by the reactants or products. Some of the supports used are silica, alumina, zeolites, porous vycor glass and clays.

Zeolites are microporous crystalline aluminosilicates frequently employed in supported catalysts. They have a rigid, 3-dimensional crystalline structure consisting of a network of interconnected tunnels and cages. They have a pore with a fixed dimension and volume. The fixed pore dimensions allow zeolites to use for specific applications. Zeolites are useful for selective catalysis because of their uniform pore volume distribution. The intrinsic pore volumes can control the selectivity of a catalytic reaction through transport or diffusional limitations, and product trapping. The transport restrictions are dependent on the pore dimensions and molecule size. The disadvantage of zeolites is that the pore-blocking can occur.

Silica is used as supports for catalyst systems. It has an amorphous structure. It is porous and consists of siloxane and silanol groups. It was used to catalyze the cracking of hydrocarbons. This form of cracking is where the large molecules in oil are converted into small, highly volatile molecules. However because the size of the pores of silica was so variable (ranging from 0.1 nm to 50 nm) and the fact that their shape was so alterable, they were hardly ideal catalysts. Due to the large size of their cavities, large products were able to form in the cavities thus lowering the reactivity.

Clays have layer crystalline structure and are subjected to shrinking and swelling as water is absorbed and removed between the layers. They are used in organic syntheses such as alkane oxidation. Clays have been chosen as the catalytic support because of their attractive advantages as follows:⁴

1. High surface area
2. Ease of handling and use
3. Non-corrosive
4. Low cost
5. Ease of regeneration

1.3 Oxidation of cycloalkane

Oxidations of cycloalkanes are important reaction in industry, for example product of cyclohexane oxidation is cyclohexanone and cyclohexanol. Both products show the important role as intermediates for the conversion into adipic acid and caprolactam and hence to nylon, which has enormous commercial applications.⁵

Adipic acid is a very important chemical that is used all over the world to produce various products: nylon 6,6, foams, paints and tires. It is also used as a food ingredient in gelatins, desserts and other foods. Nylon and nylon 6,6 are used for everyday applications such as electrical connectors, cable tires, fishing line, fabrics, carpeting, and many other useful products. Using different reactions can also produce adipic acid. One industry reaction is by the hydrogenation of benzene into cyclohexane and then oxidation. Adipic acid can also be produced from butadiene by carboalkoxylation, but this process is not commercialized.⁶

Industrial oxidation of cyclohexane proceeded under vigorous conditions, for example at 140-165 °C and 10 atm using soluble cobalt(II) catalyst.⁷ The reaction gave less than 5% conversion. Sometimes boric acid is added to stabilize the oxidation mixture. The reaction is unselective, many products are invariably produced, such as succinic, glutaric and carproic acid because the products are more reactive than cyclohexane.⁸

Cyclododecane is oxidized with air to a mixture of cyclododecanone and cyclododecanol by using boric acid catalyst at 150-160°C and atmospheric pressure. With a 25-30% conversion, the selectivity to alcohol/ketone mixture reaches an optimum of 80-82% and ratio of 8:1 to 10:1. These products are intermediates in the production of polyamides for several special applications and they are also precursors for lauryl lactam.⁹

In this research, cyclooctane was selected to be a model substrate for oxidation reaction. The clay-supported iron catalysts were synthesized and characterized. The

conditions for oxidation of cyclooctane by the catalysts were investigated: oxidant types, catalyst types, oxidant amounts, solvent types and reaction time.

1.4 Objectives of the thesis

1. To synthesize and characterize clay-supported iron catalysts.
2. To study parameters affecting the oxidation of cyclooctane using the synthesized catalysts.
3. To test the capability of reused clay supported iron catalysts.
4. To test catalyst leaching.



สถาบันวิทยบริการ
จุฬาลงกรณ์มหาวิทยาลัย

CHAPTER II

THEORY

2.1 Clay

Clay minerals are hydrous aluminum silicates and are classified as phyllosilicates, or layer silicates. There is a considerable variation in chemical and physical properties. They have long been recognized as efficient materials for promotion of many organic reactions. Because of their small size, clay minerals have large specific surface areas (surface area per unit mass). Most chemical and physical reactions and interactions occur on the surfaces of clay particles. Therefore, whether chemical or physical phenomena are considered, the small clay particles with their large specific surface area are most important in determining the fundamental properties of clay.

All layer silicates can be imagined as constructed from two modular units: a sheet of corner-linked tetrahedra and a sheet of edge-linked octahedral. Phyllosilicate minerals have layer structures composed of shared octahedral and tetrahedral sheets. The silicon tetrahedral sheets and aluminum octahedral sheets are held together by sharing apical oxygen.

2.1.1 Tetrahedral sheets

Tetrahedral sheets, $\text{Si}_2\text{O}_5^{-2}$ are composed of individual tetrahedrons, which share every three out of four oxygens. They are arranged in a hexagonal pattern with the basal oxygens linked and the apical oxygens pointing up/down.

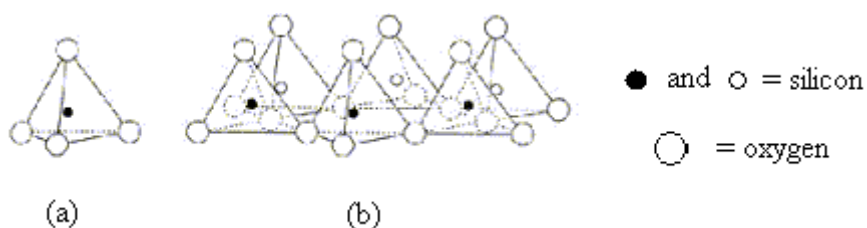


Figure 2.1 (a) A single silica tetrahedral unit (b) sheet structure of silica tetrahedra arranged in a hexagonal network.

2.1.2 Octahedral sheets

Octahedral sheets, $\text{Al}(\text{OH})_6^{-3}$ are composed of individual octahedrons that share edges composed of oxygen and hydroxyl anion groups with Al, Mg, Fe^{3+} and Fe^{2+} typically serving as the coordinating cation. These octahedrons are arranged in a hexagonal pattern.



Figure 2.2 (a) A single octahedral unit (b) sheet structure of octahedral unit arranged in a hexagonal network.

2.2 Clays structure and chemical composition

Based on their structures and chemical compositions, the clay minerals can be divided into many classes.¹⁰

2.2.1 The 1:1 layer type

The tetrahedral cation sites in the 1:1 layer type usually are all occupied by Si^{4+} and the octahedral sites by all Al^{3+} or all Mg^{2+} , this layer type usually has no

layer charge or a very small layer charge. If there is substitution in one sheet of a 1:1 layer type silicate, there often is a compensating substitution in the other sheet so that neutrality is maintained.

2.2.1.1 Kaolin

The kaolin has one layer of tetrahedral sheet and one layer of octahedral sheet in 1:1 structure. The layers are electronically neutral. The bonding between layers is by weak van der Waals bonds. Kaolinite is the most common of this group and has the chemical formula $\text{Al}_2\text{Si}_2\text{O}_5(\text{OH})_4$. In nature, kaolinite has a small net negative charge because the clay crystals have broken edges. The unit layer is about 7 Å thick, which gives rise to a characteristic X-ray diffraction peak corresponding to about 7 Å.

Four names for clay materials are associated with kaolinite: ballclay, fireclay, flintclay, and underclay. Kaolinite is formed by hydrothermal alteration of aluminosilicate minerals. It does not absorb water, does not expand when it comes in contact with water. But treatment with some organic chemicals, for example, formamide or dimethylsulfoxide, will open up kaolinite, or causes it to swell.

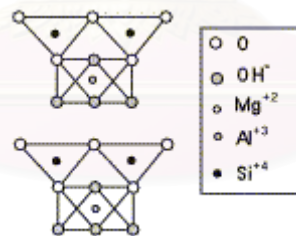


Figure 2.3 Structure of kaolinite.

2.2.2 The 2:1 layer type

They are all based on structure consisting of two tetrahedral sheets with one octahedral sheet between.

2.2.2.1 Talc-pyrophyllite, $x = 0$ (x refers to the amount of layer charge per formula unit)

Talc and pyrophyllite have the chemical formula $Mg_3Si_4O_{10}(OH)_2$ and $Al_2Si_4O_{10}(OH)_2$, respectively. They are the simplest end members of the group. The minerals of these 2:1 layer types without layer charge are important because they serve as prototypes for the discussion of the structure of other clay minerals that have a layer charge. Ideally, talc-pyrophyllite group has no tetrahedral or octahedral substitution, no layer charge, and no interlayer material. Natural materials often have small amount of substitution, which gives a small amount of ionic attraction between layers that supplements van der Waals bonding, the main force that holds these layers together.

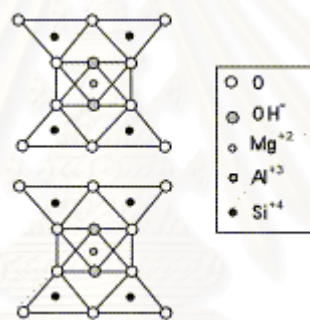


Figure 2.4 Structure of talc-pyrophyllite.

2.2.2.2 Smectite, $x \sim 0.2-0.6$

The smectite group of clays has a 2:1 layer type that is similar to that of pyrophyllite, but can also have significant amounts of Mg and Fe substituting into the octahedral sheets. These isomorphous substitutions lead to net negative charges on the clay structure, which must be satisfied by the presence of charge-balancing cations somewhere else in the structure. The interlayer is hydrated, which allows cations to move freely in and out of the structure. Because the interlayer is open and hydrated, cations may be present within the interlayer to balance negative charges on the sheets themselves. The most important aspect of the smectite group is the ability for water molecules to be absorbed between the layers, causing the volume of the minerals to

increase when they come in contact with water. Thus, the smectites are expanding clays. The basal spacing expands to 10-20 Å. The most common smectite is, with a general chemical formula of montmorillonite is $(\frac{1}{2}\text{Ca,Na})(\text{Al,Mg,Fe})_4(\text{Si,Al})_8\text{O}_{20}(\text{OH})_4 \cdot n\text{H}_2\text{O}$. Montmorillonite is the main constituent of bentonite, derived by weathering of volcanic ash. Montmorillonite can expand by several times its original volume when it comes in contact with water.

2.3 Properties of clay ¹¹

2.3.1 Ion exchange

Isomorphous substitution of cations in the lattice by lower valent ions, such as the substitution of aluminum for silicon, magnesium and/or ferrous ion for aluminum or sometimes lithium for magnesium, leaves a residual negative charge in the lattice that is balanced by other cations. These can be readily replaced by other cations when brought into contact with these ions in aqueous solution.

2.3.2 Swelling

Many clay minerals absorb water between their layers, which move apart and the clay swells. For efficient swelling, the energy released by cations and/or layer solvation must be sufficient to overcome the attractive forces (such as hydrogen bonding) between the adjacent layers. In 1:1 clay minerals (kaolinite), water forms strong hydrogen bonds with hydroxyl groups on hydrophilic octahedral layers, allowing swelling to occur.

With 2:1 clay minerals, the ability to swell depends on the solvation of interlayer cation and layer charge. Clays with 2:1 structures and low layer charge (e.g. talc and pyrophyllite) have very low concentration of interlayer cations and therefore do not swell readily. At the other extreme, those with very high layer charges (e.g. mica) have strong electrostatic forces holding alternate anionic layers and the interlayer cations together, thus preventing swelling. Those with univalent interlayer cations swell most readily and with divalent, trivalent and polyvalent cations, swelling

decreases accordingly. The extent of swelling can be observed by measuring interlayer separations using powder X-ray diffraction.

2.3.3 Intercalation and cation-exchange

In swelling clay mineral, such as, smectites, the interlayer cations can undergo exchange with cations from external solutions. The concentration of exchangeable cations is called CEC, usually measured in milliequivalents per 100 g of dried clay. Since smectites have the highest concentration of interlayer cations, they have the highest cation exchange capacities (typically 70-120 mequiv. /100 g). Structural defects at layer edges give rise to additional CEC and a small amount of anion exchange capacity.

Several methods to determine the CEC have been developed. In the early days determination of CEC was performed by saturating the clay with one cation, then washing out excess salt and finally replacing the cation by several exchange/washing cycles with another cation. The collected solutions were employed for the determination of the amount of the replaced cation. Another method was developed by saturating the clay with NH_4^+ ions. The amount of ammonium ions adsorbed was determined. Further methods were proposed by using cationic surfactants. The general problem when using surfactants is that an excess will adsorb on the clay, requiring determination of the point when the equivalent amount is adsorbed. Finally, metal-organic complexes are employed as exchange cations. The affinity of the clay minerals towards this type of cation is high, so that complete exchange can be achieved in one single treatment step. An excess of the complex is added to the clay dispersion and one has only to determine the remaining concentration after the exchange reaction. Cobalt hexaamine, silver thiourea, copper bisethylenediamine or copper triethylenetetramine can be used for this purpose.¹²

2.3.4 Acidity

The interlayer cations contribute to the acidity of clay minerals. Some of these cations may be protons or polarizing cations (e.g. Al^{3+}) which give rise to strong Brønsted acidity. The higher electronegativity of M^+ , the stronger are the acidic

sites generated. Brönsted acidity also stems from the terminal hydroxyl groups and from the bridging oxygen atoms.

In addition, clay minerals have layer surface and edge defects, which would result in weaker Brönsted and/or Lewis acidity, generally at low concentrations. The Hammett scale usually expresses the acid strength. On this scale, the acidity of clay minerals can be comparable to the concentrated sulfuric acid. The surface acidity of natural clays with Na^+ or NH_4^+ as interstitial cations ranges from +1.5 to -3. Washing of the clay with mineral acid, such as HCl, brings down the Hammett (H_0) function from -6 to -8, which is between conc. HNO_3 (-5) and H_2SO_4 (-12).

2.4 Oxidants¹³

2.4.1 Air

Air is the cheapest oxidant is used only rarely without irradiation and without catalyst. Examples of oxidations by air alone are the conversion of aldehydes into carboxylic acids (autoxidation) and the oxidation of acylloins to α -diketones. Usually, exposures to light, irradiation with ultraviolet light, or catalysts are needed.

2.4.2 Oxygen, O_2

Oxygen exists in two states. Stable ground-state oxygen (triplet oxygen) has two odd electrons with parallel spins. It behaves like a diradical and is paramagnetic. In excited-state oxygen (singlet oxygen), the two odd electrons possess antiparallel spins. Such a molecule is unstable, with a half-life of 10^{-6} s, and is diamagnetic. Each form reacts differently with organic molecules.

2.4.3 Ozone, O_3

A blue gas or dark blue liquid (*bp.* -106-116, or -125 °C), depending on the source of data), is used in a mixture with oxygen. Passing ozone-containing oxygen through solutions of organic compounds in solvents carries to ozonations. Cooling with dry-ice-acetone bath (-78 °C) is frequently needed to prevent the decomposition

of ozonides, some of which is unstable at room temperature. The most common solvents are pentane, cyclohexane, dichloromethane, chloroform, methanol, acetic acid, and acetate.

2.4.4 Hydrogen peroxide, H_2O_2

Hydrogen peroxide is an effective oxidant that could be used in many industrial processes. Because the only by-product of oxidation using hydrogen peroxide is water, it could become the ultimate green chemical for the manufacture of many oxygenated petrochemicals. However, the current method for producing is inefficient and too costly. It is commercially available in aqueous solutions of 30% or 90% concentration. The 30% hydrogen peroxide is a colorless liquid (d 1.110) and it is stabilized against decomposition, which occurs in the presence of traces of iron, copper, aluminum, platinum, and other transition metals. The 30% hydrogen peroxide does not mix with nonpolar organic compounds. The 90% hydrogen peroxide is stable at 30°C (the decomposition rate is 1%/year), it decomposed slowly at high temperatures and rapidly with boiling at 140°C. The pure hydrogen peroxide solution is stable with weak decomposition. However, when it comes in contact with heavy metals or various organic compounds, or mixes with impurities, it produces oxygen gas and decomposition heat. When formic or acetic acid is used, the reacting species is the corresponding peroxy acid. Under such conditions, the products of oxidation by hydrogen peroxide resemble those obtained with peroxy acid.

2.4.5 *Tert*-butyl hydroperoxide, $(\text{CH}_3)_3\text{COOH}$

Tert-butyl hydroperoxide is commercially available as a 70% or 90% solution containing water and *tert*-butyl alcohol. It must be handled with extreme care, because it may decompose violently in present of strong acid and some transition metals, especially manganese, iron, and cobalt. Oxidation with *tert*-butyl hydroperoxide consists of epoxidation of alkene in the presence of transition metals. In this way, α,β -unsaturated aldehyde and ketone are selectively oxidized to epoxide without the involvement of the carbonyl function. Other applications of *tert*-butyl hydroperoxide are the oxidation of lactam to imide, of tertiary amine to amine oxide, and of phosphite to phosphate. In the presence of a chiral compound, enantioselective

epoxidation of alcohol is successfully accomplished with mordenite to high enantiomeric excesses.

2.4.6 Peroxyacetic acid (peracetic acid), $\text{CH}_3\text{CO}_3\text{H}$

Peroxyacetic acid is slightly yellow liquid, easy to volatile and easily soluble in water, ethanol and ethyl ether. It is unstable and easy to decompose. It is mainly used as disinfectant and germicide in workshop, pharmaceutical room, drinking water, environment, medical treatment and sanitation and as oxidant in organic synthesis. It can be formed *in situ* from 30% or 90% hydrogen peroxide, usually in the presence of catalytic amounts of sulfuric or perchloric acid and sometimes also in the presence of acetic anhydride. The reaction of hydrogen peroxide with acetic acid to form peroxyacetic acid is reversible. The presence of substrate to be oxidized drives the oxidation to completion at moderate temperatures (25-70 °C). External cooling is frequently necessary because the reaction is strongly exothermic.

The most important applications of peroxyacetic acid are the epoxidation and *anti* hydroxylation of double bonds. Occasionally, it is used for the dehydrogenation, oxidation of aromatic compounds and oxidation of alcohol to ketone. The last reaction is catalyzed by chromium trioxide. The role of peroxyacetic acid is to reoxidize the trivalent chromium.

2.4.7 Iodosobenzene, $\text{C}_6\text{H}_5\text{IO}$

Iodosobenzene is prepared by way of iodobenzene diacetate. It is used for conversion of acetylene into α -dicarbonyl compound, of alcohol to aldehyde or ketone, of aldehyde into acid. Similar reactions can be accomplished by *p*-iodosotoluene or *o*-iodosobenzoic acid.

2.4.8 Potassium permanganate, KMnO_4

Potassium permanganate is dark-purple crystals with a metallic luster (d 2.7, solubility 6.6% in cold water and 22% in boiling water), soluble in acetone without

reacting with the solvent. It is applied most frequently in aqueous solution but can be used in the presence of organic solvents such as petroleum ether, benzene, dichloromethane, *tert*-butyl alcohol, acetone, acetic acid, acetic anhydride, and pyridine. Oxidation in organic solvent can also be carried out with potassium permanganate adsorbed on molecular sieve, bentonite, montmorillonite, or copper sulfate pentahydrate.

Potassium permanganate furnishes three oxidation equivalents per mole (three oxygens per two mols). Its reduction to manganese dioxide liberates potassium hydroxide. Therefore, most oxidation with potassium permanganate takes place in alkaline medium. Some oxidations occur at/or require lower pH, which can be attained by using buffer such as carbon dioxide, sodium bicarbonate, or sulfuric acid.

The performance of oxidation by potassium permanganate can be depending on concentration of the oxidation system and temperature. Usually, a slight excess of the reagent over the stoichiometric amount required. Adding methanol or ethanol to the mixture destroys an excess of potassium permanganate. This reagent is used to oxidize alkene to α -diketone, cleaves double bond to form carbonyl compound or carboxylic acid, and converts acetylenes into dicarbonyl compound or carboxylic acid.

สถาบันวิทยบริการ
จุฬาลงกรณ์มหาวิทยาลัย

CHAPTER III

LITERATURE REVIEWS

3.1 Homogeneous iron catalyzed oxidation

In 1990, Sheu, *et. al.*¹⁴ studied oxidation of alkanes and alkene in the presence of hydrogen peroxide using bis(picolinato)iron(II), (2,6-dicarboxylatopyridine)iron(II) and their μ -oxo dimers as catalysts ($\text{Fe}(\text{PA})_2$, $\text{Fe}(\text{DPA})$, $(\text{PA})_2\text{FeOFe}(\text{PA})_2$ and $(\text{DPA})\text{FeOFe}(\text{DPA})$, respectively). The reactions were employed in pyridine/acetic acid solvent. The presence of substantial amounts of water reduced the reaction efficiency but did not reduce the selectivity for ketone. The use of acetonitrile in place of the pyridine/acetic acid solvent system greatly reduced the efficiency and eliminates any selectivity. It was found that the $\text{Fe}(\text{PA})_2$ complex was the best catalyst (72% cyclohexane conversion at 22°C, 4 hours).

In 1990, Balavoine, *et. al.*¹⁵ reported selective oxidation of saturated hydrocarbons into ketones using ferrous picolinate (or 1,10-phenanthroline-2-carboxylate) catalyst with hydrogen peroxide in pyridine solution. When catalytic amount of catalyst was used, strong acid such as acetic acid was necessary for the reaction. The cyclic voltammetry results demonstrated that iron(II) was preferentially coordinated with picolinate or 1,10-phenanthroline-2-carboxylate more than other carboxylic acid ligands. These complexes gave high selectivity in the oxidation (ketone: alcohol = 9.6 and 27.6, respectively). The most efficient catalysts were $[\text{Fe}(\text{pic})_2\text{py}_2]$ and $[\text{Fe}(\text{o-phenCO}_2)]$. Electrochemical study showed that hydrogen peroxide oxidized Fe(II) into Fe(III)-OH.

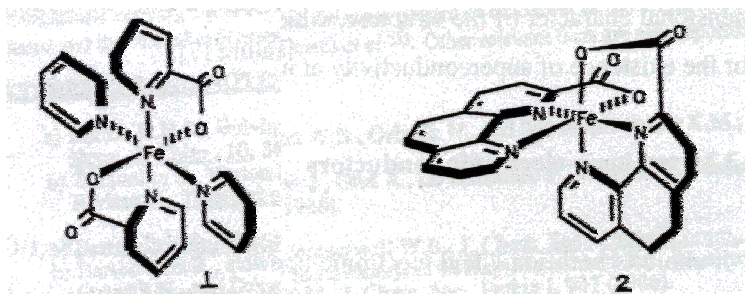


Figure 3.1 Structure of $[\text{Fe}(\text{pic})_2\text{py}_2]$ and $[\text{Fe}(\text{o-phenCO}_2)]$.

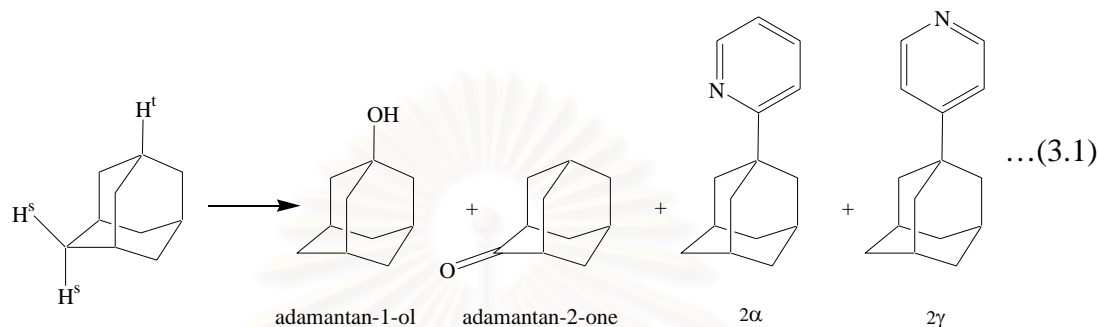
In 1992, Barton, *et. al.*¹⁶ reported oxidation of saturated alkane using iron(III) and Cu(II) as catalysts. The GoChAgg system, employing a Cu(II) catalyst and hydrogen peroxide in pyridine/acetic acid, showed similar result with iron(III) catalyzed process (GoAgg^{II}). The alkyl hydroperoxide intermediates in the GoChAgg system was proved and the reactions follow the pathway alkane → intermediate → alkyl hydroperoxide → alcohol or ketone. The relative reactivity of GoChAgg system was studied for a series of cycloalkanes. The chemical properties of Cu-intermediate and the Fe-intermediate were different. Thus, it can be deduced that the reactivity depended on metal and involved two chemically different non-radical species.

In 1993, Randolph *et. al.*¹⁷ reported oxidation of cyclohexane using (μ -oxo)diferric complex catalyst with *tert*-butyl hydroperoxide. The reactions were carried out in acetonitrile under ambient temperature and pressure under an argon atmosphere. Products of oxidation were cyclohexanol, cyclohexanone, and (*tert*-butylperoxy)cyclohexane. $[\text{Fe}_2(\text{TPA})_2\text{O}(\text{OAc})](\text{ClO}_4)_3$ (TPA = tris(2-pyridylmethyl) amine, OAc = acetate) was an efficient catalyst. It was characterized to have a (μ -oxo)(μ -carboxylato)diferric core. TPA ligands coordinated with two iron centers differ in their binding modes, with the tertiary amine on one iron center trans to the oxo bridge and one of the pendant pyridines on the other iron center trans to the oxo bridge. Stability of the catalyst was investigated after the reaction. Type of products depended on the solvents and the nature of the tripodal ligands. Addition of dimethyl sulfide (to trap two-electron oxidants) inhibited (*tert*-butylperoxy) cyclohexane formation.

In 1996, Snelgrove, *et. al.*¹⁸ studied the selected alkyl hydroperoxides as mechanistic probes for oxidation of cyclooctane using *tert*-alkyl hydroperoxides. It was found that the products were formed by alkoxy radical-induced reactions. The GoAgg^V condition involves free-radicals and Fe(III)/Fe(IV) couple, not a radical-free Fe(III)/Fe(V) couple.

In 1996, Perkins¹⁹ studied mechanism of alkane oxidation using an oxygen source or oxidizing agent and source of ferric iron catalyst. In case of adamantane, the results demonstrated secondary position was more reactive to oxidation than tertiary

position (*ca.* 7:1). The secondary position was predominantly oxidized to ketone. The tertiary position occurred hydroxylation and adamantylation of pyridine solvent (to give 2α and 2γ in Equation 3.1). The difference could be explained that the tertiary alkyl-to-iron bond is weak, dissociated into radical. Secondary alkyl-to-iron bond is so strong that it was negligibly dissociated.



In 1997, Chavasiri, *et. al.*²⁰ reported the effect of 1,3-dicarbonyl ligands on alkane oxidation in Gif-type system. The ligand coordinated around iron was found to control the outcome of the reaction. Rate of the oxidation reaction depended on the ratio of iron(III) to 1,3-dicarbonyl compound and type of ligand. The electron releasing group of 1,3-dicarbonyl ligands could enhance the rate of oxidation. The suitable ratio of iron(III) to 1,3-dicarbonyl compounds was 1:3.

In 1998, Schuchardt, *et. al.*²¹ reported oxidation of cyclohexane using soluble iron and copper such as $\text{Fe}(\text{tma})_3$ (tris(trimethylacetate)iron(III)), $\text{Cu}(\text{tma})_2$ (bis(trimethylacetate)copper(II)), $\text{Fe}(\text{fod})_3$ (tris(1,1,1,2,2,3,3-heptafluoro 7,7-dimethyl-4,6-octanodionate)iron(III)) and $[\text{Cu}(\text{en})_2](\text{NO}_3)_2 \cdot 2\text{H}_2\text{O}$ ([bis(ethylenediamine) copper(II)] nitrate dihydrate) as catalysts with *tert*-butyl hydroperoxide. The selective product was cyclohexanol. The copper catalysts were more efficient and selective under 25 bar of oxygen at 70°C for 24 hours (5% conversion and 97% selectivity). The iron catalysts were deactivated by over-oxidation of cyclohexane to adipic acid which complexed the active center.

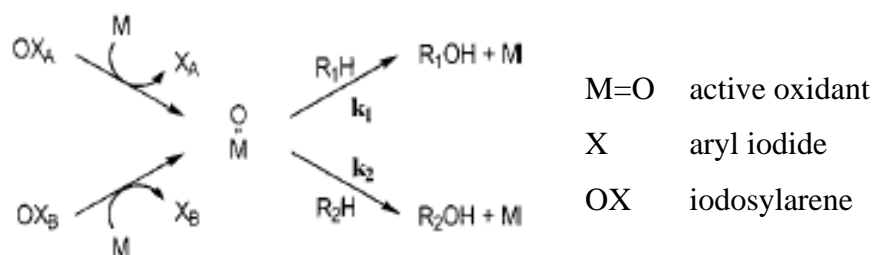
In 1998, Barton, *et. al.*²² reported co-oxidation of cyclohexane with aromatic derivatives using hydrogen peroxide as oxidant with iron(III) picolinate catalyst. Reaction was performed in mixed solvent of pyridine and acetonitrile. By variation of amounts of cyclohexane and the aromatic derivatives, the results showed that

cyclohexane was about 10 times more reactive than the aromatic. Furthermore by variation of the degree of hindrance of the aromatic, the results showed effect of size of iron species or electrophilic reagent.

In 1999, Mizuno, *et. al.*²³ reported the oxidation of cyclohexane, cyclohexene, and *trans*-stilbene using iron substituted silicotungstates as catalysts with hydrogen peroxide oxidant. The reactions were carried out in acetonitrile under argon. The results showed $\gamma\text{-SiW}_{10}[\text{Fe}(\text{OH})_2]_2\text{O}_{38}^{6-}$ gave the best catalytic activity (25.3 % conversion and turnover = 53). The activity of catalysts decreased in the following order: $\gamma\text{-SiW}_{10}[\text{Fe}(\text{OH})_2]_2\text{O}_{38}^{6-} > \alpha\text{-SiW}_{11}\text{Fe}(\text{OH})_2\text{O}_{39}^{5-} > \alpha\text{-SiW}_9[\text{Fe}(\text{OH})_2]_3\text{O}_{37}^{7-} > \alpha\text{-SiW}_{12}\text{O}_{40}^{4-}$. The efficiency of catalysts depended on structure of catalysts. *Di*-iron substituted silicotungstate, $\gamma\text{-SiW}_{10}[\text{Fe}(\text{OH})_2]_2\text{O}_{38}^{6-}$ showed higher catalytic performance than *non*-, *mono*-, and *tri*-iron substituted silicotungstates.

In 1999, Simões, *et. al.*²⁴ reported the oxidation of cyclohexane in the presence of catalytic amount of the Keggin-type heterotungstates $[\text{PW}_{11}\text{O}_{39}]^{7-}$ and $[\text{PW}_{11}\text{M}(\text{L})\text{O}_{39}]^{(7-m)-}$ (M^{m+} = first row transition metal cation, L = H₂O or CH₃CN). Reactions were carried out in acetonitrile using tetra n-butylammonium salts as catalysts and hydrogen peroxide as oxidant. Products were cyclohexanol, cyclohexanone, and cyclohexyl hydroperoxide. When the reaction was left for long time under reflux, higher conversion was observed, but selectivity was lost. The results showed that $[\text{PW}_{11}\text{O}_{39}]^{7-}$ and $[\text{PW}_{11}\text{Fe}(\text{H}_2\text{O})\text{O}_{39}]^{4-}$ gave high catalytic activity.

In 2000, Collman, *et. al.*²⁵ reported competitive oxidations of alkane substrates using Fe(TP_{F5}P)Cl ([5,10,15,20-tetrakis-(pentafluorophenyl)porphyrinato] iron(III) chloride) with various iodosylarenes (iodosobenzene, pentafluoriodosobenzene, or iodosobenzene diacetate) as the oxygen source. The product was alcohol and byproduct was aryl iodide. The proposed mechanism was shown in [Scheme 3.1](#).



Scheme 3.1 Mechanism of two-substrate competitive reaction.

The results indicated that oxidation rate ratio (k_1/k_2) depended on type of oxidant. The active oxidizing species generated from the reaction of $Fe(TP_{F5}P)Cl$ with iodosylarene oxidants were different from one another. Each substrate was oxidized to the corresponding alcohol in quantitative yield based on oxidant consumption. The yield of ketone from over-oxidation was compared with alcohol. They found that it depended on type of oxidant. They proposed that the active oxidant was a complex between the catalyst and the terminal oxidant.

In 2002, Nizova, *et. al.*²⁶ synthesized a dinuclear iron(III) complex $[Fe_2(HPTB)(\mu-OH)(NO_3)_2] \cdot (NO_3)_2 \cdot CH_3OH \cdot 2H_2O$ (HPTB = N,N,N',N'-tetrakis(2-benzimidazolymethyl)-2-hydroxo-1,3-diaminopropane). It was used to catalyze oxidation of alkanes with hydrogen peroxide in acetonitrile solvent at room temperature. In the low concentration of the complex, it could not catalyze the oxidation. But when adding some amino acids (such as pyridine-2 carboxylic acid, pyridine-2, 3-dicarboxylic acid, or picolinic acid) to the reaction mixture, the cyclohexane oxidation was observed. Alkyl hydroperoxide was a main product. Ketone and alcohol were formed in lower yields. From kinetic study, the first order with respect to both hydrogen peroxide and alkane concentration were observed. The proposed mechanism was described *via* formation of hydroxyl radical.

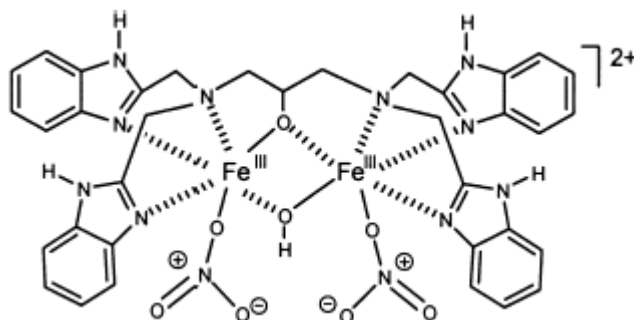


Figure 3.2 Structure of $[\text{Fe}_2(\text{HPTB})(\mu\text{-OH})(\text{NO}_3)_2]^{2+}$ cation.

In 2002, Grootboom, *et. al.*²⁷ reported the use of $\text{Cl}_{16}\text{PcFe}^{\text{II}}$ (polychlorophthalocyanine) and $[\text{Fe}^{\text{II}}\text{TSPc}]^{4-}$ (tetrasulfophthalocyanine) complexes to catalyze oxidation reaction of cyclohexane. The products: cyclohexanone, cyclohexanol and cyclohexanediol were obtained after the reaction was performed for 2 hours at room temperature. Effect of oxidant was studied by varying different type of oxidants: *tert*-butyl hydroperoxide, *m*-chloroperoxybenzoic acid (*m*-CPBA) and hydrogen peroxide. *Tert*-butylhydroperoxide was found to be the best oxidant. The relative yield of the products depended on oxidant and the catalysts. $[\text{Fe}^{\text{II}}\text{TSPc}]^{4-}$ was more active than $\text{Cl}_{16}\text{PcFe}^{\text{II}}$.

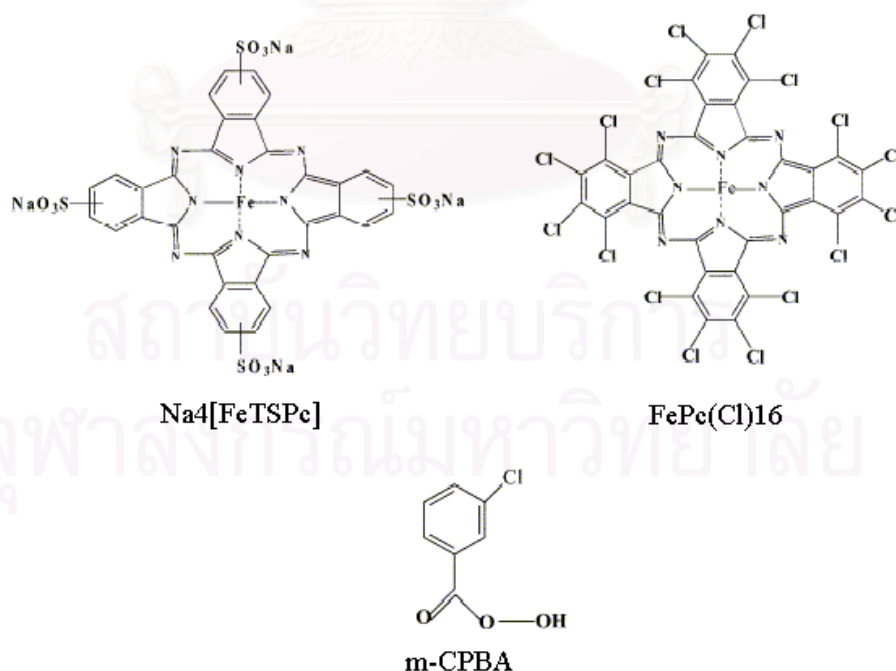


Figure 3.3 Structures of Fe(II) tetrasulfophthalocyanine ($\text{Na}_4[\text{FeTSPc}]$), Fe(II) perchlorinated phthalocyanine ($\text{FePc}(\text{Cl})_{16}$) and *m*-CPBA.

In 2003, Haber, *et. al.*²⁸ studied effect of substituents on metalloporphyrins for catalytic activity in oxidation of cyclooctane with molecular oxygen (air pressure 10 atm and reaction temperature 120 °C) to cyclooctanone and cyclooctanol without the use of reducing agent. The metalloporphyrin catalysts were manganese, iron and cobalt. It was found that the efficiency depends on the number of halogen substituents in the porphyrin ring. The yield of products showed an almost linear correlation with the number of halogen substituents and redox potential of metalloporphyrins.

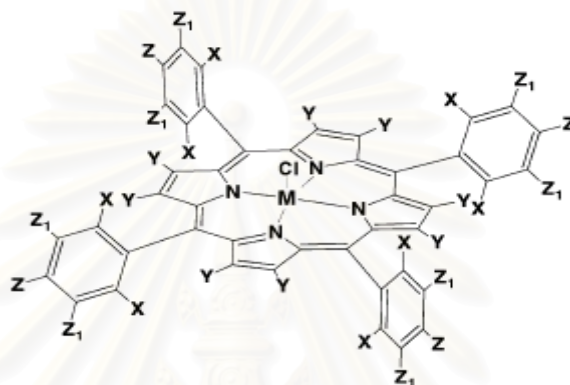
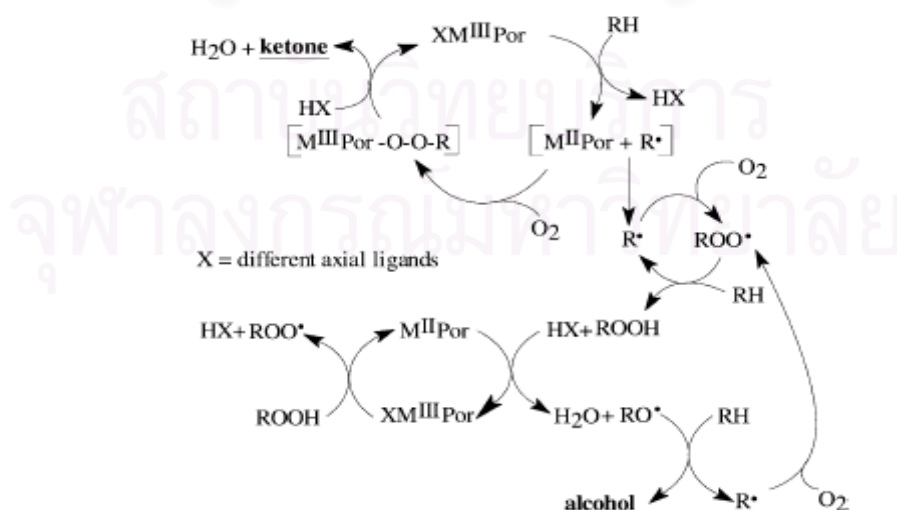


Figure 3.4 Structure of the metalloporphyrin.

The manganese complex showed highest yield and selectivity. The main product was cyclooctanone. The proposed mechanism was the radical process initiated by axial ligand of metalloporphyrins and proceeding through the formation of a metalloporphyrin-cycloalkylperoxy complex, which decomposed yielding ketone and through homolytic decomposition of a cycloalkylhydroperoxide yielding alcohol.



Scheme 3.2 Proposed mechanisms in oxidation of hydrocarbons with metalloporphyrins.

3.2 Heterogeneous iron catalyzed oxidation

In 1986, Herron, *et. al.*²⁹ synthesized iron phthalocyanine encapsulated inside zeolite X and Y and used for oxidation reaction of alkanes using iodosobenzene oxidant. The catalysts were characterized by XRD, diffuse reflectance Vis-UV, and elemental analysis. The oxidation reaction was performed in mild condition (room temperature, overnight). The results of methylcyclohexane oxidation showed that turnover increased when loading metal level decreased. It was explained by pore mechanism of the complexes. Competitive oxidation between cyclohexane and cyclododecane showed stereoselectivity of the smaller substrate.

In 1995, Jun, *et. al.*³⁰ reported cyclohexane oxidation using supported metal catalysts with hydrogen peroxide *in-situ* produced by palladium catalyst. The catalysts were metal chloride and metal tetraphenylporphyrin (TPPCL) (metal = Mn^{2+} , Fe^{2+} , Co^{3+} , Ni^{3+} and Cu^{2+}). Four kinds of 4-vinylpyridine (PVP) copolymer with styrene (S) or divinylbenzene (DVB) were used as supports: PVP-s (10%S), PVP-2d (2%DVB), PVP-6d (6%DVB) and PVP-24d (24%DVB). The reactions were performed in acetone as solvent and the selective product was cyclohexanol. It was found that supported $FeCl_2$ and $FeTPPCL$ showed higher catalytic activity. The reactivity of the catalysts depended on solubility of the supports in acetone and amount of the crosslinking degree of copolymer. The activity of catalysts decreased in the following order: PVP-s > PVP-24d > PVP-2d > PVP-6d.

In 1995, Delaude, *et. al.*³¹ studied oxidation of selected alcohols, benzylamine, thiophenol and aniline in hydrocarbon solvents by using K10 montmorillonite clay catalyst and potassium ferrate (IV) as oxidant at room temperature. The high yields of product were obtained within few hours. It was found that solvent such as cyclohexane was not inert and turn into significant amounts of cyclohexanone and cyclohexanol. The amount of water in clay affected catalytic activity. The reactions did not occur with the dried catalyst.

In 1999, Park, *et. al.*³² reported cyclohexane oxidation using heterogeneous metal oxide such as Fe_3O_4 , Fe_2O_3 , FeO , TiO_2 , MnO_2 , MoO_2 , WO_3 and ZnO as catalysts. The reaction was performed in pyridine/acetic acid and zinc under air (1

atm) at room temperature. The strong acidic and high oxidation state metal oxide showed higher activity and selectivity ratio of cyclohexanone to cyclohexanol. The Fe_3O_4 catalyst showed the best result (5.55% conversion and 10.32% selectivity) and the recycle process showed that the catalysts did not lose their activity.

In 1999, Langhendries, *et. al.*³³ reported the use of zeolite Y, USY and activated carbon supported iron-phthalocyanine to catalyze oxidation reaction of hydrocarbon using *t*-butyl hydroperoxide as oxidant. The reactions were performed in both batch and continuous reaction conditions. The catalytic activity depended on the polarity of the solid support material. The rate of reaction was increased when the Si/Al ratio of zeolite was increased. A similar reactivity trend was observed both in the batch and continuous reactions. Rapid deactivation was observed for the activated carbon supported catalyst under continuous reaction and no leaching occurred with the zeolite-encapsulated catalysts.

In 1999, Carvalho, *et. al.*³⁴ synthesized and characterized $\text{M}(\text{NC}_3)_2\text{Si-MCM-41}$ ($\text{M} = \text{Cu}(\text{II})$ and $\text{Fe}(\text{III})$) and M-MCM-41 catalysts. These catalysts were employed in the oxidation reaction of cyclohexane with aqueous hydrogen peroxide (reaction temperature 100°C , 12 hours). They found that $\text{M}(\text{NC}_3)_2\text{Si-MCM-41}$ were more active than M-MCM-41 . The activity of catalysts decreased in the following order: $\text{Fe}(\text{NC}_3)_2\text{Si-MCM-41} > \text{Fe-MCM-41} > \text{Cu}(\text{NC}_3)_2\text{Si-MCM-41} > \text{Cu-MCM-41}$. However, when the catalysts were recycled, leaching of the metal was observed.

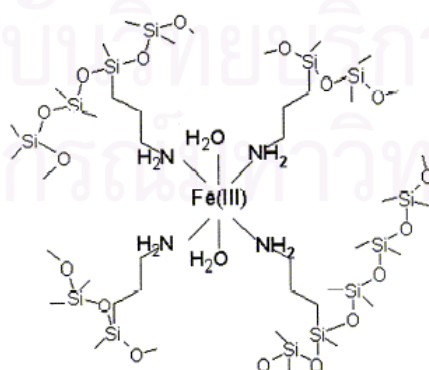


Figure 3.5 Proposed structure of the active site of $\text{Fe}(\text{NC}_3)_2\text{Si-MCM-41}$.

In 1999, Álvalo, *et. al.*³⁵ synthesized Fe³⁺-picolinate (Fe-PA) catalysts inside micropore of zeolite Y and mordenite by using encapsulation method. The catalysts were performed in the oxidation reaction of cyclohexane using hydrogen peroxide oxidant and mixed acetonitrile/pyridine as solvent. It was found that mordenite was more efficient support than zeolite Y (49.1% conversion and 93% selectivity). The catalysts showed similar catalytic activity and selectivity to homogeneous complex.

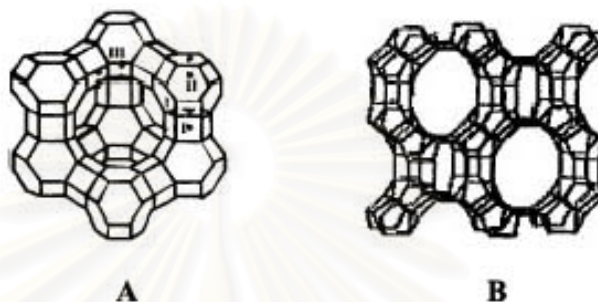


Figure 3.6 Geometry of (A) zeolite Y and (B) mordenite.

In 2000, Rosa, *et. al.*³⁶ reported the immobilization of FeP1 (iron(III) 5,10,15,20-tetrakis(4-*N*-methylpyridyl)porphyrin) and FeP2 (iron(III) 5-mono(2,6-dichlorophenyl)10,15,20-tris(4-*N*-methylpyridyl)porphyrin) into zeolite X. These solids were efficient catalysts for oxidation of cyclohexane in dichloroethane by using iodosobenzene as oxidant (reaction temperature 25°C). The catalytic efficiency and selectivity of these solids were higher than those of the iron porphyrins in solution.

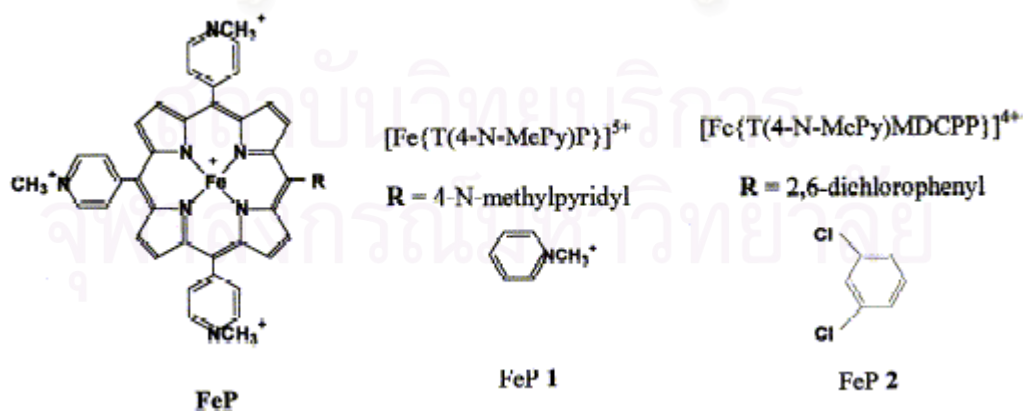


Figure 3.7 Structures of iron porphyrins.

In 2001, Manfred, *et. al.*³⁷ reported the use of silica supported iron(II) to catalyze oxidation reaction of cyclohexane to cyclohexanone using hydrogen peroxide as oxidant under mild condition (reaction temperature 31°C, 24 hours). Moderate yield (38%) was obtained and the low leaching of the iron species was observed. In addition, the stability of the catalyst was studied by repeated oxidation. It showed almost the same catalytic activity after 6 cycles.

In 2001, Perkas, *et. al.*³⁸ reported oxidation of cyclohexane to cyclohexanone and cyclohexanol using nanostructure iron oxide (Fe_2O_3), cobalt oxide (Co_3O_4), Co and Fe powder and iron supported on titania ($\text{Fe}_2\text{O}_3/\text{titania}$) as catalyst. Oxidant was molecular oxygen (1 atm) and isobutyraldehyde was employed as an activator. The activities of catalysts decrease in the following order: $\text{Fe}_2\text{O}_3/\text{titania} > \text{Fe}_2\text{O}_3 > \text{Co}_3\text{O}_4 > \text{Co powder} \sim \text{Fe powder}$. The catalytic activity was depending on particle size of the catalysts.

In 2002, Machado, *et. al.*³⁹ reported the use of immobilized FeTMPy^{5+} (iron(III) tetrakis(1-methyl-4-pyridiniumyl)porphyrin) and MnTMPy^{5+} (manganese(III) tetrakis(1-methyl-4-pyridiniumyl)porphyrin) on the surface of montmorillonite and Brazilian natural clays to catalyze oxidation reaction of cyclohexane (room temperature, 4 hours). The selective product was cyclohexanol. The catalytic activities were depending on concentration of the porphyrin immobilized in the clay, metal ion species, solvent and concentration of iodosylbenzene oxidant. The best catalytic result was obtained with MnTMPy^{5+} immobilized in montmorillonite clay (82% cyclohexanol and 12% cyclohexanone).

In 2002, Nakagaki, *et. al.*⁴⁰ reported the immobilization of FeTPPCl (5,10,15,20-tetraphenylporphyrin iron(III) chloride) and FeTMPyPCl_5 (5,10,15,20-tetrakis(4-*N*-methylpyridyl)porphyrin iron(III) pentachloride) into porous vycor glass and used these materials as catalyst in oxidation reaction of cyclohexane and cyclohexene using iodosylbenzene as oxidant. The catalytic efficiency of these materials was higher than the iron porphyrins in solution (homogeneous catalysis). The highest yield (alcohol product) and selectivity were obtained when reaction performed in dichloromethane.

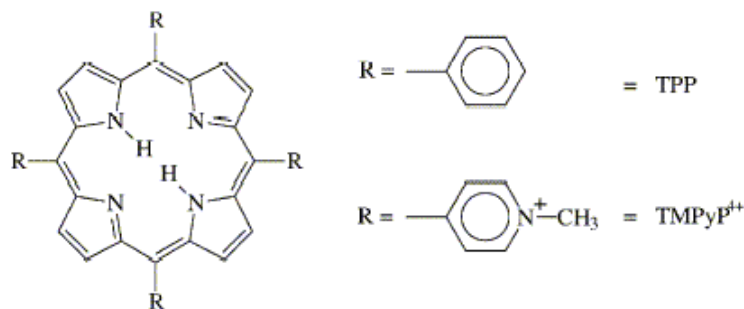


Figure 3.8 Structures of TPP and TMPyP porphyrins.

In 2002, Srivastava, *et. al.*⁴¹ synthesized and characterized mesoporous iron oxide catalyst by using sonochemical technique. The catalyst was employed in the oxidation of cyclohexane with isobutyraldehyde and molecular oxygen (O_2 1 atm, reaction temperature 70°C , and reaction time 15-17 hours). The mesoporous Fe_2O_3 catalyst showed 36% conversion of cyclohexane and cyclohexanone:cyclohexanol = 5:1.

In 2003, Kopylovich, *et. al.*⁴² synthesized binary Fe(III)-Cr(III) hydroxides by hydrolysis of Fe(III) and Cr(III) in their single or binary nitrate solution. After thermolysis process, the products were obtained and characterized by potentiometric titration, thermal analysis, IR spectroscopy and X-ray powder diffraction. The aquahydroxo complexes and metal hydroxides were employed to catalyze in homogeneous and heterogeneous oxidation of alkanes using hydrogen peroxide oxidant. Ketones and alcohols were formed at room temperature. For homogeneous system, the Fe(III) species gave the best catalytic activity. Synergistic effect was not observed. In case of heterogeneous metal oxide catalysts, the synergistic effect was observed. The binary Fe(III)-Cr(III) hydroxide was the best catalyst, with a maximum yield of 30% (TON=30). In addition, the product of oxidation also depended on pH.

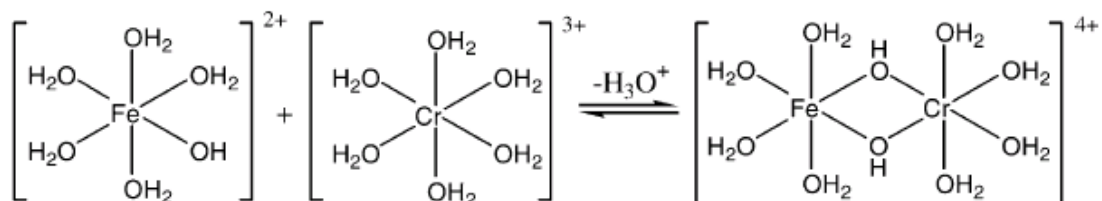


Figure 3.9 The heteropolynuclear hydrolysis of binary mixture.

In 2004, Faria, *et. al.*⁴³ synthesized aminofunctionalized phyllosilicates, Talx and Silx, as supports for 5,10,15,20-tetrakis (pentafluorophenyl) porphyrin iron(III) chloride [FeTFPPCl] through covalent binding, where x = 1-3 represents the length of the organic chain binding the ironporphyrin to the support. The catalysts were characterized by UV-Vis, IR, and ESR and used as catalysts for oxidation of alkanes and alkenes by iodosobenzene and hydrogen peroxide. FeTalx was more efficient than the corresponding FeSilx. For hydrogen peroxide oxidant, FeTalx systems were better catalysts for hydrocarbon oxidation than the homogeneous ironporphyrin.

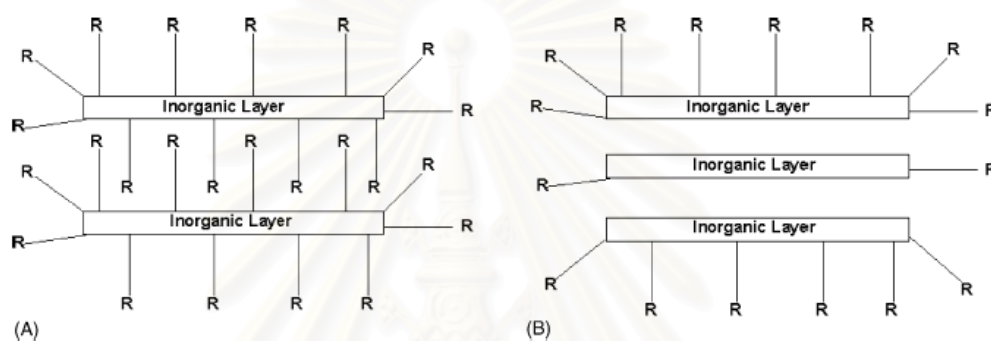


Figure 3.10 Gallery space and surface of the phyllosilicate (A) Silx and (B) Talx, where R is the attached organic group bound to the inorganic backbone.

In 2004, Nakagaki, *et. al.*⁴⁴ synthesized silanized kaolinite support (**4**) by silanization reaction between kaolinite and 3-aminopropyltriethoxysilane (3-APTS) after intercalation with urea and delamination under ultrasonic treatment. Then silanized kaolinite (**4**) was immobilized by electrostatic interaction with 5,10,15,20-tetrakis(2,6-difluoro-3-sulfonatophenyl) porphyrinato iron(III) chloride [(FeTDFSPP)Cl]⁴⁻ (**3**). Kaolinite-iron(III) porphyrin (**5**) was obtained and characterized by UV-Vis, FT-IR, ESR, ¹H NMR, AAS, TG/DSC, and XRD. Catalyst (**5**) was used for oxidation of cyclooctane, heptane, and cyclohexane with iodosobenzene oxidant. It showed high catalytic activity. Hydrogen peroxide was also used as oxidant but lower yields were obtained.

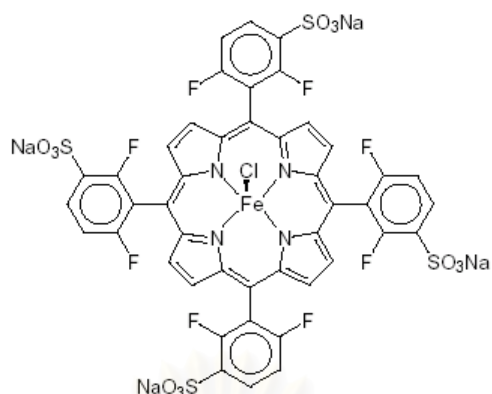


Figure 3.11 Structure of the iron porphyrin $\text{Na}_4[\text{Fe}(\text{TDFSPP})\text{Cl}]$.

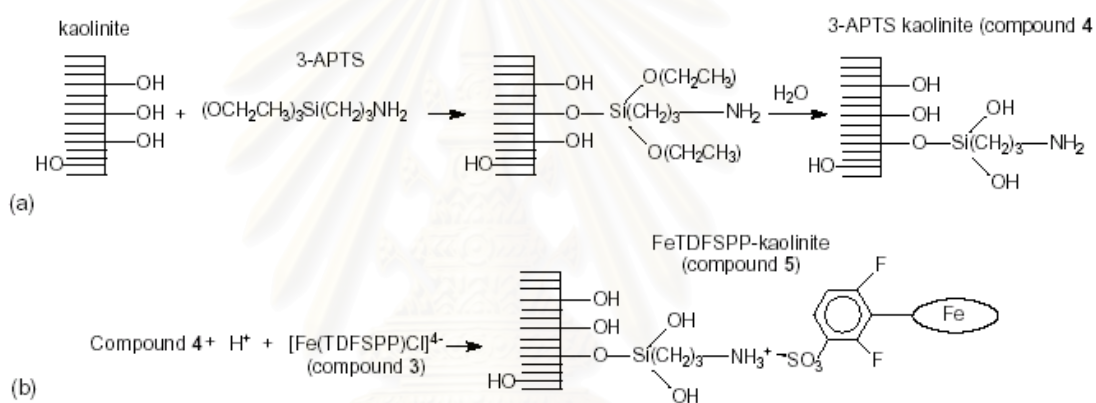


Figure 3.12 Synthesis of 3-aminopropyltriethoxysilanzed kaolinite (**4**) and 5,10,15,20 -tetrakis(2,6-difluoro-3-sulfonatophenyl) porphyrinato iron(III) silanzed kaolinite (**5**).

สถาบันวิทยบริการ
จุฬาลงกรณ์มหาวิทยาลัย

CHAPTER IV

EXPERIMENTAL

In the present study of oxidation of cyclooctane with clay-supported iron catalysts, the experiment was divided into four steps.

1. Preparation and characterization of clay-supported iron catalysts
2. Oxidation of cyclooctane with the prepared catalysts
3. Reusability of clay-supported iron catalysts
4. Test of metal leaching

The details of the experiments were explained in the following.

4.1 Equipment

Some reactions were done in an inert gas atmosphere (prepurified nitrogen) using standard Schlenk technique. All equipments used in the oxidation of cyclooctane compounds are listed as follows:

4.1.1 Schlenk line

Schlenk line consists of nitrogen and vacuum line. The vacuum line was equipped with a solvent trap and a vacuum pump, respectively. The nitrogen line was connected to the moisture trap and the oil bubble that contained enough oil to provide a seal from the atmosphere. The Schlenk line is shown in Figure 4.1.

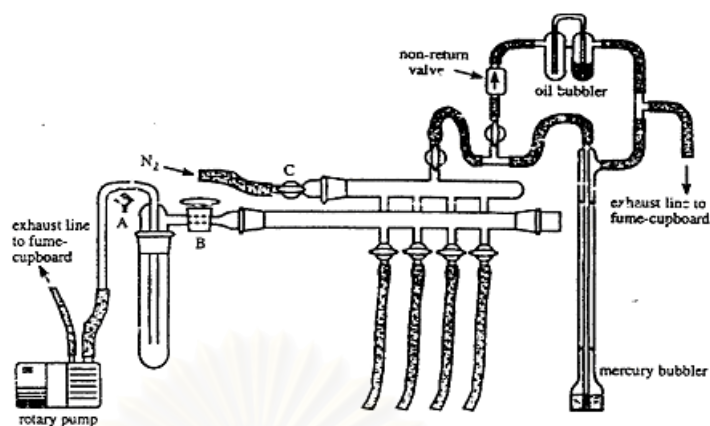


Figure 4.1 Schlenk line.

4.1.2 Schlenk flask

A Schlenk flask has a side arm to connect to the Schlenk line. A typical model is shown in Figure 4.2.



Figure 4.2 Round-bottomed Schlenk flask.

4.1.3 Vacuum pump

A pressure of 10^{-3} - 10^{-1} mmHg was adequate for the vacuum supply to the vacuum line in the Schlenk line using Edward RV5 vacuum pump.

4.1.4 Inert gas supply

Ultra high purity nitrogen gas (99.99%) was purified by passing through three columns packed with 4°A molecular sieve, NaOH and P₂O₅, respectively. The inert gas was used to feed into nitrogen line of Schlenk line.

4.1.5 Heating bath

The heating silicone oil bath with thermometer was used for high temperature reaction.

4.2 Chemicals

All chemicals used in this experiment were analytical grade.

Table 4.1 Chemicals and suppliers

Reagents and Solvents	Supplier
Bentonite clay	Cernic International Co., Ltd., Thailand
Kaolinite clay	Cernic International Co., Ltd., Thailand
Talcum clay	Cernic International Co., Ltd., Thailand
2-Aminophenol	Fluka Chemie A.G., Switzerland
2,2'-Bipyridyl	Fluka Chemie A.G., Switzerland
Chloroform	Merck, Germany
Cyclooctane	Fluka Chemie A.G., Switzerland
Dichloromethane	Lab Scans Co., Ltd., Ireland
Ethylbenzene	Fluka Chemie A.G., Switzerland
37% Hydrochloric acid	Lab Scans Co., Ltd., Ireland
48% Hydrofluoric acid	BDH Laboratory Supplies, England

Table 4.1 Chemicals and suppliers (continued)

Reagents and Solvents	Supplier
30% Hydrogen peroxide	Merck, Germany
Iron(III) acetylacetonate	Merck, Germany
Iron(III) chloride anhydrous	Aldrich Chemical Co., Inc., USA
Iron(III) nitrate nonahydrate	Fluka Chemie A.G., Switzerland
Iron(II) sulfate heptahydrate	Scharlau Chemie S. A., Spain
Iodobenzene diacetate	Aldrich Chemical Co., Inc., USA
Methanol	Lab Scans Co., Ltd., Ireland
65% Nitric acid	Merck, Germany
Picolinic acid	Fluka Chemie A.G., Switzerland
Potassium hydroxide	Merck, Germany
Pyrazine-2-carboxylic acid	Fluka Chemie A.G., Switzerland
Pyridine	Fluka Chemie A.G., Switzerland
2-Pyridine carboxaldehyde	Fluka Chemie A.G., Switzerland
Silica(60), 0.06-0.2 mm	Scharlau Chemie S. A., Spain
Sodium acetate trihydrate	Merck, Germany
Sodium hydroxide	Merck, Germany
Sodium sulfate anhydrous	Merck, Germany
Sodium sulfite	Merck, Germany
98% Sulfuric acid	Merck, Germany
70% Tert-butyl hydroperoxide in water	Merck, Germany
80% Tert-butyl hydroperoxide in di-tert-butylperoxide	Merck, Germany
Ultra high purity nitrogen gas (99.99%)	Thai Industry Gas Co., Ltd., Thailand

4.3 Analytical Measurements

4.3.1 Fourier transform infrared spectrometer (FT-IR)

Fourier transform infrared spectra were recorded on Nicolet FT-IR Impact 410 Spectrophotometer at Department of Chemistry, Chulalongkorn University. The solid samples were prepared by pressing the sample with KBr. Infrared spectra were recorded between 400 cm^{-1} to $4,000\text{ cm}^{-1}$ in transmittance mode.

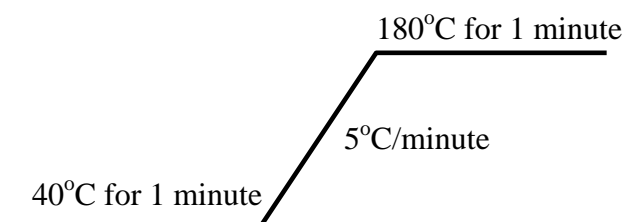
4.3.2 UV-Visible spectrometer (UV-vis)

UV-Visible spectra were recorded on Milton Roy Spectronic 3000 Array at Department of Chemistry, Chulalongkorn University.

4.3.3 Gas chromatography (GC)

Gas chromatography analyses were performed on a Shimadzu GC-14B gas chromatograph equipped with a flame ionization detector and a 30 m (0.25 mm i.d., 0.25 μm film thickness) DB-1 capillary column. The condition used for the determination of %conversion of substrate and %yield of products was set as follows:

Carrier gas	: Nitrogen
Carrier gas pressure	: 50 kPa
Detector temperature	: 220 °C
Injection temperature	: 220 °C
Programmed temperature	:



4.3.4 X-ray diffractometer (XRD)

The XRD patterns of catalysts were obtained on Rigaku, DMAX 2002 Ultima Plus X-ray powder diffractometer equipped with a monochromator and a Cu-target X-ray tube (40 kV, 30 mA) and angles of 2θ ranged from 2-60 degree at Department of Chemistry, Faculty of Science, Chulalongkorn University.

4.3.5 X-ray fluorescence spectrometer (XRF)

Iron content in the catalyst was determined using a SISON S X-ray fluorescence spectrometer ARL 8410 at the Department of Science Service, Ministry of Science and Technology.

4.3.6 Atomic absorption spectrometer (AAS)

Iron content of the catalyst and leached ones were performed on filtrates using a Varian Spectra-AA300 atomic absorption spectrometer with air/acetylene flame at the Scientific and Technological Research Equipment Center, Chulalongkorn University.

Atomic absorption spectroscopy technique was used to determine iron content in catalysts. The solid catalysts were digested in a 100 mL Teflon beaker. 0.040 g of catalyst was added with 10 mL of concentrated HCl and subsequently with 10 mL of 48% HF to remove the silica in a form of volatile SiF_4 species. The solid was heated but not boiled to dryness on the hot plate. The removal of silica was repeated three times. An amount of 10 mL of a mixture of 6 M HCl: 6 M HNO_3 at a ratio 1:3 was added and further heated to dryness. 5 mL of 6 M HCl was added to the beaker and warmed for 5 minutes to complete dissolution. The solution was transferred to a 50 mL polypropylene volumetric flask and made up the volume by adding deionized water. Then the flask was capped and shaken thoroughly.

4.3.7 Scanning electron microscope (SEM)

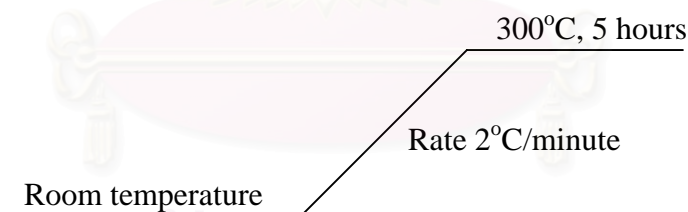
The SEM photograph, energy dispersive x-ray (EDX) and x-ray mapping were observed using a JEOL JSM-5800LV scanning electron microscopy and EDX spectrometer, Oxford Instrument (Link ISIS series 300) at the Scientific and Technological Research Equipment Center, Chulalongkorn University.

4.3.8 Nitrogen adsorption/desorption (Brunauer-Emmett-Teller method, BET)

BET specific surface area of the catalysts was carried out using a Quantachrome Autosorb-1 nitrogen adsorptometer at Department of Chemistry, Faculty of Science, King Mongkut's Institute of Technology, Lad-Krabang Campus.

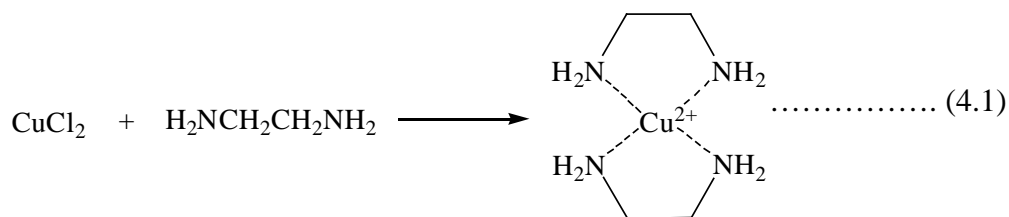
4.3.9 Furnace

Calcination of the catalyst was performed in a Carbolite RHF 1600 muffle furnace in air. The condition used for the calcination of the catalysts was set as follows:



4.4 Determination of cation exchange capacity

Cation exchange capacity (CEC) of clays and the catalysts were determined using copper bisethylenediamine cations ($\text{Cu}(\text{EDA})_2^{2+}$).¹² An 0.05 M solution of $\text{Cu}(\text{EDA})_2^{2+}$ was prepared by mixing the appropriate volumes (1:2) of 1 M CuCl_2 and 1 M EDA solutions (with slight excess of the latter to ensure the complete formation of the complex) and making up to the required volume.



Cation exchange capacity (CEC) was determined by weighing 0.5 g of dried clay or catalyst in a centrifugal tube. 5 mL of the complex solution was diluted with deionized water to 25 mL and added to the clay. The samples were shaken for 30 minutes and then centrifuged. The concentration of the complex remaining in the supernatant was determined by photometry.

4.5 Preparation of clay supported iron catalysts

The clay supported iron catalysts were prepared by ion exchange method.

4.5.1 Bentonite supported iron catalysts

All catalysts were characterized by FT-IR, XRD and AAS techniques.

A. Bentonite-supported iron (II) sulfate catalysts

Ben/FeSO₄ : Bentonite (10.0 g) was suspended in acetone (30 mL) and stirred at room temperature for 24 hours. Then 1 M of iron(II) sulfate solution was added dropwise and stirred 24 hours. The solid was either centrifuged and washed with deionized water to remove excess iron compound or evaporated solvent. The resulting solid was dried at 100°C overnight. Amount of iron solution was varied: 11, 22 and 44 mmol (11, 22 and 44 mL or 2.5, 5 and 10 equivalents with respect to exchangeable cation of bentonite, respectively).

B. Bentonite-supported iron (III) chloride catalysts

Ben/FeCl₃ : The catalysts were prepared using the same method described in A. but used solution of 1 M iron(III) chloride. Amount of iron solution was varied: 7.5

and 15 mmol (7.5 and 15 mL or 2.5 and 5 equivalents with respect to exchangeable cation of bentonite, respectively).

C. Bentonite-supported iron (III) nitrate catalysts

Ben/Fe(NO₃)₃ : The catalyst was prepared using the same method described in A. but used 7.5 mL of 1 M iron(III) nitrate solution (7.5 mmol or 2.5 equivalents with respect to exchangeable cation of bentonite).

D. Bentonite-supported iron (III) acetylacetonate catalysts

Ben/Fe(acac)₃ : The catalysts were prepared using the same method described in A. but used solution of 0.5 M iron(III) acetylacetonate. Amount of iron solution was varied: 3, 7.5 and 15 mmol (6, 15 and 30 mL or 1.0, 2.5 and 5 equivalents with respect to exchangeable cation of bentonite, respectively).

E. Bentonite-supported iron (III) bipyridine catalyst⁴⁵

Ben/Fe(bpy)₂Cl₃ : Bentonite (5.0 g) was slowly added to 0.06 M solution of iron(III) chloride in 100 mL methanol to exchange cation with iron(III). The suspension was stirred at room temperature for 24 hours. The orange solid was filtered, washed with methanol and dried at 50°C under vacuum. Then 1.0 g of dried solid was added to a solution of 2,2'-bipyridine (2.18 mmol, 0.40 g) in 100 mL of CH₂Cl₂. The suspension was heated under reflux condition for 24 hours, filtered and washed with CH₂Cl₂ to remove unreacted ligands. The obtained pink solid was dried under vacuum at 50°C.

F. Bentonite-supported iron (III) picolinate catalysts

Ben/Fe(picolinate)₂Cl₃: The catalyst was prepared using the same manner described in E. but used picolinic acid (2.18 mmol, 0.27 g) in methanol.

G. Bentonite-supported iron (III) pyrazinate catalysts

Ben/Fe(pyrazinate)₂Cl₃ : The catalyst was prepared by two methods. First, pyrazine-2-carboxylic acid (white solid) and sodium hydroxide was dissolved in deionized water at 80°C. Then starting catalyst, bentonite supported iron chloride was slowly added into the mixture, stirred for few hours. The color did not change to purple as expected. After filtered, washed with diluted sodium hydroxide solution and dried at 100°C, the obtained solid was a mixture of white flake and orange powder. This was concluded that no iron complex was incorporation into the bentonite. It might be due to the iron species of Ben/FeCl₃ which was identified as iron oxide, inactive in complexation.⁴⁶ Second method, the catalyst was prepared using the same manner described in E. but used pyrazine-2-carboxylic acid (2.18 mmol, 0.27 g) in methanol in stead of 2,2'-bipyridine. Therefore in this work, only the latter was used to study.

4.5.2 Kaolinite- and talcum-supported iron catalysts

mTalc: Modified talcum was prepared following previous report but used [(H₅C₂O)₃Si(CH₂)₃]₂S₄ silane (Si 69) instead of 3-aminopropyltrimethoxysilane.⁴⁷ Talcum was initially activated by heating at 150°C for 24 hours. Then 2.5 g of activated talcum was suspended in 125 mL of xylene at 80°C. 5 mL Si 69 was added and the reaction mixture was maintained during two days under this condition. The modified talcum was filtered, washed with ethanol and vacuum dried at 60°C.

Kao/FeSO₄ and Talc/FeSO₄: The preparation of these catalysts followed the procedure in [section 4.5 A](#). but using kaolinite or talcum instead of bentonite.

The prepared catalysts were characterized by FT-IR, XRD and AAS techniques.

4.5.3 Silica-supported iron catalysts³⁷

SiO₂/FeSO₄ : The catalysts were prepared by mixing silica 60 (13.26 g) with FeSO₄·7H₂O (0.58 and 2.9 g) in 50 mL methanol. The mixture was stirred for 24

hours, filtered and vacuum dried. Iron content in the catalyst was determined by AAS technique.

4.6 Synthesis of goethite

The preparation of a goethite was modified according to the previous report.⁴⁸ A 50 mL of 2.5 M KOH solution was mixed with 200 mL of 0.15 M Fe(NO₃)₃ solution and the mixture was stirred vigorously. Then the precipitate was formed and aged for 48 hours at 80°C after that the solid was centrifuged and re-dispersed in 0.01 M HNO₃ solution, this process was repeated five times and again three times with deionized water instead of HNO₃ solution. The orange precipitate was dried under vacuum and identified by FT-IR and XRD.

4.7 Preparation of iodosobenzene oxidant

The preparation of iodosobenzene was modified from previous report.⁴⁹ The starting material iodobenzene diacetate was hydrolyzed in base to form iodosobenzene as shown in [Equation 4.1](#).



Finely ground iodobenzene diacetate 3.2 g (10 mmol) was placed in a 50 mL beaker, and 15 mL of 3 M sodium hydroxide solution was added under vigorous stirring for 20 minutes. The lumps of solid were formed. A 10 mL of deionized water was added, the mixture was stirred, and the crude solid iodosobenzene was collected on a Buchner funnel. The wet solid was suspended in 20 mL of deionized water, and suctioned, washed with chloroform. The iodosobenzene was separated by filtration and air dried. The weight of the compound was 2.0 g (92% yield); m.p. 210 °C.

4.8 Oxidation procedure for cyclooctane

In a round bottom flask, connected with a condenser, cyclooctane, solvent and the catalyst were mixed. Then the oxidant was added into the reaction mixture. The mixture was stirred for the desired time and temperature. After the reaction finished, 1

mL of the reaction mixture was taken, acidified with 25% H_2SO_4 and extracted with diethyl ether, neutralized with saturated solution of NaHCO_3 and dried over anhydrous Na_2SO_4 . Products were analyzed by GC (using ethylbenzene as internal standard).

To determine the %products, GC technique was used to detect products from the oxidation of cyclooctane, cyclooctanone and cyclooctanol. The peaks area of both were calculated and converted to mole, then to percentage based on the initial amount of cyclooctane. The sum of both products led to %yield. As in this work, only two products were obtained, therefore, in this report, %yield of product was represented by %conversion.

$$\% \text{Yield} = \% \text{Conversion} = \% \text{cyclooctanone} + \% \text{cyclooctanol}.$$

According to the oxidation procedure, various effects in the oxidation reaction of cyclooctane were investigated.

A. Effect of catalyst types

The prepared catalysts were used to investigate the oxidation.

B. Effect of oxidant types

Different types of oxidants were investigated: 70% *tert*-butyl hydroperoxide, 80% *tert*-butyl hydroperoxide in di-*tert*-butylperoxide, 30% hydrogen peroxide and iodosobenzene.

C. Effect of oxidant amounts

Amount of 70% *tert*-butyl hydroperoxide oxidant was varied: 5, 10 and 20 mmol.

D. Effect of solvent types

Different types of solvents were investigated: acetone, acetonitrile, acetonitrile/pyridine and dichloromethane.

E. Effect of reaction time

Effect of reaction time was investigated: 24, 48 and 72 hours.

4.9 Homogeneous iron compound catalysts

In order to compare the catalytic activity between supported catalyst and homogeneous catalyst, the homogeneous iron catalysts were investigated: FeSO_4 , FeCl_3 , $\text{Fe}(\text{acac})_3$, $\text{Fe}(\text{pyrazinate})_2\text{Cl}_3$, $\text{Fe}(\text{picolinate})_2\text{Cl}_3$ and $\text{Fe}(\text{acac})_3$.

The oxidation reaction was carried out in the same manner described in [section 4.8](#). Cyclooctane, solvent and the catalyst were mixed in a round bottom flask that connected a cooling condenser. Then the oxidant was added into the reaction mixture. The mixture was stirred for the desired time and temperature. After the reaction finished, 1 mL of the reaction mixture was taken, acidified with 25% H_2SO_4 and extracted with diethyl ether, neutralized with saturated solution of NaHCO_3 and dried over anhydrous Na_2SO_4 .

In case of $\text{Fe}(\text{pyrazinate})_2\text{Cl}_3$ and $\text{Fe}(\text{picolinate})_2\text{Cl}_3$, they were prepared *in situ* using 0.14 mmol of iron(III) chloride and 0.43 mmol of pyrazine-2-carboxylic acid or picolinic acid in mixed solvent (pyridine: acetic acid ratio 10:1 v/v).

4.10 Test of iron leaching

In a round bottom flask, 0.4 g of the catalyst was suspended in solvent (10 mL). A 70% tert-butyl hydroperoxide (0.7 mL) was subsequently added. The mixture was stirred at 70°C for 24 hours. Then the mixture was centrifuged and filtered. The filtrate was extracted with deionized water and the organic layer was removed. The aqueous solution was transferred to 25 mL of volumetric flask. The leaching iron was determined by atomic absorption spectrometer.

4.11 Reusability of clay-supported iron catalysts

After being used in the reaction, the catalyst was removed from the reaction mixture by filtration, washed with diethyl ether and dried at 100°C overnight. Then it was reused for oxidation by adding fresh cyclooctane and 70% *tert*-butyl hydroperoxide at 70°C for 24 hours.



สถาบันวิทยบริการ
จุฬาลงกรณ์มหาวิทยาลัย

CHAPTER V

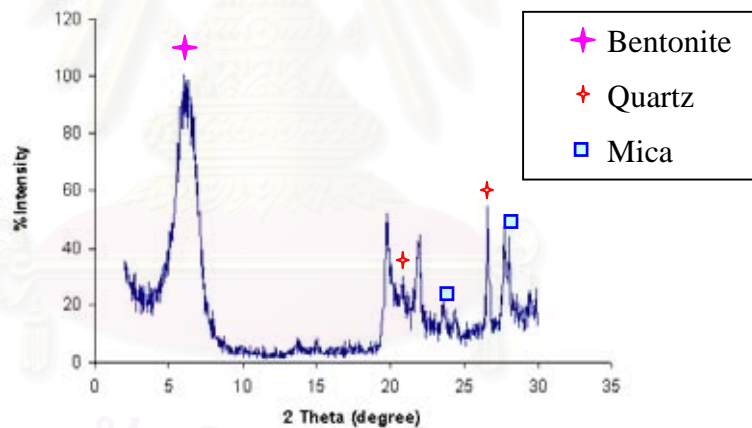
RESULTS AND DISCUSSION

5.1 Characterization of clays

Raw clays: bentonite, kaolinite, and talcum were characterized by x-ray diffraction and fourier transform infra-red techniques.

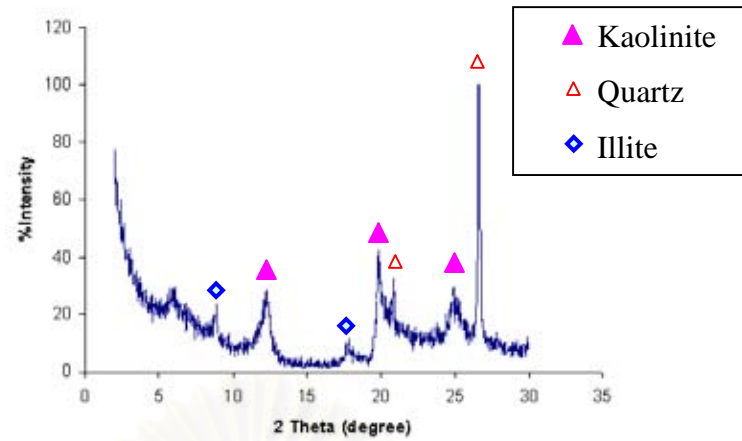
5.1.1 X-ray diffraction (XRD)

Structures of clays were investigated by XRD technique, XRD patterns were shown in [Figure 5.1](#).

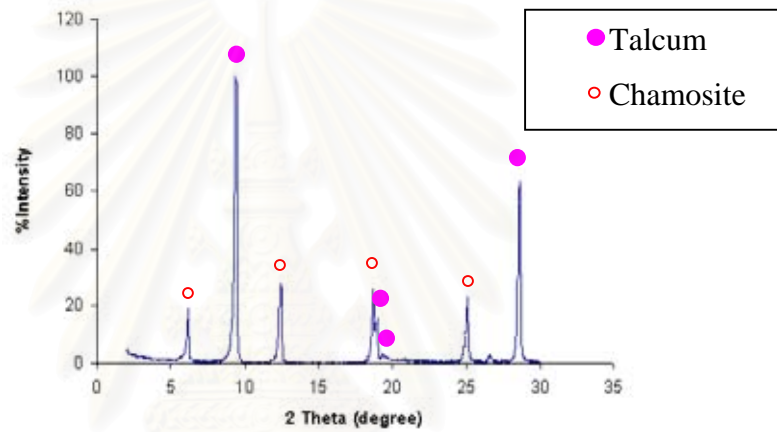


(a) Bentonite clay

Figure 5.1 XRD patterns of clays (a) bentonite, (b) kaolinite and (c) talcum.



(b) Kaolinite clay



(c) Talcum clay

Figure 5.1 (cont.) XRD patterns of clays (a) bentonite, (b) kaolinite and (c) talcum.

The XRD patterns (Figure 5.1) exhibited the characteristic patterns of bentonite, kaolinite, and talcum, respectively.

In Figure 5.1(a), montmorillonite was main composition in bentonite as shown from the characteristic peak at 2θ about 7.5. The other phases were calcium mica and quartz. Calcium mica ($\text{Al}_3\text{Ca}_{0.5}\text{Si}_3\text{O}_{11}$) showed characteristic peak at 2θ 23.7 and 27.8. Quartz (SiO_2) showed characteristic peak at 2θ 20.8 and 26.6.

According to the patterns in [Figure 5.1\(b\)](#), the sample consisted of kaolinite (characteristic peak at 2θ 12.3, 19.8 and 24.9), illite ($((K,H_3O)Al_2Si_3AlO_{10}(OH)_2)$) at 2θ 8.8 and 17.7 and quartz.

The pattern of talcum in [Figure 5.1\(c\)](#) showed characteristic peak at 2θ 9.4, 18.9, 19.4 and 28.6. It also consisted of chamosite ($((Fe,Al,Mg)_6(Si,Al)_4O_{10}(OH)_8)$) at 2θ 6.2, 12.4, 18.7 and 25.1.

5.1.2 X-ray fluorescence (XRF) and Atomic absorption spectrometer (AAS)

The iron content in raw clays was determined by AAS technique. The XRF data were taken from result of Cernic International Co., Ltd. The results were shown in [Table 5.1](#).

Table 5.1 The iron content in the raw clay using XRF and AAS techniques

Clay	Iron content (% weight Fe_2O_3)	
	XRF	AAS
Bentonite	3.1	3.0
Kaolinite	1.4	1.5
Talcum	Nd	0.2

Nd = not determined.

The iron content of raw clays increased in the following order: bentonite > kaolinite > talcum. The XRF and AAS techniques showed similar results. The iron contents depended on the source of clays.

5.1.3 Fourier transform infra-red spectrometer (FT-IR)

The FT-IR technique was used to characterize functional group of clays. The FT-IR spectra of clay presented the characteristic absorption peaks. The FT-IR spectra and data of bentonite, kaolinite, and talcum were shown in [Figure 5.2](#) and [Table 5.2](#), respectively.

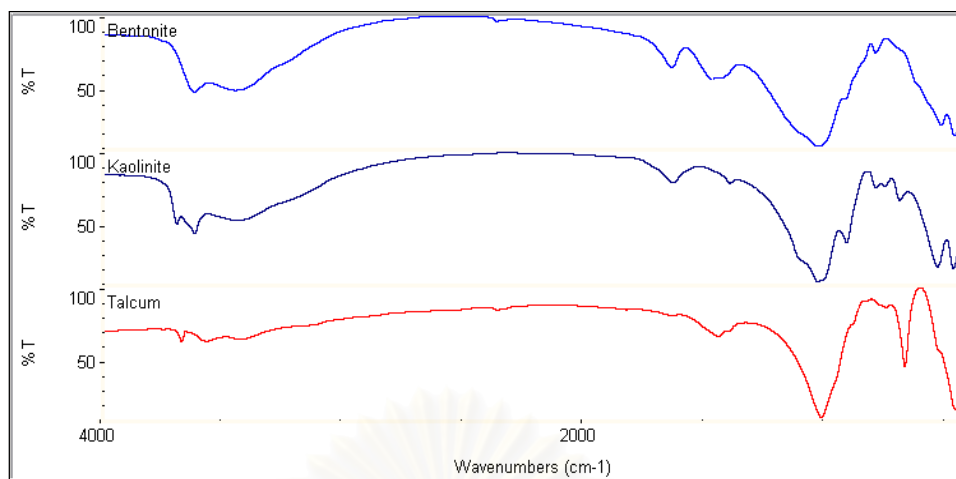


Figure 5.2 FT-IR spectra of bentonite, kaolinite and talcum clay.

Table 5.2 The assignment for the FT-IR spectra of clays

Wave number (cm ⁻¹)			Assignment
Bentonite	Kaolinite	Talcum	
3624	3618	3678	O-H stretching
1396	1396	1391	O-H bending
1026	1031	1015	Si-O stretching
911	906	-	Al-OH bending

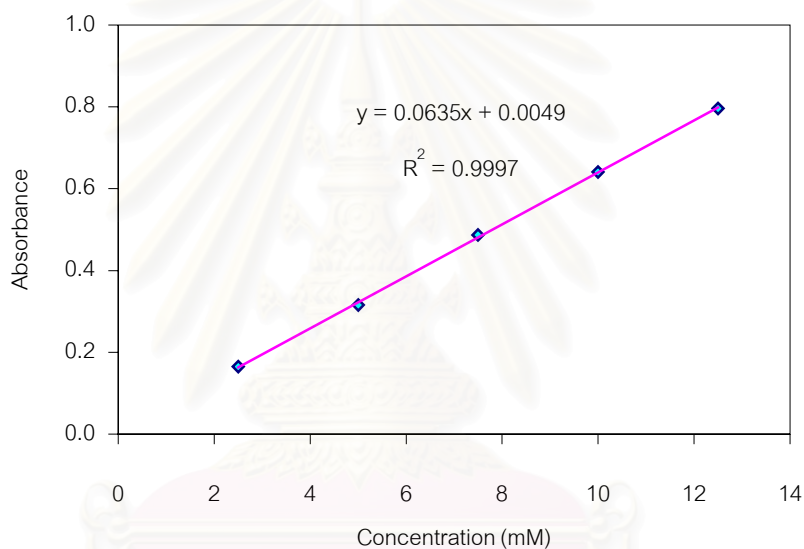
FT-IR spectra of three types of clays showed O-H octahedral stretching at 3624-3678 cm⁻¹, O-H octahedral bending at 1391-1396 cm⁻¹, Si-O tetrahedral stretching at 1015-1026 cm⁻¹ and Al-OH vibration at 906-911 cm⁻¹. The interpretations of the spectra were difficult at wavenumber below 900 cm⁻¹, because of the overlapping bands in this region.

5.1.4 Cation exchange capacity

Cation exchange capacity of clays was determined using copper bisethylenediamine complex (Cu(EDA)₂²⁺). Concentration of Cu(EDA)₂²⁺ was measured by UV-Vis spectrometry. A calibration curve of Cu(EDA)₂²⁺ was plotted. The result was indicated in [Table 5.3](#) and [Figure 5.3](#).

Table 5.3 UV-Vis data of Cu(EDA)_2^{2+} complex at $\lambda_{\text{max}} = 548 \text{ nm}$

Concentration of Cu(EDA)_2^{2+} (mM)	Absorbance
12.5	0.796
10.0	0.641
7.5	0.487
5.0	0.316
2.5	0.165

**Figure 5.3** Calibration curve of Cu(EDA)_2^{2+} complex at $\lambda_{\text{max}} = 548 \text{ nm}$.**Table 5.4** Cation exchange capacity of clays

Clay	Run no.	Absorbance ($\lambda_{\text{max}} = 548 \text{ nm}$)	CEC (meq/g)	CEC avg. (meq/g)
Bentonite	1	0.191	0.71	0.71
	2	0.191	0.71	
Kaolinite	1	0.495	0.23	0.24
	2	0.482	0.25	
Talcum	1	0.639	0.00	0.00
	2	0.640	0.00	

As seen from Table 5.4, the CEC of bentonite is higher than that of kaolinite. This is in good agreement with their structure and charge.^{10, 12} Bentonite is classified as smectite group, has a 2:1 layer type and amount of layer charge per formula unit ~ 0.2-0.6. The layers of kaolinite are electronically neutral (1:1 layer type) but it shows some CEC, this might be due to the existence of illite which has amount of layer charge per formula unit ~ 0.6-0.9 (see section 5.1.1). Talcum has no CEC as it has no layer charge.

5.2 Preparation and characterization of clay supported iron catalysts

The clay-supported iron catalysts prepared from ion-exchange process between cation of clays and iron solution were characterized by XRD, XRF and FTIR.

5.2.1 X-ray diffraction (XRD)

The XRD patterns of the clay-supported iron catalysts were illustrated in Figures 5.4 – 5.7.

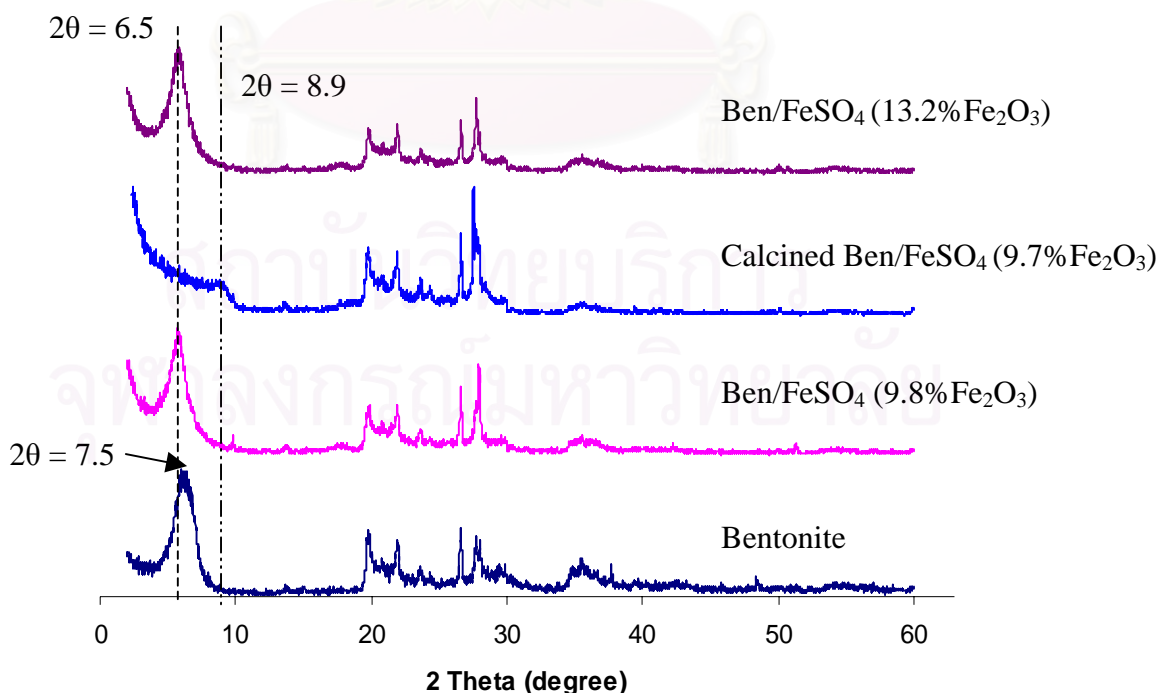


Figure 5.4 XRD patterns of bentonite supported iron(II) sulfate catalysts.

From Figures 5.4, XRD patterns of the clay supported iron(II) sulfate catalysts after calcinations revealed the disappearance of water adsorbed on clay, as seen from the increasing of 2θ values (from 6.5 to 8.9 degree) or in other words, d_{001} -spacing values of calcined catalyst decreased from 13.6 to 10.0 Å. For the uncalcined iron catalysts, the results showed that after loading iron onto the bentonite, the 2θ angles shift slightly to lower values (from 7.5 to 6.5 degree). This could be an evidence of the intercalation of iron into the clay structure. As seen in previous report,⁴⁷ $Mn_2C_{38}N_6H_{42}Br_4$ complex could be intercalated into the montmorillonite interlayer by using cation exchange process and it was found that the d_{001} -spacing shifted from 12.2 to 13.7 Å. However, for higher angle, 2θ values 35.6, the ambiguity result was found, this is due to the overlapping peak of montmorillonite and iron oxide phase.

Figures 5.5 shows XRD patterns of the bentonite supported iron(III) compound catalysts.

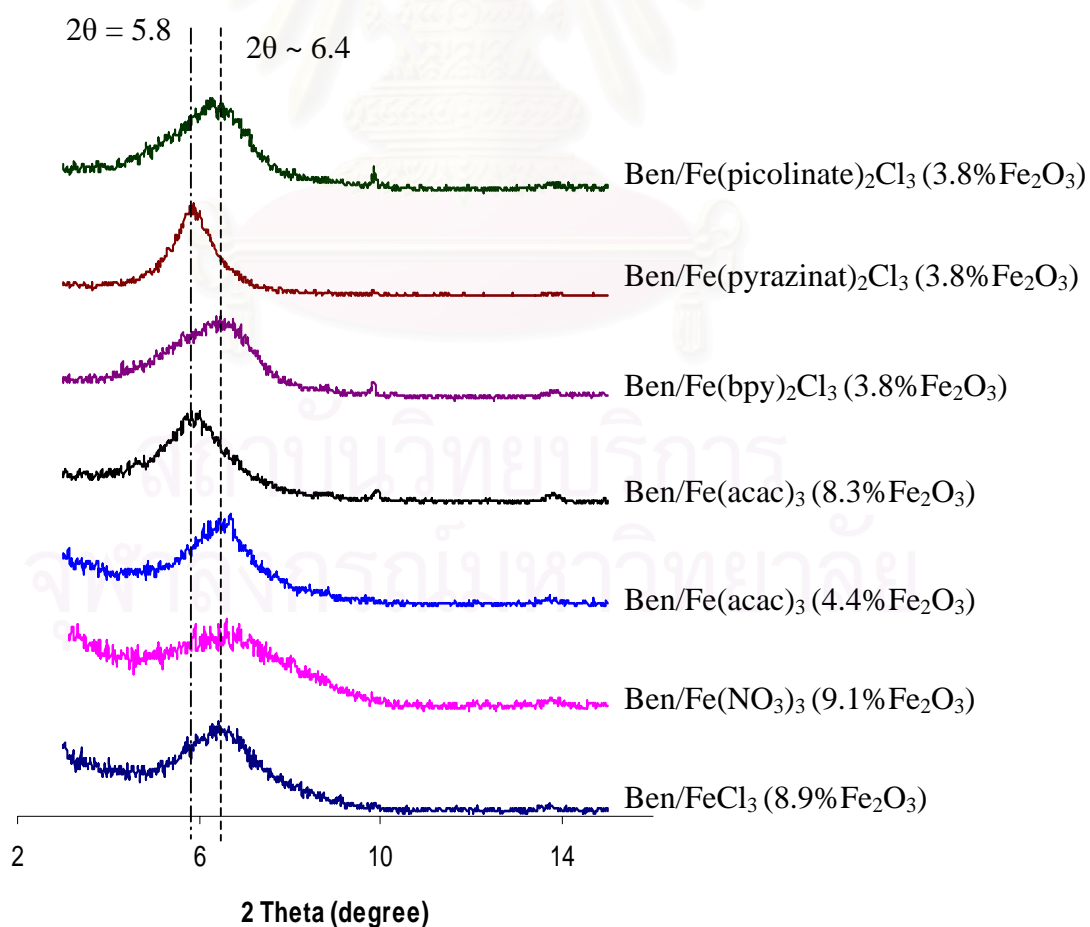


Figure 5.5 XRD patterns of bentonite supported iron(III) compound catalysts.

The XRDs were all similar except Ben/Fe(acac)₃ (8.3%Fe₂O₃) and Ben/Fe(pyrazinate)₂Cl₃. These results showed that types of iron compound have no effect on the layer structure of bentonite.

For the Ben/Fe(acac)₃ with 8.3%Fe₂O₃ and Ben/Fe(pyrazinate)₂Cl₃ catalysts, different results were observed, there was a drastic increase of d-spacing. For the former case, it might be due to a large amount of the iron(III) acetylacetonate molecules intercalated between the clay surfaces, causing an increase of d-spacing. In the latter case, it was thought that more iron complexes were formed between the layers of clay structure, this was also noticed from the color change while mixing Fe-clay with ligand solution.

Figure 5.6 shows XRD patterns of the kaolinite supported iron whereas Figure 5.7 shows XRD patterns of the talcum supported iron(II) sulfate.

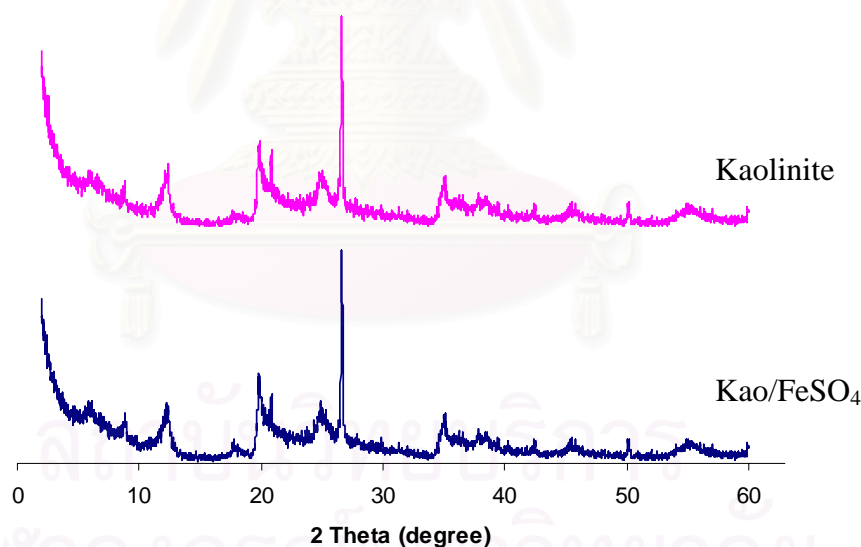


Figure 5.6 XRD patterns of kaolinite supported iron(II) sulfate catalysts.

The XRD patterns of kaolinite supported catalysts revealed that the layer structure remained unchanged when clays supports were loaded with iron compound. The same result was observed in the case of talcum supported iron catalyst (Figure 5.7).

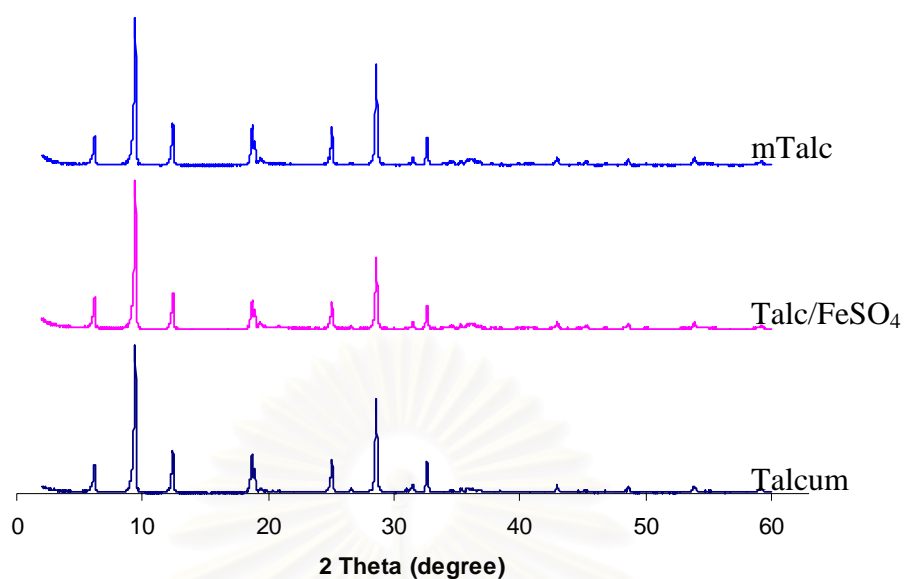


Figure 5.7 XRD patterns of talcum supported iron(II) sulfate catalysts.

For the attempt to modify surface of talcum with silane, from comparison between mTalc and talcum XRD patterns, it was shown that they are similar, 2θ values unchanged. These indicated that the silane could not intercalate into layer structure of talcum. This result was different from previous report,⁵⁰ which used aminated trialkoxysilane as modifier. It might be caused by different size of intercalant.

5.2.2 X-ray fluorescence (XRF) and atomic absorption spectrometer (AAS)

The iron content in the bentonite-supported iron catalysts was determined either by XRF or AAS, shown in [Table 5.5](#).

Table 5.5 The iron content in the clay supported iron catalysts using XRF and AAS

Catalysts	Loaded iron mmol/g	Iron content (% weight Fe ₂ O ₃)	
		XRF	AAS
Ben/FeSO ₄	1.1	10.0	8.8
Ben/FeSO ₄	2.2	11.5	9.8
Calcined Ben/FeSO ₄	2.2	11.4	9.7
Ben/FeSO ₄	4.4	-	13.2
Ben/FeCl ₃	0.75	9.7	8.9
Ben/FeCl ₃	1.5	-	10.5
Calcined Ben/FeCl ₃	1.5	-	10.4
Ben/Fe(NO ₃) ₃	0.75	-	9.1
Ben/Fe(acac) ₃	0.3	-	3.5
Ben/Fe(acac) ₃	0.75	-	4.4
Calcined Ben/Fe(acac) ₃	0.75	-	4.4
Ben/Fe(acac) ₃	1.5	-	8.3
Ben/Fe(bpy) ₂ Cl ₃	0.12	-	3.8
Ben/Fe(pyrazinate) ₂ Cl ₃	0.12	-	3.8
Ben/Fe(picolate) ₂ Cl ₃	0.12	-	3.8
Kao/FeSO ₄	2.2	-	4.4
Talc/FeSO ₄	2.2	-	2.3
SiO ₂ /FeSO ₄	0.16	-	0.6
SiO ₂ /FeSO ₄	0.79	-	5.0

From XRF and AAS results, the iron content in the catalyst depended on amount of iron loading. Therefore bentonite supported iron(II) sulphate catalysts loaded with different amount of iron solution possess iron content of 8.8, 9.8 and 13.2%, respectively. The same trend was observed in bentonite supported iron(III) chloride and iron(III) acetylacetonate catalysts. It can also be seen that calcination of the catalyst does not affect iron content.

When using different type of iron compound supported onto clay, the results showed that for iron(III) compounds, the iron content on the clay supports were not different, $\text{FeSO}_4 \sim \text{FeCl}_3 \sim \text{Fe}(\text{NO}_3)_3$ (8.8, 8.9, 9.1 % Fe_2O_3 , respectively). On the contrary, for $\text{Fe}(\text{acac})_3$, the iron content was much lower (4.4% Fe_2O_3). This might be due to the hindrance of the acetylacetonate ligand which made it difficult to access into layer clay.

Compared the type of clay, the iron content of different clays increased in the following order: $\text{Ben}/\text{FeSO}_4 > \text{Kao}/\text{FeSO}_4 > \text{Talc}/\text{FeSO}_4$ (9.8, 4.4 and 2.3% Fe_2O_3 respectively). This agreed well with cation exchange capacity (CEC) data.

For silica support, the iron content also depended on amount of loading iron.

5.2.3 Fourier transform infra-red spectrometer (FT-IR)

After iron was loaded onto clay, the catalysts obtained were characterized by FT-IR. Effect of iron loading was shown in Table 5.6.

Table 5.6 The assignment for the FT-IR spectra of bentonite supported iron(II) sulfate catalysts

Catalyst	Iron content (% Fe_2O_3)	wave number (cm^{-1})			
		O-H stretching	O-H bending	Si-O stretching	Al-O vibration
Bentonite	3.0	3624	1396	1026	911
Ben/FeSO_4	8.8	3625	1398	1040	920
Ben/FeSO_4	9.8	3624	1402	1042	917
Ben/FeSO_4	13.2	3624	1402	1042	922

From Table 5.6, the bentonite supported iron(II) sulfate catalysts with different amount of iron were observed by FT-IR technique. The results indicated that the absorption bands of O-H bending (1398 and 1402), and Si-O stretching (1042) shift to higher values resulting from the incorporation of metal and formation of Si-O-Fe

bonds when comparing with bentonite.⁵¹ However, amount of iron content in the clay did not affect FT-IR spectrum.

FT-IR spectra of various supported on bentonite were shown in Figure 5.8 and summarized in Table 5.7.

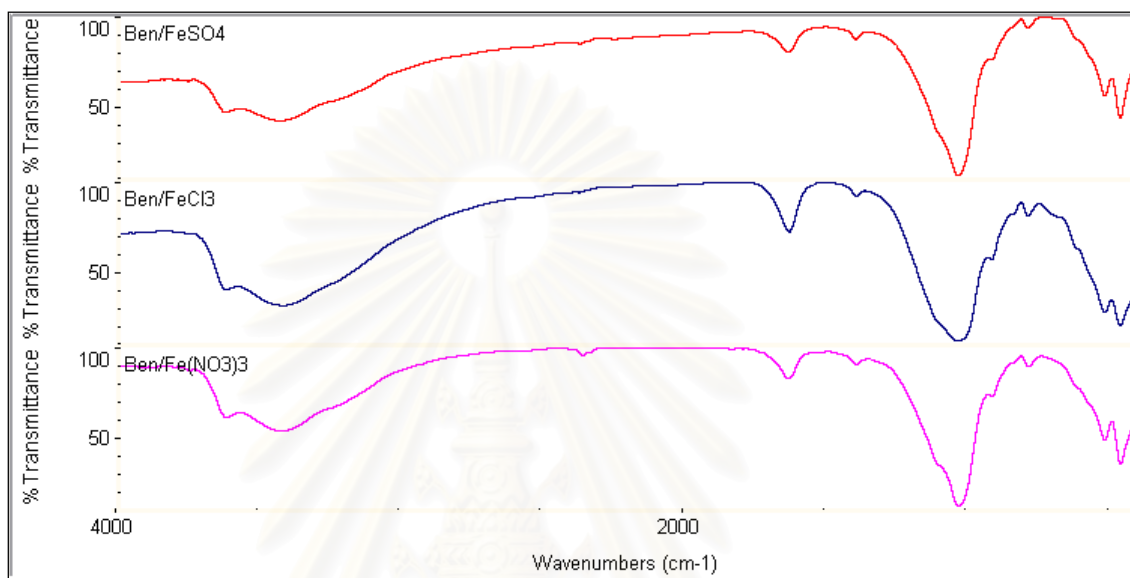


Figure 5.8 FT-IR spectra of bentonite supported FeSO₄, FeCl₃ and Fe(NO₃)₃ catalysts.

Table 5.7 The assignment for the FT-IR spectra of bentonite supported iron compound catalysts

Wave number (cm ⁻¹)			Assignment
Ben/FeSO ₄	Ben/FeCl ₃	Ben/Fe(NO ₃) ₃	
3624	3624	3627	O-H stretching
1402	1402	1398	O-H bending
1042	1042	1042	Si-O stretching
917	917	917	Al-O vibration

For all three bentonite supported iron catalysts, the absorption bands were shifted to higher wave numbers. These results indicated the incorporation of metal.⁵¹ The similar results were found in the calcined catalysts. However, when comparing

the FT-IR spectra of bentonite supported iron(III) acetylacetonate catalysts with and without calcination, different result was obtained, see Figure 5.9.

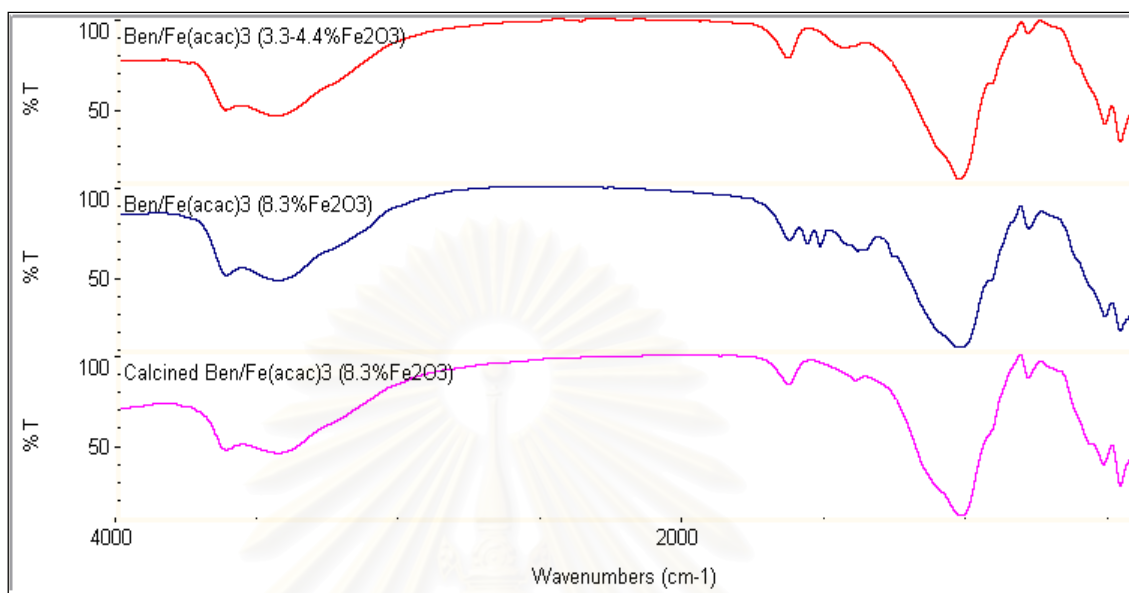


Figure 5.9 FT-IR spectra of uncalcined and calcined Ben/Fe(acac)₃ catalysts.

Table 5.8 The assignment for the FT-IR spectra of bentonite supported iron(III) acetylacetonate catalysts

Wave number (cm ⁻¹)			Assignment
Ben/Fe(acac) ₃ (3.3-4.4 %Fe ₂ O ₃)	Ben/Fe(acac) ₃ (8.3 %Fe ₂ O ₃)	Calcined Ben/Fe(acac) ₃ (8.3 %Fe ₂ O ₃)	
3624	3624	3624	O-H stretching
1400	1402	1402	O-H bending
-	1565	-	C=O stretching
-	1521	-	CH ₃ stretching
1042	1042	1042	Si-O stretching
917	917	917	Al-O vibration

Ben/Fe(acac)₃ catalysts were prepared to possess various amount of iron: 3.3, 3.5 4.4 and 8.3 %Fe₂O₃. It could be seen that only the sample of high amount of iron (8.3 % Fe₂O₃) peaks belonging to acetylacetonate ligand could be observed, CH₃ stretching at 1521 cm⁻¹ and C=O stretching at 1565 cm⁻¹. Absorption peaks of bentonite were found at 3624, 1402, 1042 and 917 cm⁻¹. But after calcination, the acetylacetonate absorption peak disappeared.

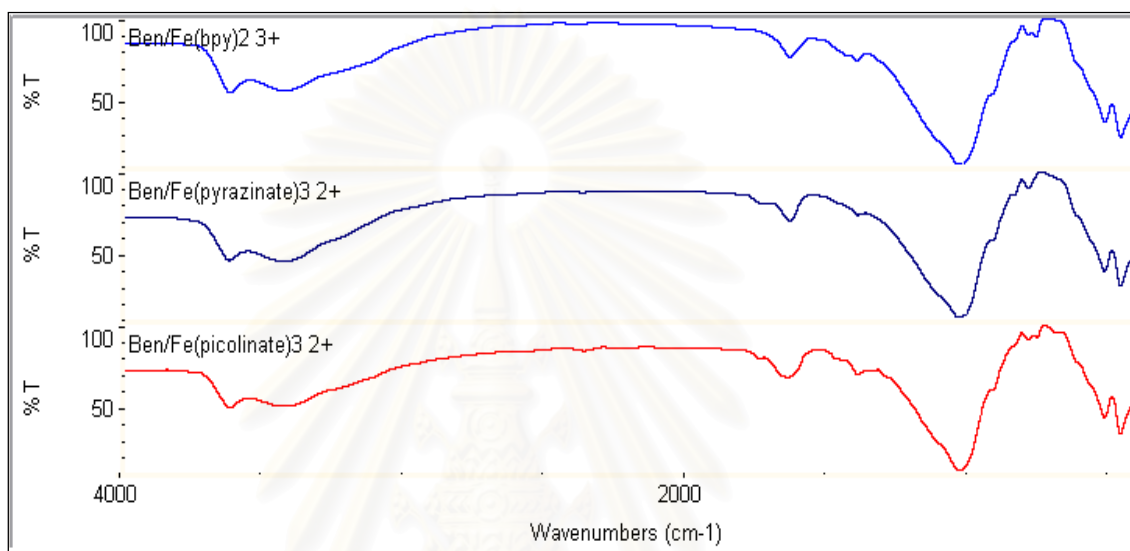


Figure 5.10 FT-IR spectra of bentonite supported Fe(bpy)₂Cl₃, Fe(pyrazinate)₂Cl₃ and Fe(picolinate)₂Cl₃ catalysts.

Table 5.9 The assignment for the FT-IR spectra of bentonite supported iron(III) complex catalysts

Wave number (cm ⁻¹)			Assignment
Ben/ Fe(bpy) ₂ Cl ₃	Ben/(pyrazinate) ₂ Cl ₃	Ben/(picolinate) ₂ Cl ₃	
3624	3624	3624	O-H stretching
-	1747	1742	C=O stretching
1400	1400	1400	O-H bending
1042	1042	1042	Si-O stretching
917	917	917	Al-O vibration

The FT-IR spectra in [Figure 5.10](#) showed absorption peak of bentonite, O-H stretching at 3627 cm^{-1} , O-H bending at 1400 cm^{-1} and Si-O stretching at 1042 cm^{-1} , respectively. The C=O stretching absorption peak of the ligand could be observed at 1747 and 1742 cm^{-1} for Ben/Fe(pyrazinate) $_2\text{Cl}_3$ and Ben/Fe(picolate) $_2\text{Cl}_3$ respectively.

FT-IR spectra of kaolinite supported iron compound catalysts were indicated in [Figure 5.11](#) and [Table 5.10](#).

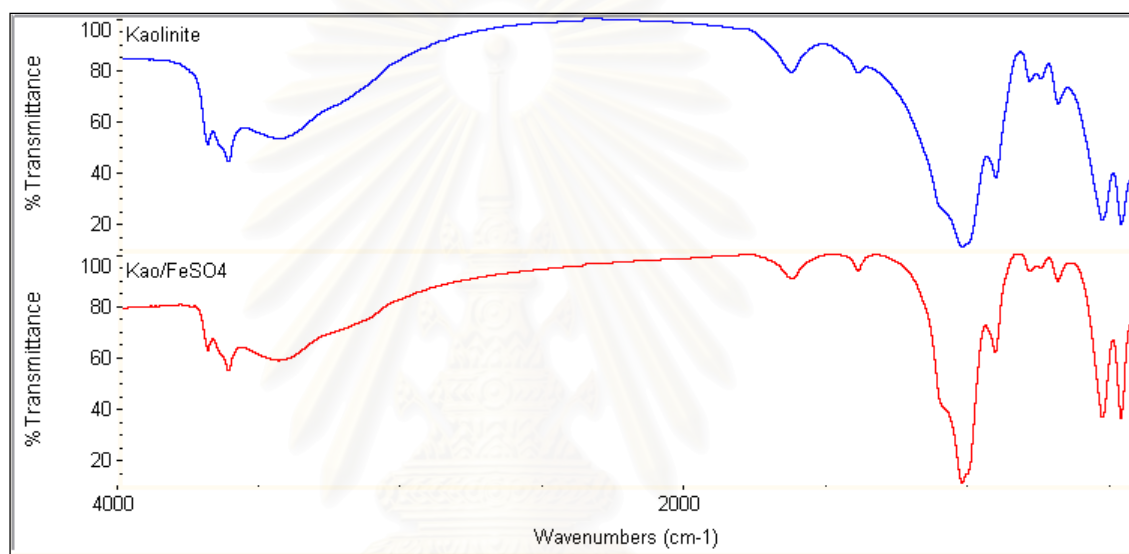


Figure 5.11 FT-IR spectra of kaolinite and Kao/FeSO $_4$ catalysts.

Table 5.10 The assignment for the FT-IR spectra of kaolinite and Kao/FeSO $_4$

Wave number (cm^{-1})		Assignment
Kaolinite	Kao/FeSO $_4$	
3618	3618	O-H stretching
1396	1396	O-H bending
1031	1037	Si-O stretching
906	911	Al-OH bending

It was observed that the absorption band shifted to higher wave numbers. It could be concluded in the same way as bentonite-supported iron compounds that metal was incorporated and Si-O-Fe bonds were formed.

Figure 5.12 and Table 5.11 shows FT-IR spectra of the talcum supported iron compound catalysts.

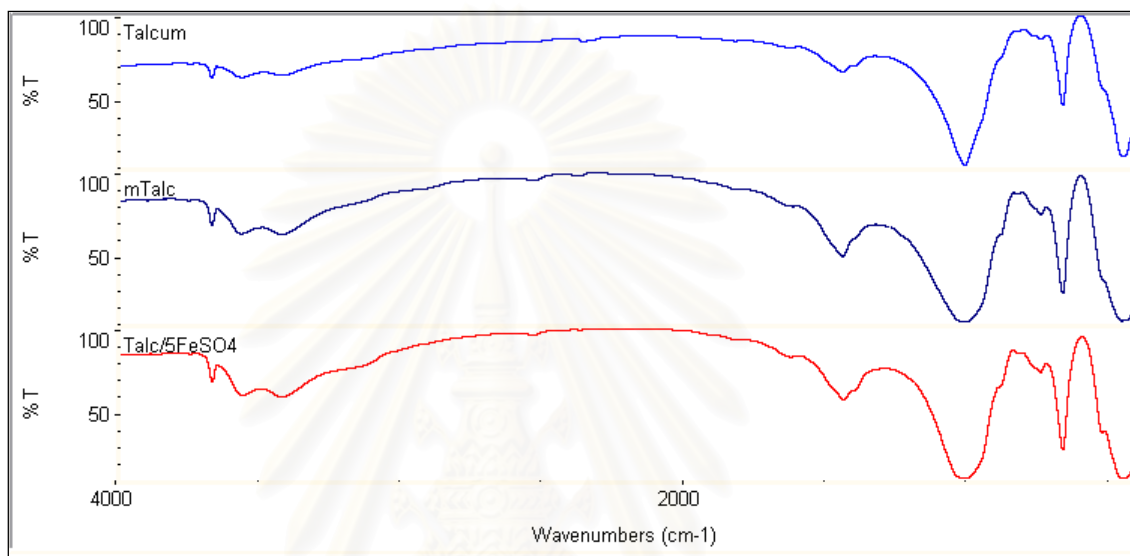


Figure 5.12 FT-IR spectra of talcum, mTalc and Talc/FeSO₄ catalysts.

Table 5.11 The assignment for the FT-IR spectra of talcum, mTalc and Talc/FeSO₄

Wave number (cm ⁻¹)			Assignment
Talcum	mTalc	Talc/FeSO ₄	
3678	3678	3678	O-H stretching
1444	1444	1444	O-H bending
1015	1015	1015	Si-O stretching

FT-IR of talcum showed O-H octahedral stretching at 3678 cm⁻¹, O-H octahedral bending at 1444 cm⁻¹ and Si-O tetrahedral stretching at 1015 cm⁻¹, respectively.

Attempt to modify talcum with silane was not successful. FT-IR spectrum reveals the original talcum. The result was in agreement with the XRD result (see Figure 5.7).

5.2.4 Cation exchange capacity (CEC)

To investigate site of loaded iron in the catalysts, CEC of the catalysts was determined and the results were indicated in Table 5.12.

Table 5.12 Cation exchange capacity of catalysts

Entry	Catalyst	Fe ₂ O ₃ (% weight)	CEC avg. (meq/g)
1	Ben/FeSO ₄	9.8	0.70
2	Calcined Ben/FeSO ₄	9.7	0.58
3	Ben/FeSO ₄	13.2	0.66
4	Ben/FeCl ₃	8.9	0.71
5	Ben/FeCl ₃	10.5	0.70
6	Ben/Fe(acac) ₃	3.5	0.70
7	Ben/Fe(acac) ₃	4.4	0.63
8	Ben/Fe(acac) ₃	8.3	0.59

In the literature, there was a report about the iron species in iron supported on clay.⁵² The data from electron spin resonance (ESR) technique showed that there were different species of iron present. One type was isolated iron species located in the layer of the clay, which is probably resulted from the substitution on aluminium atom in octahedral unit. This type of iron species will show comparable CEC to the original clay. The second one was iron species belonging to oxide clusters which might reside on surface of the clay layer. The third type was isolated iron species as extra-framework species or intercalating between clay layers and balanced the charge on clay. For the both latter species, CEC of the catalysts would be decreased when compared with raw clay.

From the present results, it was observed that the catalysts containing low iron content had comparable CEC to the starting clay. These might be discussed that most iron species resided between clay layers and could be re-exchanged with copper ion in the CEC testing solution.

On the contrary, the catalysts containing high iron content had decreasing CEC values compared to the starting clay. This indicated that coagulation of iron and iron cluster were formed on the clay surface.

Comparison between uncalcined and calcined catalyst in entries 1 and 2, the calcined catalyst showed smaller CEC because the pillar iron oxide was formed when the catalyst was calcined at high temperature (300°C).

5.2.5 Scanning electron microscope (SEM)

The principle of SEM is based on irradiation of sample by a focused electron beam, which results in imaging of secondary or back-scattered electrons and energy analysis of x-rays for view and cross-section surface imaging and composition analysis of sample.

The morphology of the catalysts with SEM was investigated. The results were collected in [Figure 5.13](#).

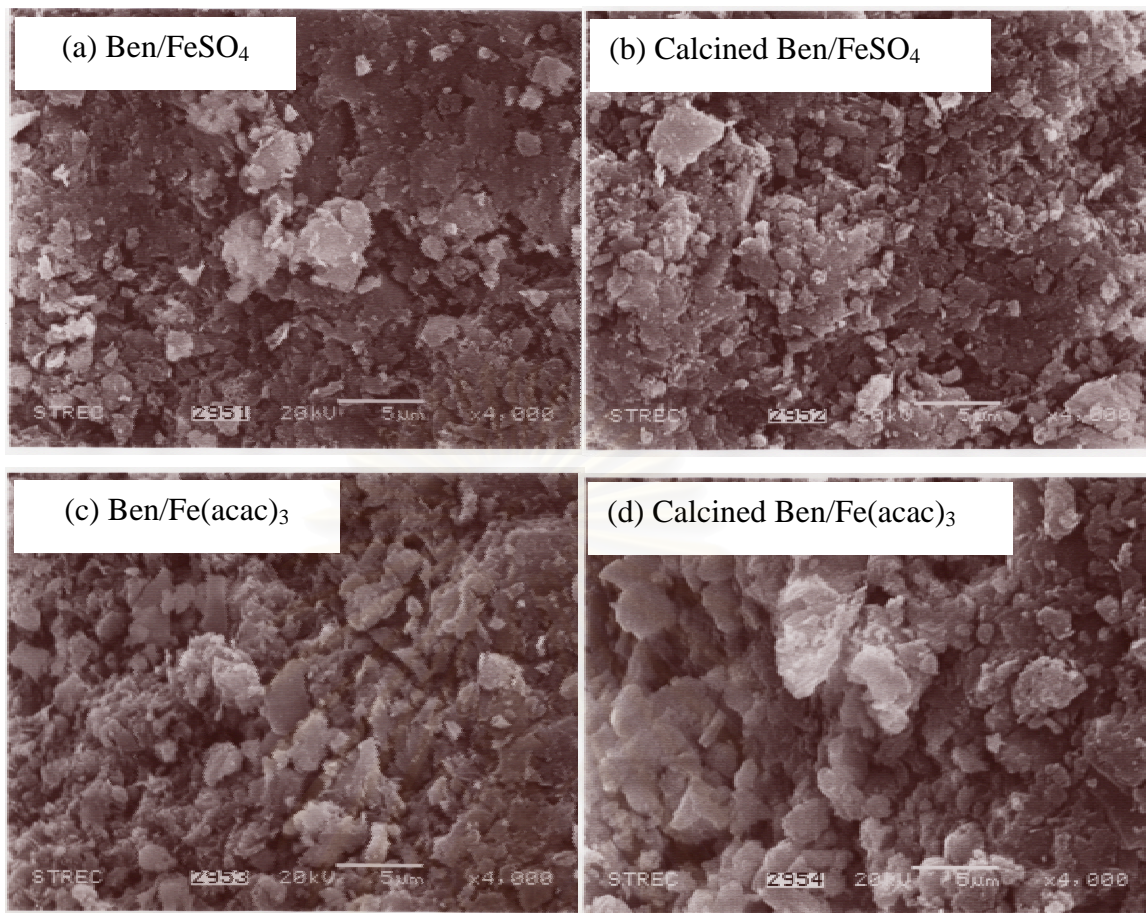


Figure 5.13 SEM photographs of the bentonite supported iron catalysts.

SEM photographs of the catalysts reveal layer structure. These confirmed that loaded iron did not destroy clay structure.

In addition, energy dispersive x-ray (EDX) was used to determine the chemical composition of a microscopic area of a solid sample. From qualitative EDX results it can be seen that the catalysts had iron species on the surface.

X-ray mapping of the catalysts shows iron distributions on the surface. From x-ray mapping photographs in [Figure 5.14](#), the left-hand picture shows sites of iron species while the right-hand one shows SEM photograph. All catalyst exhibited good iron distribution on the surface.

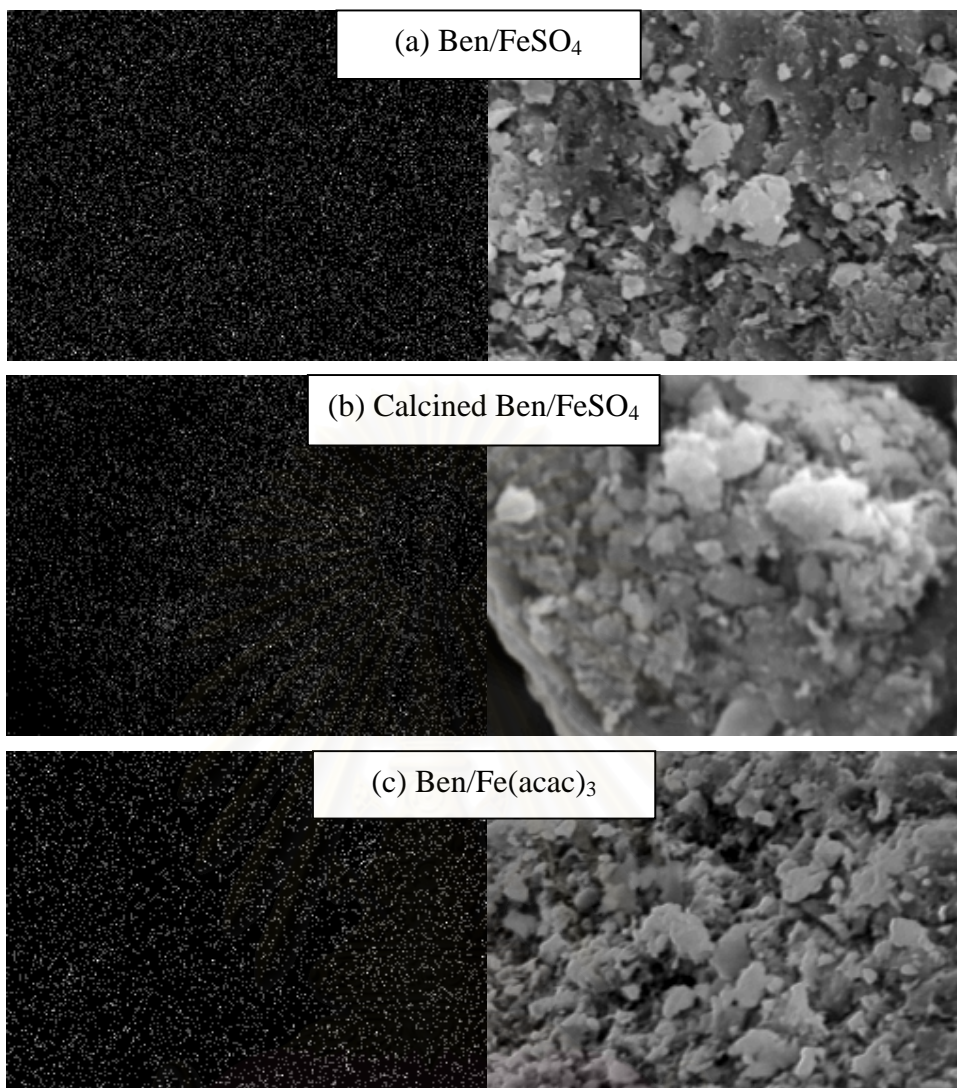


Figure 5.14 Iron distributions on surface of the bentonite supported iron catalysts.

5.2.6 Nitrogen adsorption/desorption (Brunauer-Emmett-Teller method, BET)

Nitrogen adsorption/desorption is a commonly applied technique to determine various characteristics of porous materials. The most widely used procedure for the determination of the surface area of porous materials is the Brunauer-Emmett-Teller (BET) method. The BET surface area is calculated by constructing the so-called BET plot using the relative pressure. In BET method, a single layer of nitrogen molecules is formed on the surface (monolayer).

BET specific surface areas of Ben/Fe(acac)₃ catalysts were indicated in [Table 5.13](#).

Table 5.13 BET specific surface area of Ben/Fe(acac)₃ catalysts

Catalyst	Iron content (%weight Fe ₂ O ₃)	Specific surface area (BET) (m ² g ⁻¹)
Bentonite	3.0	58
Ben/Fe(acac) ₃	3.5	71
Ben/Fe(acac) ₃	8.3	52

The results showed when iron content increased, specific surface areas of the catalysts were decreased. This might be explained by agglomeration of iron species on the clay surface.⁵³

5.3 Preparation and characterization of goethite

As previously reported that the bentonite supported iron nitrate catalyst had some goethite particle as inhomogeneous composition,⁵⁴ in this work, goethite was synthesized and investigated its activity in cyclooctane oxidation. Goethite is iron oxide hydroxide mineral, α -Fe^{III}O(OH). The synthesized goethite was characterized by XRD and FT-IR.

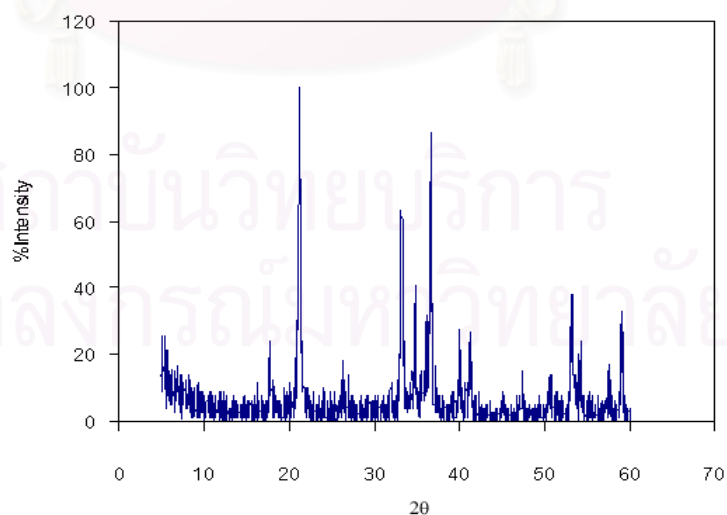
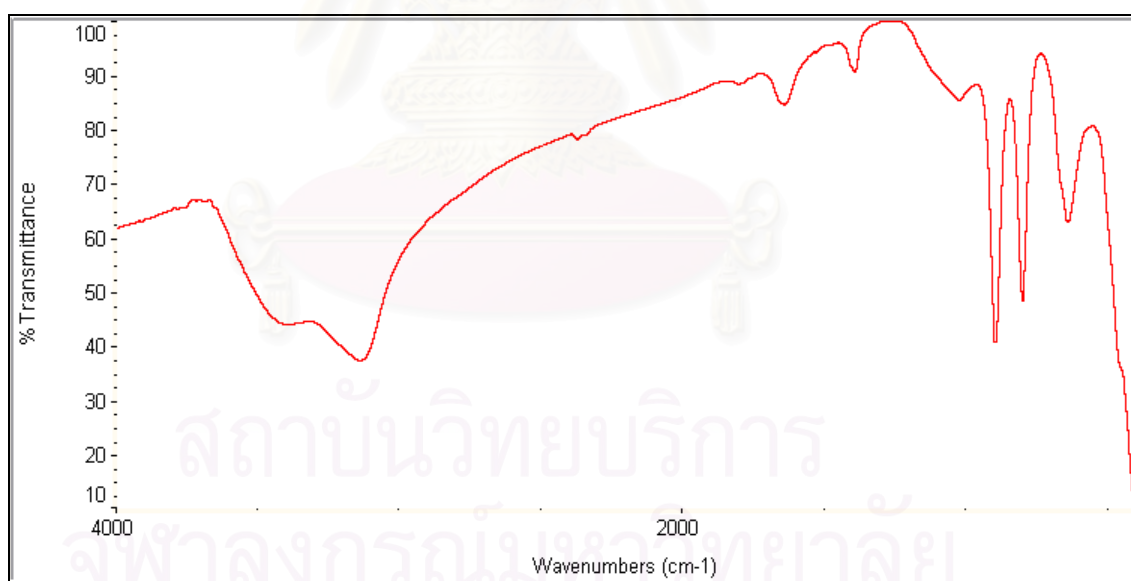
**Figure 5.15** XRD pattern of goethite.

Table 5.14 XRD data of goethite

2θ (degree)	d (Å)
100.0	4.2
61.3	2.7
36.0	2.6
81.3	2.4
25.3	2.3
25.3	2.2
32.0	1.7
25.3	1.6

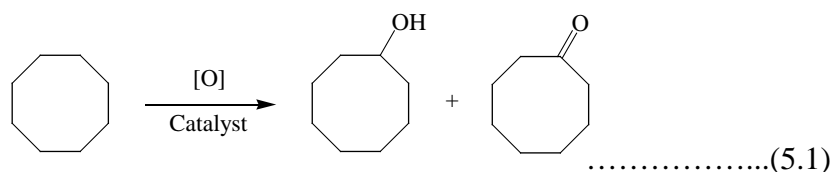
The XRD pattern of the synthesized goethite exhibited single phase of goethite.⁴⁸ From the FTIR result in Figure 5.16, it could be observed the absorption band of O-H stretching at 3424 cm^{-1} and O-H bending at 1383 cm^{-1} .

**Figure 5.16** FT-IR spectrum of goethite.

5.4 Oxidation of cyclooctane

Oxidation of cyclooctane was performed to compare the catalytic efficiency of the prepared supported catalysts. % Yield of products was derivable from GC results

and showed the existence of cyclooctanol and cyclooctanone. All yields were based on cyclooctane substrate.



The parameters studied were iron amount, oxidant types, oxidant amount, solvent types, and reaction time.

5.4.1 Optimization of reaction condition

A. Effect of iron amounts

Cyclooctane oxidation was performed using bentonite supported iron(II) sulfate catalysts which contain different amount of iron. Weight of catalyst as fixed at 0.4 g, amount of iron was calculated according based on its iron content (see [Table 5.5](#)). Products of cyclooctane oxidation were shown in [Table 5.15](#).

Table 5.15 Oxidation of cyclooctane using iron(II) sulfate supported on bentonite catalysts

Entry	Catalyst	Amount of iron (mmol)	% Conversion	%Selectivity	
				-none	-nol
1	Bentonite	0.17	3	68	32
2	Ben/FeSO ₄	0.44	13	89	11
3	Ben/FeSO ₄	0.49	6	81	19
4	Calcined Ben/FeSO ₄	0.49	6	73	27
5	Ben/FeSO ₄	0.66	3	90	10
6	Calcined Ben/FeSO ₄	0.66	3	79	21

Condition: catalyst 0.40 g, cyclooctane 20 mmol, TBHP 10 mmol, 24 hours, 70°C,

The catalyst was calcined at 300°C for 5 hours.

It could be seen that bentonite alone is able to catalyze oxidation of cyclooctane. This might be due to the iron impurity in bentonite.

The activity test revealed that amount of the metal on the support affected catalytic activity. The catalyst with 0.44 mmol of iron showed high %conversion (entry 2). Activity was decreased when iron loaded was increased beyond 0.44 mmol (entries 3 and 5). It was reported that high catalytic activity was obtained with low concentration of the catalyst.³⁹

It was reported that concentration of iron in preparative procedure of iron oxide affected catalytic activity, the diluted iron solution (0.5 M) resulted in the smaller sized iron oxide and provided higher %conversion than the 1.0 M solution.³⁷

For high iron loading, aggregation of the iron was occurred and lower catalytic activity was obtained.²⁷ In silica support it was found that when amount of iron content was decreased ten-fold, catalytic activity was drastically increased.⁵⁵

In the case of product selectivity, for the calcined catalysts, it was found that selectivity to cyclooctanone decreased whereas selectivity to cyclooctanol increased (entries 3 vs. 4, and 5 vs. 6). It might be explained by hydrophilicity of clay surface.¹² In general, molecules of water always solvate around cations which intercalate into layer structures of clay and it will be lost by calcination method. This is also seen in XRD results in this work, section 5.2.1.

Uncalcined catalysts had higher hydrophilicity than calcined ones therefore cyclooctanol which is polar will favor to reside longer time on the surface of clay and reacted further to produce cyclooctanone.⁵⁶

In the literature, low conversions of the heterogeneous catalysts were usually observed. For example, in cyclohexane oxidation, limited catalytic activity was found. Zeolite Y supported-iron phthalocyanin catalyst could catalyze cyclohexane oxidation. Yield of 8% was obtained when the reaction was performed in acetone for

4 hours, using 0.1 g of the catalyst (9.2 μmol of iron) and 9.2:7.3 mol ratio of cyclohexane:TBHP.³³

Cyclohexane oxidation was previously reported using copper containing silicate catalyst in the presence of TBHP oxidant for 24 hours at 75°C. The results showed yield of 4.3% when used 0.1 g catalyst with 0.29 μmol of copper, cyclohexane (95 mmol) and TBHP (9.5 mmol).⁵¹

B. Effect of oxidant types

Effect of oxidant was investigated. Traditional oxidants such as chromate or permanganate are rather inefficient and show low selectivity in alkane oxidation.⁵⁷ Therefore in this work, 70% *tert*-butyl hydroperoxide, 30% hydrogen peroxide and iodosobenzene were investigated and compared with KMnO_4 . The results were indicated in Table 5.16.

Table 5.16 Effect of oxidants for cyclooctane oxidation using calcined Ben/ FeSO_4 catalyst

Entry	Oxidant	Solvent	%Conversion	%Selectivity	
				-none	-nol
1	70% TBHP	-	6	73	27
2	30% H_2O_2	-	0	0	0
3	PhIO	Acetone	0	0	0
4	KMnO_4	Acetone	0	0	0

Condition: catalyst 0.40 g (iron 0.49 mmol), cyclooctane 20 mmol and oxidant 10 mmol, 24 hours

The results showed that *tert*-butyl hydroperoxide gave more %conversion than other solvents tested while hydrogen peroxide, iodosobenzene and permanganate could not catalyze the oxidation. These agreed with that report,⁵⁸ *tert*-butyl hydroperoxide showed higher %conversion than H_2O_2 in cyclohexane oxidation using iron(II) salophen complex catalyst (10.6 and 5.1 %conversion, respectively). The

reaction was performed in mixed pyridine and acetonitrile (cyclohexane:oxidant:catalyst = 120:60:1 mole ratio). It should be mentioned that in the case of using H₂O₂, catalytic activity is limited due to the tendency of H₂O₂ to decompose when use supported iron compound.^{24, 44}

It was reported that iron porphyrin supported on montmorillonite gave 0.01 and 2 %conversion in cyclohexane oxidation using H₂O₂ and PhIO oxidants for 4 hours when the reaction performed in mixed dichloromethane/acetonitrile by using the catalyst with iron 2.3 %weight, 1:20 mol ratio of catalyst:PhIO.³⁹ Besides that iron porphyrin immobilized on silanized kaolinite was used to catalyze the oxidation in previous report.⁴⁴ The reaction was performed at room temperature for 6 hours, 20 mg of the catalyst with iron 12 µmol/g and 1:10 mole ratio of catalyst:oxidant in dichloromethane, the result showed 0.1 %conversion.

In this work, when using permanganate oxidant, it was observed brown precipitate of magnesium dioxide, occurred from the reduction of permanganate.¹³

C. Effect of oxidant amount

Effect of oxidant amount was collected in [Table 5.17](#).

Table 5.17 Oxidation of cyclooctane using calcined Ben/FeSO₄ catalyst

Entry	Amount of TBHP (mmol)	%Conversion	%Selectivity	
			-none	-nol
1	5	2	71	29
2	10	3	75	25
3	20	8	79	21
4	40	11	82	18

Condition: catalyst 0.4 g (iron 0.49 mmol), cyclooctane 20 mmol, acetonitrile 11.5 mL and pyridine 3.5 mL as solvent, 24 hours, 70°C

Following previous result,²² mixed solvent (acetonitrile: pyridine ratio 23: 7 v/v) was selected to study oxidation of cyclooctane with varying amount of oxidant. From Table 5.17, the result on the effect of oxidant amount indicated that the %conversion was enhanced with increasing amount of oxidant. This result agrees with the previous report,²¹ oxidation of cyclohexane using bis(ethylenediamine)copper(II) nitrate dihydrate catalyst at 70°C for 24 hours. The oxidation products were increased from 0 to 5.9% when *tert*-butyl hydroperoxide was increased from 0 to 15 mmol, respectively.

D. Effect of solvent types

The solvent effect was investigated using acetone, dichloromethane, and acetonitrile/pyridine (7.7:2.3), and acetonitrile. The results were collected in Table 5.18.

Table 5.18 Effect of type of solvents for cyclooctane oxidation using calcined Ben/FeSO₄ catalyst

Entry	Solvent (mL)	%Conversion	%Selectivity	
			-none	-nol
1	-	6	73	27
2	Acetone (10)	5	84	16
3	CH ₃ CN:Py (7.7:2.3)	3	76	24
4	CH ₂ Cl ₂ (10)	1	77	23
5	CH ₃ CN (10)	1	87	13

Condition: catalyst 0.40 g (iron 0.49 mmol), cyclooctane 20 mmol, TBHP 10 mmol, 24 hours, 70°C

The results show that the oxidation could occur in the absence of solvent. This was an advantage of this system. For acetone, even though it gave moderate %conversion (entry 2), but it is easy to volatile. Other solvents tested, dichloromethane, acetonitrile and mixed solvent (acetonitrile/ pyridine) showed lower %conversion. The catalytic activity was found to be depended on type of solvent.

It was reported that acetone is better solvent than acetonitrile and dichloromethane when using iron(III)-alumina catalysts for benzene oxidation at 60°C for 6 hours and using 10:1 mol ratio of H₂O₂:benzene.⁵⁹

E. Effect of reaction time

Oxidation of cyclooctane was monitored with time, the results were shown in [Table 5.19](#).

Table 5.19 Effect of time for cyclooctane oxidation using calcined Ben/FeSO₄ catalyst

Entry	Reaction time (hrs)	% Conversion	%Selectivity	
			-none	-nol
1	24	3	80	20
2	48	3	79	21
3	72	5	79	21

Condition: catalyst 0.40 g (iron 0.66 mmol), cyclooctane 20 mmol, TBHP 10 mmol, and acetone 10 mL as solvent, 70°C

%Conversion was increased slowly with time but %selectivity was not changed. These suggested that cyclooctanol and cyclooctanone products were simultaneously formed.

5.4.2 Bentonite supported iron compound catalysts

The results of cyclooctane oxidation using iron(III) chloride and iron(III) nitrate supported on bentonite are collected in [Table 5.20](#).

Table 5.20 Oxidation of cyclooctane using iron(III)chloride supported on bentonite catalysts

Entry	Catalyst	Amount of iron (mmol)	%Conversion	%Selectivity	
				-none	-nol
1	Ben/FeCl ₃	0.45	11	78	22
2	Ben/FeCl ₃	0.52	5	80	20
3	Calcined Ben/FeCl ₃	0.52	5	77	23

Condition: catalyst 0.40 g, cyclooctane 20 mmol, TBHP 10 mmol, 24 hours, 70°C

When the amount of iron content in the catalyst increased, %conversion decreased, this might be explained by agglomeration of iron on support increased when large amount of iron solution was loaded onto clay in the preparation method (entries 1 and 3). It was reported that when an aqueous solution of iron(III) chloride was kept for a long time, goethite separates due to hydrolysis.⁴⁶ Thus, when the solution was stirred for a long time with bentonite for ion exchange, it was believed that the deposited species might be goethite.

To investigate iron compound type affecting the oxidation of cyclooctane, activity of different iron compound supported on bentonite catalysts were compared and shown in Table 5.21.

Table 5.21 Results from different types of iron catalysts

Entry	Catalyst	Amount of iron (mmol)	%Conversion	%Selectivity	
				-none	-nol
1	Ben/FeSO ₄	0.44	13	89	11
3	Ben/FeCl ₃	0.45	11	78	22
5	Ben/Fe(NO ₃) ₃	0.46	13	76	24

Condition: catalyst 0.40 g, cyclooctane 20 mmol, TBHP 10 mmol, 24 hours, 70°C

The results indicated that Fe(II) and Fe(III) had comparable activity. This result might be explained that iron(II) was transformed to iron(III) in the preparation

process, the same explanation was reported for iron(II) sulfate added into alumina support.⁵⁹

5.4.3 Bentonite supported iron(III) complex catalysts

The results of cyclooctane oxidation using bentonite supported iron(III) acetylacetonate catalysts were demonstrated in Table 5.22.

Table 5.22 Oxidation of cyclooctane using bentonite supported iron(III) acetylacetonate catalyst

Entry	Catalyst	Amount of iron (mmol)	%Conversion	%Selectivity	
				-none	-nol
1	Ben/Fe(acac) ₃	0.18	15	80	20
2	Ben/Fe(acac) ₃	0.22	17	82	18
3	Calcined Ben/Fe(acac) ₃	0.22	9	68	32
4	Ben/Fe(acac) ₃	0.42	5	64	36

Condition: catalyst 0.40 g, cyclooctane 20 mmol, TBHP 10 mmol, 24 hours, 70°C

Amount of loaded iron affected %conversion. The results showed Ben/Fe(acac)₃ with 0.22 mmol of iron content gave the highest %conversion.

As seen in entries 2 and 3, the calcined catalyst shows lower % conversion, since acetylacetonate ligand was lost from the catalyst. It was reported that acetylacetonate ligand increased rate of reaction.²⁰

From the results in section 5.4.1 B, it was found that TBHP was the best oxidant. So for further experiments, different types of TBHP were studied. The results were indicated in Table 5.23.

Table 5.23 Oxidation of cyclooctane using Ben/Fe(acac)₃ catalyst

Entry	Type of TBHP	% Conversion	%Selectivity	
			-none	-nol
1	70% in water	17	82	18
2	70% in water/ molecular sieve	14	64	36
3	80% in di- <i>tert</i> -butylperoxide	15	86	14

Condition: catalyst 0.4 g (iron 0.22 mmol), cyclooctane 20 mmol, oxidant 10 mmol, 24 hours, 70°C

From the results, it seemed that using aqueous condition, a little better %conversion can be obtained (entry 1). In entries 2 and 3 it can be seen that attempt to get rid of water from the reaction using molecular sieve or using TBHP in organic solvent did not increase the %conversion. In the literature, it was reported that montmorillonite K10 with potassium ferrate oxidant which was used to catalyze the oxidation of benzyl alcohol showed decreased activity in the absence of water.³¹ The reactions were performed in cyclohexane solvent at 75°C for 24 hours. The results showed 0.2 and 2.2 %conversion for dry K10 and crude K10, respectively.

Besides using acetylacetonate ligand, other kinds of ligand containing donor atom were also tested as it was found that these ligands bonded on the metal can increase reactivity with electrophilic oxidizing agents, contributing to increase in the catalytic activity.³⁹ Oxidation of cyclooctane using bentonite supported iron(III) complexes as catalyst were shown in Table 5.24.

Table 5.24 Oxidation of cyclooctane using bentonite supported iron(III) complexes catalyst

Entry	Catalyst	Amount of iron (mmol)	% Conversion	% Selectivity	
				-none	-nol
1	Ben/Fe(acac) ₃	0.18	15	80	20
2	Ben/Fe(bpy) ₂ Cl ₃	0.19	7	75	25
3	Ben/Fe(pyrazinate) ₂ Cl ₃	0.19	7	68	32
4	Ben/Fe(picolate) ₂ Cl ₃	0.19	11	81	19

Condition: catalyst 0.40 g, cyclooctane 20 mmol, 70% TBHP 10 mmol, 24 hours, 70°C

Among iron (III) complexes studied in this work: Ben/Fe(acac)₃, Ben/Fe(picolate)₂Cl₃, Ben/Fe(pyrazinate)₂Cl₃ and Ben/Fe(bpy)₂Cl₃, the reactivities seem to depend on the ligand.⁶⁰

For Ben/Fe(acac)₃ in entry 1, the arrangement of the acetylacetonate ligand is more flexible, which is likely to allow the access of the cyclooctane to the iron active sites.

In the case of Ben/Fe(bpy)₂Cl₃ catalyst in entry 2, the %conversion was low. It was usually observed the negative effect when bipyridine ligand was involved in the reaction, e.g. cyclohexane oxidation with iron(II) sulfate in the presence of bipy, using hydrogen peroxide oxidant.⁶¹

For Ben/Fe(pyrazinate)₂Cl₃ and Ben/Fe(picolate)₂Cl₃ in entries 3 and 4, Ben/Fe(picolate)₂Cl₃ showed higher activity, both have similar structure. Therefore the difference is stemmed from the electronic effect of the ligand. The picolate ligand has one nitrogen atom, it can stabilize the iron cation more than the pyrazinate ligand which possess two nitrogen atoms.

For Ben/Fe(picolate)₂Cl₃ in entry 4, the result was in agreement with the previous report.³⁵ Iron(III) picolate encapsulated in mordenite showed 12 %conversion of cyclohexane when used 1 g of the catalyst, 0.56 mmol of cyclohexane and 0.15 mmol of H₂O₂ in mixed acetonitrile and pyridine for 24 hours.

5.4.4 Kaolinite and talcum supported iron catalysts

The oxidation of cyclooctane was comparatively performed using other clays: kaolinite and talcum supported with iron (II) sulfate. The results were shown in [Table 5.25](#).

Table 5.25 Oxidation of cyclooctane using kaolinite and talc supported iron catalysts

Entry	Catalyst	Amount of iron (mmol)	% Conversion	%Selectivity	
				-none	-nol
1	Kaolinite	0.08	5	70	30
2	Kao/FeSO ₄	0.22	5	81	19
3	Talcum	0.01	2	67	33
4	Talc/FeSO ₄	0.12	2	67	33

Condition: catalyst 0.40 g, cyclooctane 20 mmol, TBHP 10 mmol, 24 hours, 70°C

Kaolinite alone showed oxidation activity (5 %conversion). This might be due to the presence of iron and illite impurities. After being loaded with iron, the result showed increase of iron and believed that agglomeration of iron occurred (see section 5.12). This iron species with small amount could not catalyze the oxidation thus %conversion of the catalyst was comparable to the support. Similar result was found in the case of Talc/FeSO₄ catalyst which talcum had no CEC.

5.4.5 Silica supported iron(II) sulfate catalysts

As previously seen in [section 5.1.1](#), the XRD patterns of clays in indicated quartz as impurity, so in order to verify the activity of quartz in the oxidation reaction, silica was chosen as support. The results of cyclooctane oxidation using silica supported iron catalysts were shown in [Table 5.26](#).

Table 5.26 Oxidation of cyclooctane using silica supported iron(II) catalysts

Entry	Catalyst	Amount of iron (mmol)	%Conversion	%Selectivity	
				-none	-nol
1	SiO ₂ /FeSO ₄	0.03	4	76	24
2	SiO ₂ /FeSO ₄	0.25	6	86	14

Condition: cyclooctane 20 mmol, TBHP 10 mmol, catalyst 0.40 g, 24 hours, 70°C

When loaded with iron(II) sulfate, %conversion was increased a little to 4%. In the literature, 0.1% conversion was obtained in cyclohexane oxidation with silica supported ironporphyrin catalyst (iron 0.3 μmol/g). The reaction was performed in dichloromethane for 1 hour using iodosobenzene oxidant (mole ratio 30:1:61000 of oxidant:catalyst:cyclohexane).⁵⁵

5.4.6 Iron oxide catalysts

Oxidation of cyclooctane using goethite and hematite were investigated. The results were shown in [Table 5.27](#).

Table 5.27 Oxidation of cyclooctane using iron oxides catalyst

Catalyst	Amount of iron (mmol)	%Conversion	%Selectivity	
			-none	-nol
Goethite	1.7	5	74	26
	4.5	3	67	33
Hematite	2.0	3	74	26

Condition: cyclooctane 20 mmol, and TBHP 10 mmol, 24 hours, 70°C

Both iron oxides gave low %conversion in cyclooctane oxidation. The results demonstrated that when the amount of goethite increased, %conversion decreased. This might be due to the coagulation of iron species to become inactive form. Nanostructured amorphous Fe₂O₃ was reported to catalyze the oxidation of

cyclohexane when using 1 atm of dioxygen/ isobutyraldehyde in the presence of acetic acid at 30°C for 16 hours to give 1.5 %conversion.³⁸

5.4.7 Homogeneous iron catalysts

In order to compare the catalytic activity between supported catalyst and homogeneous catalyst, some homogeneous iron catalysts were also prepared and investigated. The selected iron catalysts were Fe(pyrazinate)₂Cl₃, Fe(picolate)₂Cl₃ and Fe(acac)₃. The results were indicated in Table 5.28.

Table 5.28 Cyclooctane oxidation using homogeneous iron catalysts

Entry	Catalyst	Amount of iron (mmol)	% Conversion	%Selectivity	
				-none	-nol
1	FeSO ₄ ·7H ₂ O	0.10	4	86	14
2	FeCl ₃	0.10	6	79	21
3	Fe(acac) ₃	0.10	9	71	29
4	Fe(pyrazinate) ₂ Cl ₃	0.10	5	83	17
5	Fe(picolate) ₂ Cl ₃	0.10	6	72	28

Condition: cyclooctane 20 mmol, TBHP 10 mmol, 24 hours, 70°C

The condition used for the clay-supported iron compound catalysts in this work was selected to study in the homogeneous system except that a much lower amount of catalyst was used in the homogeneous system. Iron complexes: Fe(pyrazinate)₂Cl₃ and Fe(picolate)₂Cl₃ were prepared *in situ* using iron(III) chloride as starting material and used excess ligand (pyrazine-2-carboxylic acid or picolinic acid). It was known that excess ligand had not any negative influence on the performance of the catalyst.

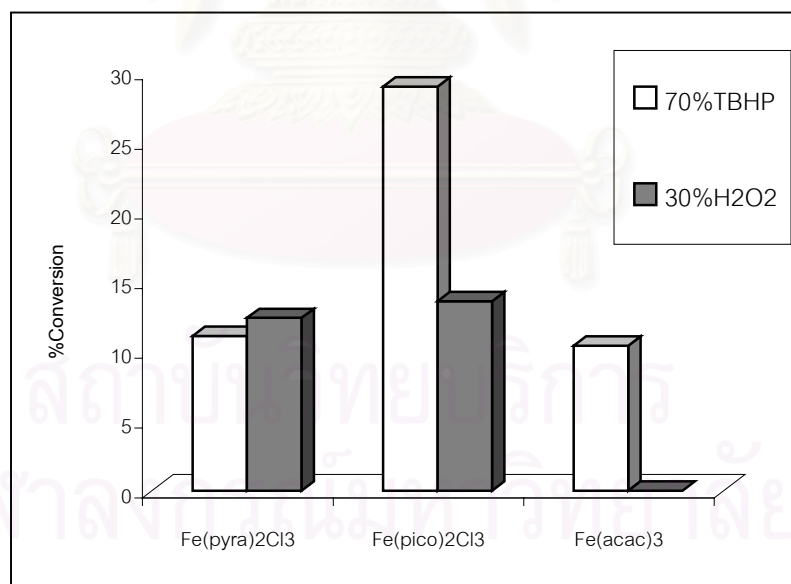
From the results shown in Table 5.28, Fe(acac)₃ gave higher %conversion than other complexes tested. According to the previous report, iron complex containing 1,3-dicarbonyl ligand was found to be a good catalyst for cyclohexane oxidation using hydrogen peroxide in mixture of pyridine and acetic acid.²⁰

To further compare catalytic activity of the homogeneous iron catalysts, effect of oxidant was studied by comparing two types of oxidant: 70% *tert*-butyl hydroperoxide and 30% hydrogen peroxide. The results were shown in Table 5.29.

Table 5.29 Effect of oxidants for cyclooctane oxidation using homogeneous iron catalysts

Catalyst	TBHP			H ₂ O ₂		
	% Conversion	%Selectivity		% Conversion	%Selectivity	
		-none	-nol		-none	-nol
Fe(pyrazinate) ₂ Cl ₃	11	100	-	12	78	22
Fe(picolate) ₂ Cl ₃	29	96	4	14	79	21
Fe(acac) ₃	10	79	21	0	-	-

Condition: catalyst 0.14 mmol, cyclooctane 1.42 mmol, oxidant 2.84 mmol, pyridine: acetic acid (10:1 v/v) 10 mL as solvent, 3.5 hours, RT



The *in situ* prepared Fe(pyrazinate)₂Cl₃ and Fe(picolate)₂Cl₃ were used to catalyze oxidation reaction of cyclooctane using mixed solvent (pyridine: acetic acid ratio 10:1 v/v).¹⁸ As pyridine is believed to be essential to the system as a trap for hydroxyl radical and acetic acid serves as a proton source to transform superoxide ion

to hydroperoxyl radical (HOO•).¹⁴ It was reported that in acetic acid neither inactivated hydrogen peroxide (without iron) nor iron(III) alone did not oxidize the substrate.⁶²

Under the same reaction condition, comparing between different catalysts, Fe(picolate)₂Cl₃ gave higher % conversion in TBHP than Fe(pyrazinate)₂Cl₃. This is in good agreement with those reported.^{27, 61, 63} This might be due to their structures (Figure 5.17). It was reportedly found that small concentration of picolinic acid could accelerate the oxidation while pyrazinic acid required higher concentration.²⁶

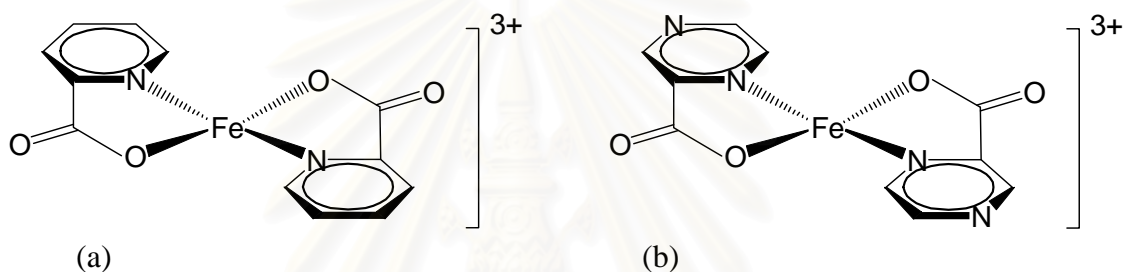


Figure 5.17 Structures of (a) Fe(picolate)₂³⁺ and (b) Fe(pyrazinate)₂³⁺.

The results in Table 5.29 showed that 70% TBHP was the better oxidant than 30% H₂O₂. These agreed with the results in section 5.4.1 B.

In this work, the homogeneous system required shorter reaction time than the heterogeneous one but solvent was needed. Furthermore, the clay supported iron catalysts had some advantages over the homogeneous system: easily separated from the reaction and could be reused.

5.5 Test of leaching

Iron leached from catalyst was studied in some selected polar solvents: acetonitrile/pyridine (3:1) and dichloromethane.

Table 5.30 Amount of iron leached from calcined Ben/FeSO₄ catalyst

Entry	Solvent	Initial amount of iron (mg)	Leached amount of iron (mg)
1	-	28.5	0.020
2	CH ₂ Cl ₂	28.5	0.018
3	ACN:Py (3:1)	28.5	0.038

Condition: TBHP 10 mmol, Ben/FeSO₄ 0.40 g (iron 0.49 mmol), solvent 10 mL, 24 hours, 70°C,

Amount of leached iron from the Ben/5FeSO₄ catalyst was little even when polar solvent was used therefore it could be neglected (~ 0.1%). These indicated that iron species bond strongly with clay support.

5.6 Recycling of clay supported iron catalyst

Recycling Ben/FeSO₄ catalyst was investigated. The results were collected in [Table 5.31](#).

Table 5.31 Oxidation of cyclooctane using recycled calcined Ben/FeSO₄ catalyst

Entry	Recycle time	%Conversion	%Selectivity	
			-none	-nol
1	Fresh	6	73	27
2	1	6	68	32
3	2	5	63	37
4	3	5	65	35

Condition: catalyst 0.4 g (iron 0.49 mmol), cyclooctane 20 mmol, TBHP 10 mmol, 24 hours, 70°C,

It was shown that the catalyst can be reused, with slightly decreasing activities. These results correspond with the results of amount of leached iron ([Table](#)

5.29). In addition, XDR pattern of the reused catalyst was unchanged, which demonstrates stability of the catalyst.

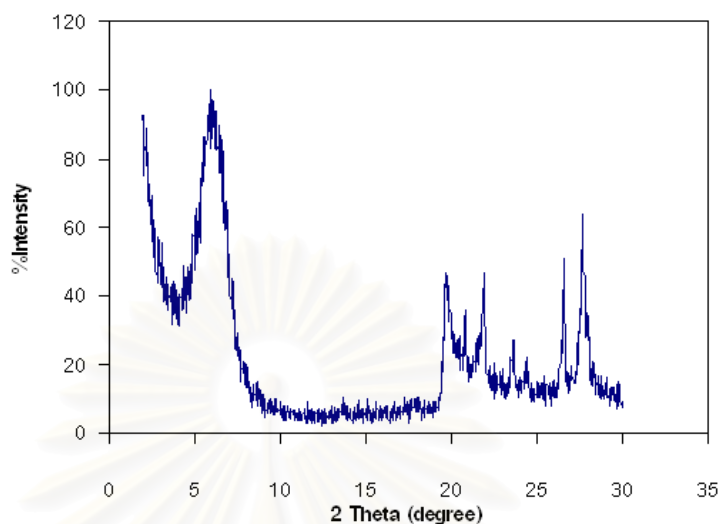


Figure 5.18 XRD pattern of calcined Ben/FeSO₄ catalyst after reusing.

5.7 Proposed Mechanism

Mechanism of cyclooctane oxidation reaction was investigated. The addition of triphenylphosphine (PPh₃) additive to the reaction would provide some clues for the mechanism. The results were shown in Table 5.32.

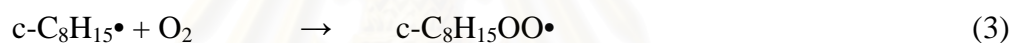
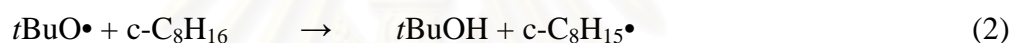
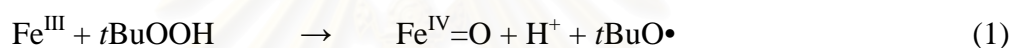
Table 5.32 Comparison %selectivity of cyclooctane oxidation between before and after adding PPh₃

Entry	Catalyst	Amount of iron (mmol)	PPh ₃	%Selectivity	
				-none	-nol
1	Ben/FeSO ₄	0.49	Before added	82	18
2	Ben/FeSO ₄	0.49	After added	47	53
3	Ben/Fe(acac) ₃	0.22	Before added	82	18
4	Ben/Fe(acac) ₃	0.22	After added	56	44

Condition: catalyst 0.4 g, cyclooctane 20 mmol, TBHP 10 mmol, 24 hours, 70°C,

After treatment of reaction solution with PPh₃, the GC analysis will give the amount of cyclooctanone which corresponds to the real concentration of this product in the reaction solution. The amount of cyclooctanol will correspond to the sum of real concentrations of cyclooctyl hydroperoxide and cyclooctanol.⁶¹ It was observed that %selectivity of the products was changed after adding triphenylphosphine, a reducing agent. The cyclooctanol product was increased while cyclooctanone was decreased. These indicated that cyclooctyl hydroperoxide intermediate was formed in the reaction.

Therefore, in this work proposed mechanism for oxidation of cyclooctane by *tert*-butyl hydroperoxide oxidant was believed to occur *via* free radical pathway in the same fashion in the literature.¹⁸



The iron(III) compound was transformed to high valent Fe^{IV}=O species and *t*BuO• initiator radical was formed. In the next step, hydrogen was transferred between *t*BuO• and cyclooctane and *c*-C₈H₁₅• radical was formed. Then dioxygen coming from the decomposition of TBHP or from air reacted with *c*-C₈H₁₅• radical and produced cyclooctylperoxide radical (*c*-C₈H₁₅OO•) that was then converted to cyclooctanone and cyclooctanol in the final step.

CHAPTER VI

CONCLUSION AND SUGGESTIONS

6.1 Conclusion

Three types of natural clays: bentonite, kaolinite and talcum were used to prepare clays supported iron catalysts. First, clays were ion exchanged with iron ion solution, followed by reacting with ligand solution. Iron compound catalysts investigated in this work are: iron(II) sulfate, iron(III) chloride, iron(III) nitrate, iron(III) acetylacetonate, iron(III) pyrazinate, iron(III) picolinate and iron(III) bipyridine. The prepared clays supported iron catalysts were characterized by XRD, XRF or AAS, FT-IR and SEM techniques. The XRD patterns and SEM photographs of the catalysts indicated that layer structure of clay was retained. Iron content in the catalysts (determined by XRF or AAS) varied with amount of metal loaded, type of iron and type of clay which corresponded to cation exchange capacity (CEC) of raw clay.

The prepared catalysts were used for cyclooctane oxidation. Parameters affecting the reaction were studied. The results showed that %conversion increased with increasing amount of oxidant and reaction time. High catalytic activity was found when the reaction was performed at 70°C for 24 hours and used 70% TBHP (in water) as oxidant. The products identified by GC were mainly cyclooctanone and small amount of cyclooctanol.

The maximum %conversion of cyclooctane obtained in this work was 17% using bentonite supported iron(III) acetylacetonate catalyst (4.4% weight Fe_2O_3). For bentonite supported iron(III) complexes, the ligand affected catalytic activity. It was found that iron(III) acetylacetonate could catalyze the oxidation better than iron(III) pyrazinate, iron(III) picolinate and iron(III) bipyridine. In the case of different iron compound catalysts with similar iron content, the results indicated that activities of iron(II) sulfate, iron(III) chloride and iron(III) nitrate were comparable.

Considering type of clay support, the results showed that iron supported on bentonite provided higher %conversion than kaolinite and talcum. This is due to the iron content and high cation exchange capacity of bentonite.

For the reusability of the spent catalyst, the tests showed that after three cycles, its catalytic activity was slightly dropped which might be caused by the leaching of iron from the catalyst and the deactivation of iron active species.

Some homogeneous catalysts were investigated for comparison. The results revealed that in mixed solvent system (pyridine: acetic acid ratio 10:1 v/v), TBHP showed better catalytic activity than H₂O₂. It was found that iron(III) picolinate gave higher %conversion than iron(III) pyrazinate and iron(III) acetylacetonate.

Comparison between the supported and homogeneous catalysts for cyclooctane oxidation, it could be seen that the clay supported iron catalysts showed comparable catalytic activity to the iron homogeneous. The main advantages of the supported system were the reusability and the easy to be separated from the reaction. Moreover, the supported catalysts could be effective in the absence of solvent, this was a good benefit for the environment in view of the solvent contamination.

The mechanism in the cyclooctane oxidation studied in this work was proposed to occur *via* alkyl hydroperoxide intermediate in radical pathway. This was revealed and confirmed by the study which involved the addition of triphenylphosphine, widely used in the oxidation field.

6.2 Suggestions

From the results obtained, future work shall be focused on the following:

1. To modify clay before loading metal in order to increase catalytic activity in the oxidation of cyclooctane. For example, using alkylammonium cation or ethylene glycol to expand clay interlayers to allow the introduction of metal complex.

2. To study kinetic of the cyclooctane oxidation with the synthesized catalysts.



สถาบันวิทยบริการ
จุฬาลงกรณ์มหาวิทยาลัย

REFERENCES

1. Barkanova, S. V.; Derkacheva, V. M.; Dolotova, O. V.; Li, V. D.; Negrimovsky, V. M.; Kaliya, O. L.; Luk'yanets, E. A. "Homogeneous Oxidation of Aromatics in Nucleus with Peracetic Acid Catalyzed by Iron and Manganese Phthalocyanine Complexes", *Tetrahedron Letters* **1996**, *37*, 1637-1640.
2. Hagen, J. *Industrial Catalysis A Practical Approach*. Weinheim: WILEY-VCH, **1999**, 11.
3. Schuchardt, U.; Cardoso, D.; Sercheli, R.; Pereira R.; Cruz, R. S. D.; Guerreiro M. C.; Mandelli, D.; Spinacé, E. V.; Pires E. L. "Cyclohexane Oxidation Continues to be a Challenge", *Applied Catalysis A: General* **2001**, *211*, 1-17.
4. Tateiwa, J-I.; Uemura, S. "Selective Organic Synthesis Over Metal Cation-Exchanged Clay Catalyst", *Journal of the Japan Petroleum Institute* **1997**, *40*, 329-341.
5. Bayer, H.; Walter, W. *Handbook of Organic Chemistry*. London: Prentice Hall, **1996**, 398.
6. Castellan, A.; Bart, J.C.J.; Cavallaro, S. "Industrial Production and Uses of Adipic Acid", *Catalysis Today* **1991**, *9*, 237-254.
7. Parshall, G. W.; Ittel, S. D. *Homogeneous Catalysis 2nd ed.* New York: John Wiley & Sons, **1992**, 242-249.
8. Bernadou, J.; Pitie, M.; Meunier, B. "Oxidation at Carbon-1' of DNA Deoxyribose by the Mn-TMPY/KHSO₅ System Results from a Cytochrome P-45 Type Hydroxylation Reaction", *Journal of American Chemical Society* **1995**, *117*, 2935-2936.
9. Weissermel, K.; Arpe, H.-J. *Industrial Organic Chemistry Third Completely Revised Edition*. Weinheim: WILEY-VCH, **1997**, 243.
10. Moore, D.M.; Reynolds, R.C. *X-Ray Diffraction and the Identification and Analysis of Clay Materials*. New York: Oxford University Press, **1989**, 120-128.
11. Verma, R. S. "Clay and Clay-supported Reagents in Organic Synthesis", *Tetrahedron* **2002**, *58*, 1235-1255.
12. Bergaya, F.; Vayer, M. "CEC of clays: Measurement by Adsorption of a Copper Ethylenediamine Complex", *Applied Clay Science* **1997**, *12*, 275-280.

13. Hudlický, M. *Oxidations in Organic Chemistry*. Washington DC: ACS Monograph 186, **1990**, 1.
14. Sheu, C.; Rechert, S. A.; Cofré, P.; Ross, B. Jr.; Sobkowiak, A.; Sawyer, D. T.; Kanofsky, J. R. "Iron-Induced Activation of Hydrogen Peroxide for the Direct Ketonization of Methylenic Carbon [$c\text{-C}_6\text{H}_{12} \rightarrow c\text{-C}_6\text{H}_{10}(\text{O})$] and the Dioxygenation of Acetylenes and Aryloefins", *Journal of American Chemical Society* **1990**, *112*, 1936-1942.
15. Balavoine, G.; Barton, D. H. R.; Boivin, J.; Gref, A. "On the Oxidation of Saturated Hydrocarbons with H_2O_2 in the Presence of Iron(II)-Picolinate or Iron(II)-1,10-Phenanthroline 2-Carboxylate", *Tetrahedron Letters* **1990**, *31*, 659-662.
16. Barton, D. H. R.; Bévière, S. D.; Chavasiri, W.; Cshai, É.; Doller, D. "The Fuctionalisation of Saturated Hydrocarbons. Part XXI. The Fe(III)-Catalyzed and Cu(II)-Catalyzed Oxidation of Saturated Hydrocarbons by Hydrogen Peroxide: A Comparative Study", *Tetrahedron* **1992**, *48*, 2895-2910.
17. Randolph, A. L.; Jinheung, K.; Migiel, A. P.; Lawrence, Q. Jr. "Alkane Functionalization at (μ -Oxo)diiron(III) Centers", *Journal American Chemical Society* **1993**, *115*, 9524-9530.
18. Snelgrove, D. W.; MacFaul, A.; Ingold, K. L.; Wayner, D. M. "The role of alkoxy radicals in Gif (GoAgg^{V}) Chemistry", *Tetrahedron Letters* **1996**, *37*, 823-826.
19. Perkins, M. J. "A Radical Reappraisal of Gif Reactions", *Chemical Society Reviews* **1996**, 229-236.
20. Chavasiri, W.; Jang, D. O. "The Effect of 1,3-Dicarbonyl Compounds on Alkane Oxidation in Gif-Type Reactions", *Bulletin of Korean Chemical Society* **1997**, *18*, 362-363.
21. Schuchardt, U.; Pereira, R.; Rufo, M. "Iron(III) and Copper(II) Catalysed Cyclohexane Oxidation by Molecular Oxygen in the Presence of *Tert*-Butyl Hydroperoxide", *Journal of Molecular Catalysis A: Chemical* **1998**, *135*, 257-262.
22. Barton, D. H. R.; Launay, F. "The Selective Fuctionalization of Saturated Hydrocarbons. Part 44. Measurement of Size of Reagent by Variation of Steric Demands of Competing Substrates using Gif Chemistry" *Tetrahedron* **1998**, *54*, 3379-3390.

23. Mizuno, N.; Kiyoto, I; Nozaki, C.; Misono, M. "Remarkable Structure Dependence of Intrinsic Catalytic Activity for Selective Oxidation of Hydrocarbons with Hydrogen Peroxide Catalyzed by Iron-Substituted Silicotungstates", *Journal of Catalysis* **1999**, *181*, 171-174.
24. Simões, M. M. Q.; Conceição, C. M. M.; Gamelas, J. A. F.; Domingues, P. M. D. N.; Cavaleiro, A. M. V.; Cavaleiro, J. A. S.; Ferrer-Correia, A. J. V.; Johnstone, R. A. W. "Keggin-Type Polyoxotungstates as Catalysts in the Oxidation of Cyclohexane by Dilute Aqueous Hydrogen Peroxide", *Journal of Molecular Catalysis A: Chemical* **1999**, *144*, 461-468.
25. Collman, J.; Chien, A. S.; Eberspacher, T. A.; Brauman, J. I. "Multiple Active Oxidants in Cytochrome P-450 Model Oxidations", *Journal of American Chemical Society* **2000**, *122*, 11098-11100.
26. Nizova, G. V.; Krebs, B.; Süß-Fink, G.; Schindler, S.; Westerheide, L.; Cuervo, L. G.; Shul'pin, G. B. "Hydroperoxidation of Methane and Other Alkanes with H₂O₂ Catalyzed by a Dinuclear Iron Complex and an Amino Acid", *Tetrahedron* **2002**, *58*, 9231-9237.
27. Grootboom, N.; Nyokong, T. "Iron Perchlorophthalocyanine and Tetrasulfophthalocyanine Catalyzed Oxidation of Cyclohexane Using Hydrogen Peroxide, Chloroperoxybenzoic Acid and *Tert*-Butylhydroperoxide as Oxidants", *Journal of Molecular Catalysis A: Chemical* **2002**, *179*, 113-123.
28. Haber, J.; Matachowski, L.; Pamin, K.; Poltowicz, J. "The Effect of Peripheral Substituents in Metalloporphyrins on Their Catalytic Activity in Lyons System", *Journal of Molecular Catalysis A: Chemical* **2003**, *198*, 245-221.
29. Herron, N.; Stucky, G. D.; Tolman, C. A. "Shape Selectivity in Hydrocarbon Oxidations using Zeolite Encapsulated Iron Phthalocyanine Catalysts", *Journal of Chemical Society Chemical Communication* **1986**, *610*, 1521-1522.
30. Jun, K-W.; Shim, E-K.; Park, S-E.; Lee, K-W. "Cyclohexane Oxidations by Iron-Palladium Bicyclic System; Soluble Catalysts and Polymer Supported Catalysis", *Bulletin of Korean Chemical Society* **1995**, *16*, 398-400.
31. Dulaude, L.; Laszlo, P.; Lehance P. "Oxidation of Organic Substrate with Potassium Ferrate (VI) in the Presence of the K10 Montmorillonite", *Tetrahedron Letters* **1995**, *36*, 8505-8508.

32. Park, O-S.; Nam, S- S.; Kim, S-B.; Lee, K-W. "Gif-KRICT Biomimic Oxidation of Cyclohexane: The Influence of Metal Oxides", *Bulletin of Korean Chemical Society* **1999**, *20*, 49-52.
33. Langhendries, G.; Baron, G. V.; Neys, P. E. Jacobs, P.A. "Liquid-Phase Hydrocarbon Oxidation using Supported Transition Metal Catalysts: Influence of the Solid Support", *Chemical Engineering Science* **1999**, *54*, 3563-3568.
34. Carvalho, W. A.; Wallua, M.; Schuchardt, U. "Iron and Copper Immobilised on Mesoporous MCM-41 Molecular Sieves as Catalysts for the Oxidation of Cyclohexane", *Journal of Molecular Catalysis A: Chemical* **1999**, *144*, 91-99.
35. Álvalo, M.; Ferrer, B.; Garcia, H.; Sanjuán, A. "Heterogeneous Gif Oxidation of Cyclohexane Using Fe³⁺-Picolinate Complex Encapsulated within Zeolites", *Tetrahedron* **1999**, *55*, 11895-11902.
36. Rosa, I. L. V.; Manso, C. M. C. P.; Serra, O. A.; Iamamoto, "Biomimetical Catalytic Activity of Iron(III) Porphyrins Encapsulated in the Zeolite X", *Journal of Molecular Catalysis A: Chemical* **2000**, *160*, 199-208.
37. Monfared, H. H.; Ghorbani, M. "Hydrogen Peroxide Oxidation of Hydrocarbon Catalyzed by a Silica Supported Iron Precursor", *Monatshefte für Chemie* **2001**, *132*, 989-992.
38. Perkas, N.; Koltypin, Y.; Palchik, O.; Gedaken, A.; Chadrsekaran, S. "Oxidation of Cyclohexane with Nanostructured Amorphous Catalysts under Mild Conditions", *Applied Catalysis A: General* **2001**, *209*, 125-130.
39. Machado, A. M.; Wypych, F.; Drechsel, S. M.; Nakagaki, S. "Study of the Catalytic Behavior of Montmorillonite/Iron(III) and Mn(III) Cationic Porphyrins", *Journal of Colloid and Interface Science* **2002**, *254*, 158-164.
40. Nakagaki, S.; Ramos, A. R.; Benedito, F. L.; Peralta-Zamora, P.G.; Zarbin, A. J. G. "Immobilization of Iron Porphyrins into Porous Vycor Glass: Characterization and Study of Catalytic Activity", *Journal of Molecular Catalysis A: Chemical* **2002**, *185*, 203-210.
41. Srivastava, D. N.; Perkas, N.; Gedanken, A.; Felner, I. "Sonochemical Synthesis of Mesoporous Iron Oxide and Accounts of Its Magnetic and Catalytic Properties", *Journal of Physical Chemistry B* **2002**, *106*, 1878-1883.

42. Kopylovich, M. N.; Kirillov, A. M.; Baev, A. K.; Pombeiro, A. J. L. "Heteronuclear Iron(III)-Chromium(III) Hydroxo Complexes and Hydroxides, and Their Catalytic Activity Towards Peroxidative Oxidation of Alkanes", *Journal of Molecular Catalysis A: Chemical* **2003**, *206*, 163-178.
43. Faria, A. L.; Airoidi, C.; Doro, F. G.; Fonseca, M. G.; Assis, M. das D. "Anchored Ironporphyrins-the Role of Talc-Aminofunctionalized Phyllosilicates in the Catalysis of Oxidation of Alkanes and Alkenes", *Applied Catalysis A: General* **2004**, *268*, 217-226.
44. Nakagaki, S.; Benedito, F. L. Wypych, F. "Anionic Iron(III) Porphyrin Immobilized on Silanized Kaolinite as Catalyst for Oxidation Reactions", *Journal of Molecular Catalysis A: Chemical* **2004**, *217*, 121-131.
45. Niassary, M. S.; Farzaneh, F.; Ghandi, M. "Selective Hydroxylation of Cyclic Ethers with Tert-Butylhydroperoxide and Hydrogen Peroxide Catalyzed by Iron(III) and Manganese(II) Bipyridine Complexes Included in Zeolite Y and Bentonite", *Journal of Molecular Catalysis A: Chemical* **2001**, *175*, 105-110.
46. Shrigadi, N. B.; Shinde, A. B.; Samant, S. D. "Study of Catalytic of Free and K10-Supported Iron Oxyhydroxides and Oxides in the Friedel-Crafts Benzoylation Reaction using Benzyl Chloride/Alcohol to Understand Their Role in the Catalysis by the Fe-Exchange/Impregnated K10 Catalysts", *Applied Catalysis A: General* **2003**, *252*, 23-35.
47. Gournis, D.; Louloudi, M.; Karakassides, M. A.; Kolokytha, C.; Mitopoulou, K.; Hadjiliadis, N. "Heterogenous Clay-Manganese(II) Oxidation Catalyst", *Material Science and Engineering* **2002**, *C22*, 113-116.
48. Kosmulski, M.; Maczka, E.; Jarych, E.; Rosenholm, J. B. "Synthesis and Characterization of Goethite and Goethite-Hemathite Composite: Experimental Study and Literature Survey", *Advances in Colloid and Interface Science* **2003**, *103*, 57-76.
49. Sharefkin, J. G.; Saltzman, H. *Organic Synthesis Collective Volume 3*. New York: John Willey & Sons, **1963**, 60.
50. Fonseca, M. G. D.; Airoidi, C. "New Amino-Inorganic Hybrids from Talc Silylation and Copper Adsorption Properties", *Materials Research Bulletin* **2001**, *36*, 277-287.

51. Rosenira, S. da C.; Juliana, M. de S.; Ulrich, A.; Mauricio, S. D.; Ulf, S. "Copper Containing Silicates as Catalysts for Liquid Phase Cyclohexane Oxidation", *Journal of Brazil Chemical Society* **2002**, *13*, 170-176.
52. Guélou, E.; Barrault, J.; Fournier, J.; Tatibouët, J-M. "Active Iron Species in the Catalytic Wet Peroxide Oxidation of Phenol Over Pillared Clays Containing Iron", *Applied Catalysis B: Environmental* **2003**, *1346*, 1-8.
53. Parmaliana, A.; Arena, F.; Frusteri, F., Martínez-Arias, A.; Granados. M. L.; Fierro, J. L. G. "Effect of Fe-Addition on the Catalytic Activity of Silicas in the Partial Oxidation of methane to formaldehyde", *Applied Catalysis A: General* **2002**, *226*, 163-174.
54. Belaroui, L. S.; Millet, J. M. M.; Bengueddach, A. "Characterization of Latithe, a New Bentonite-Type Algerian Clay for Intercalation and Catalysts Preparation", *Catalysis Today* **2004**, *89*, 279-286.
55. Iamamoto, Y.; Idemori, Y. M.; Nakagaki, S. "Cationic Iron Porphyrins as Catalyst in Comparative Oxidation of Hydrocarbons: Homogeneous and Supported on Inorganic Matrices Systems", *Journal of Molecular Catalysis A: Chemical* **1995**, *99*, 187-193.
56. Pardo, E.; Lloret, F.; Carrasco, R.; Muñoz, M, C.; Temporal-Sánchez, T.; Ruiz-García, R. "Chemistry and Reactivity of Dinuclear Iron Oxamate Complexes: Alkane Oxidation with Hydrogen Peroxide Catalyzed by an Oxo-Bridged Diiron(III) Complex with Amide and Carboxylate Ligation", *Inorganic Chimica Acta* **2004**, *357*, 2713 –2720.
57. Costas, M.; Chen, K.; Gue, Jr., L. "Biomimetic Nonheme Iron Catalysts for Alkane Hydroxylation", *Coordination Chemistry Reviews* **2000**, *200-202*, 517-544.
58. Tongkratok, S. "Electrochemical and Catalytic Properties of Thansition Metal-Schiff Base Complexes", *Master Thesis, Program of Pretochemistry and Polymer Science, Faculty of Science, Chulalongkorn University*, **2002**.
59. Monfared, H. H.; Amouei, Z. "Hydrogen Peroxide Oxidation of Aromatic Hydrocarbon by Immobilized Iron(III)", *Journal of Molecular Catalysis A: Chemical* **2004**, *217*, 161-164.
60. Gozzo, F. "Radical and Non-Radical Chemistry of the Fenton-Like System in the Presence of Organic Substrates", *Journal of Molecular Catalysis A: Chemical* **2001**, *171*, 1-22.

61. Georgiy, B. S. “Metal-Catalyzed hydrocarbon Oxygenations in Solutions: the Dramatic Role of Additives: a Review”, *Journal of Molecular Catalysis A: Chemical* **2002**, *189*, 39-66.
62. Kowalski, J.; Ploszyńska, J.; Sobkowiak, A. “Iron(III)-Induced Activation of Hydrogen Peroxide for Oxidation of 2-Methylnaphthalene in Glacial Acetic Acid”, *Catalysis Communications* **2003**, *4*, 603-608.
63. Barton, D. H. R. “Gif Chemistry: the Present Situation”, *Tetrahedron* **1998**, *54*, 5805-5817.



สถาบันวิทยบริการ
จุฬาลงกรณ์มหาวิทยาลัย

APPENDIX

Gas chromatography analyzer was used to determine products of cyclooctane oxidation. Cyclooctanone and cyclooctanol products were identified using standard addition method.

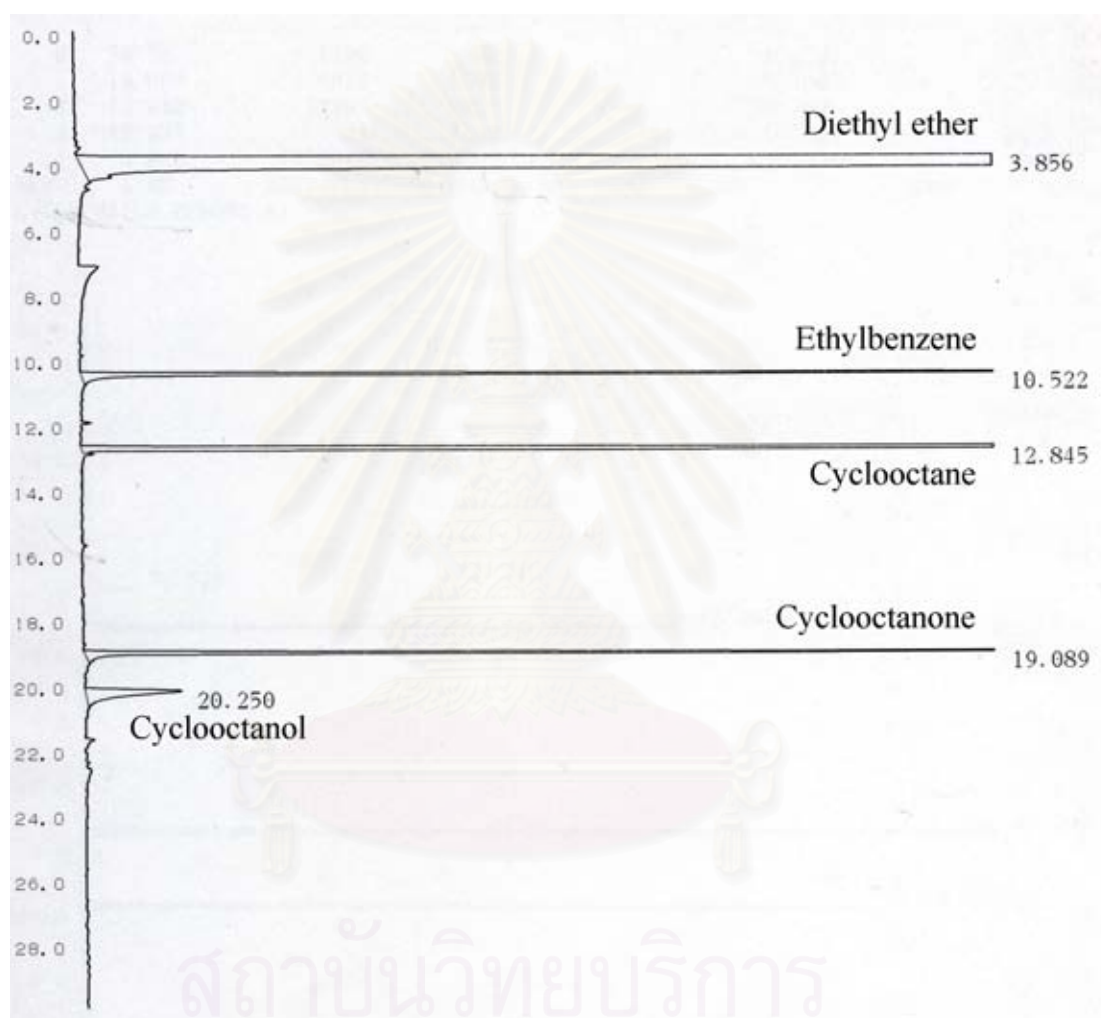


Figure A-1 A gas chromatogram of liquid products from oxidation of cyclooctane.

Calculation of the correction factor

The correction factor was calculated based upon the results obtained from gas chromatographic analysis (see also the experimental section). Ethylbenzene was internal standard.

Example:

A: exact amount of desired product prepared (mmol)

B: total volume of the reaction (mL)

C: peak area of the desired product

D: peak area of the internal standard

E: exact amount of substrate (mmol)

F: exact amount of internal standard was added (mmol)

The calculation of the correction factor can be described as follows:

The amount of the product from the reaction mixture

$$= (F \times C / D) = G$$

The amount of the product in B mL (total volume of the reaction)

$$= G \times B = H$$

Thus, the correction factor of the product can be calculated as:

$$= A / H = I$$

The calculation of the desired product can be calculated as:

$$\% \text{Yield of product} = (H \times I / E) \times 100$$

The correction factors of chemicals are listed as follows:

Cyclooctane = 0.9

Cyclooctanone = 1.0

Cyclooctanol = 1.0

Calculation of %conversion of cyclooctane

Using peak areas obtained from GC analysis

$$\% \text{conversion} = \% \text{yield of cyclooctanone} + \% \text{yield of cyclooctanol}$$

Calculation of %selectivity of cyclooctanone and cyclooctanol

Using peak areas obtained from GC analysis

%Selectivity of cyclooctanone

$$= (\% \text{yield of cyclooctanone} / \% \text{conversion}) \times 100$$

%Selectivity of cyclooctanol

$$= (\% \text{yield of cyclooctanol} / \% \text{conversion}) \times 100$$

Calculation of cation exchange capacity (CEC)

CEC was calculated based upon the results obtained from Uv-Vis spectrophotometer. The initial concentration of Cu(EDA)_2^{2+} complex was 10 mM.

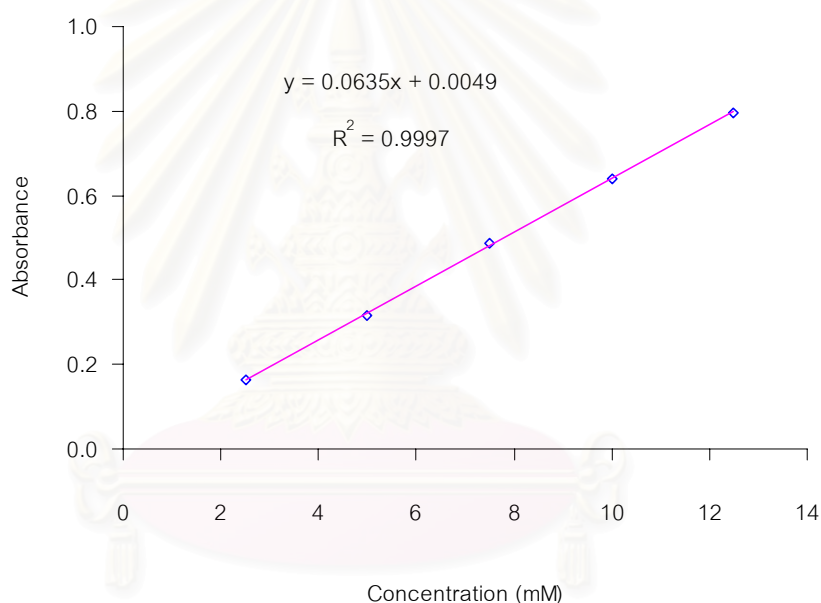


Figure A-2 Calibration curve of Cu(EDA)_2^{2+} complex at $\lambda_{\text{max}} = 548 \text{ nm}$.

From calibration curve of Cu(EDA)_2^{2+} complex at $\lambda_{\text{max}} = 548 \text{ nm}$, the linear equation, $y = 0.0635x + 0.0049$ was obtained.

Concentration of exchangeable cation

$$= \{10 - [(\text{Absorbance} - 0.0049) / 0.0635] \} * 25 / 1000$$

$$= J$$

Cation exchange capacity value (CEC)

$$\text{CEC} = J * 2 / 0.50$$

Table A-1 XRD data of Bentonite

2θ (degree)	d (Å)
7.5	11.8
19.8	4.5
21.9	4.1
26.6	3.3
27.8	3.2

Table A-2 XRD data of bentonite-supported iron compound catalysts

Catalyst	Amount of iron (%weight Fe ₂ O ₃)	2θ (degree)	d ₀₀₁ (Å)
Ben/FeSO ₄	8.8	6.5	13.7
Ben/FeSO ₄	9.8	6.5	13.6
Calcined Ben/FeSO ₄	9.7	8.9	10.0
Ben/FeSO ₄	13.2	6.5	13.6
Ben/FeCl ₃	8.9	6.4	13.7
Ben/FeCl ₃	10.5	6.4	13.8
Calcined Ben/FeCl ₃	10.5	8.9	9.9
Ben/Fe(NO ₃) ₃	9.1	6.4	13.7
Ben/Fe(acac) ₃	4.4	6.5	13.6
Ben/Fe(acac) ₃	8.3	5.8	15.3
Ben/Fe(bpy) ₂ ³⁺	3.8	6.5	13.6
Ben/Fe(pyrazinate) ₂ Cl ₃	3.8	5.9	15.2
Ben/Fe(picolate) ₂ Cl ₃	3.8	6.3	13.7

Table A-3 XRD data of kaolinite, Kao/FeSO₄ and Kao/Fe(acac)₃ catalysts

kaolinite		Kao/FeSO ₄		Kao/Fe(acac) ₃	
2θ (degree)	d (Å)	2θ (degree)	d (Å)	2θ (degree)	d (Å)
8.8	10.1	8.7	10.1	8.7	10.1
12.3	7.2	12.3	7.2	12.3	7.2
17.7	5.0	17.7	5.0	17.7	5.0
19.9	4.5	19.8	4.5	19.8	4.5
24.9	3.6	24.8	3.6	24.8	3.6
26.6	3.3	26.6	3.3	26.6	3.3

Table A-4 XRD data of talcum, mTalc and Talc/FeSO₄ catalysts

Talcum		mTalc		Talc/FeSO ₄	
2θ (degree)	d (Å)	2θ (degree)	d (Å)	2θ (degree)	d (Å)
6.2	14.2	6.2	14.2	6.2	14.3
9.4	9.3	9.4	9.4	9.4	9.4
12.4	7.1	12.4	7.1	12.4	7.1
18.7	4.7	18.8	4.7	18.7	4.7
19.3	4.6	19.0	4.7	18.9	4.7
25.1	3.6	25.1	3.6	25.1	3.6
28.6	3.1	28.6	3.1	28.6	3.1

สถาบันวิทยบริการ
จุฬาลงกรณ์มหาวิทยาลัย

Table A-5 Chemical analysis of bentonite and kaolinite from XRF data according to Cernic International Co., Ltd.

Metal oxide	% Weight	
	Bentonite	Kaolinite
SiO ₂	63.6	51.5
Al ₂ O ₃	17.6	23.0
Fe ₂ O ₃	3.1	0.37
CaO	3.0	0.37
MgO	Trace	0.12
Na ₂ O	3.4	0.22
K ₂ O	0.5	0.92
Loss on ignition	5.8	19.6

สถาบันวิทยบริการ
จุฬาลงกรณ์มหาวิทยาลัย

VITAE

Miss Parichat Damrongpong was born on June 29, 1977 in Sraraburi, Thailand. She received her Bachelor's Degree of Science in Chemistry from Srinakarinwirot University in 1998. She studied Master Degree in Inorganic Chemistry at Chulalongkorn University in 2002, she was awarded a teaching assistantship by the Faculty of Science in 2003 and was supported by a research grant from the Graduate School, Chulalongkorn University and graduated in 2004.

Her present address in 532/11 Moo 2, Phaholyothin 52 Soi, Phaholyothin Road, Klongthanone, Saimai, 10230, Bangkok. Tel 02-9942135, 01-6266717.



สถาบันวิทยบริการ
จุฬาลงกรณ์มหาวิทยาลัย